

Chpt.5 Atomic processes

5.1 Atomic data for astrophysics

5.2 Two-level system

5.3 Bremsstrahlung

5.4 Recombination and photoionization

5.4.1 Radiative recombination (free-bound) process

5.4.2 Photoionization (bound-free) process

5.4.3 Ionization energy

5.4.4 Photoionization cross section

5.4.5 Radiative recombination data

5.4.6 Radiative recombination continuum

5.4.7 Optical recombination lines

5.4.8 Radio recombination lines

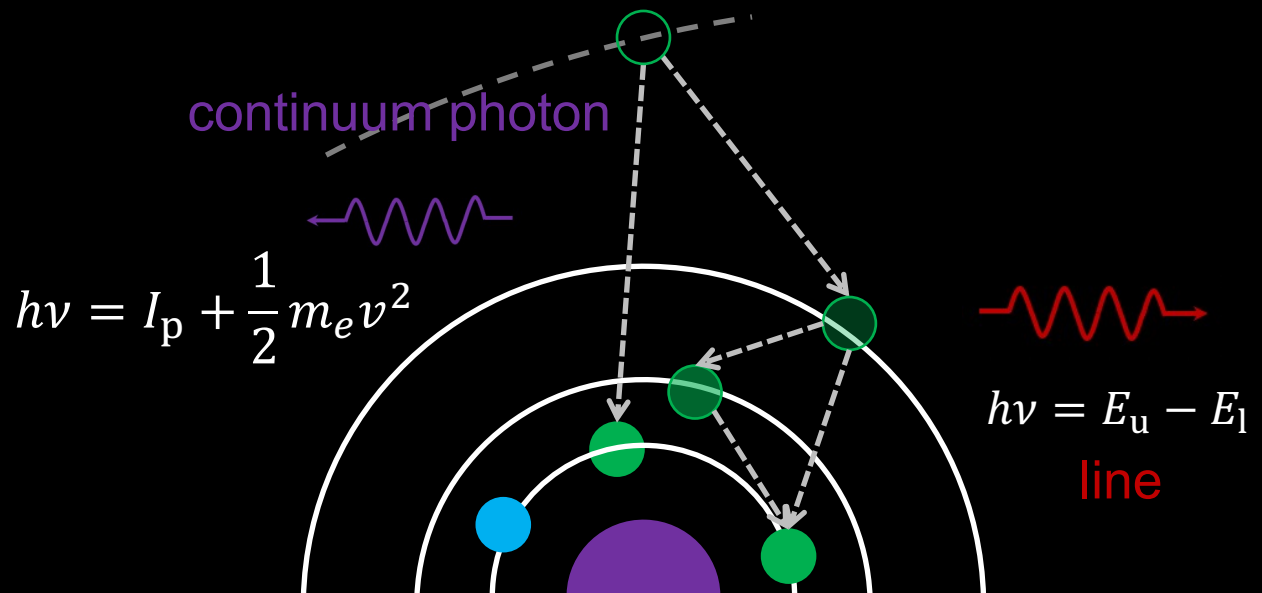
5.4.9 Dielectronic recombination

5.5 Collisional excitation and de-excitation

5.6 Other atomic processes

5.7 Astrophysical plasma models

5.4 Recombination and photoionization



Radiative recombination (free-bound) process

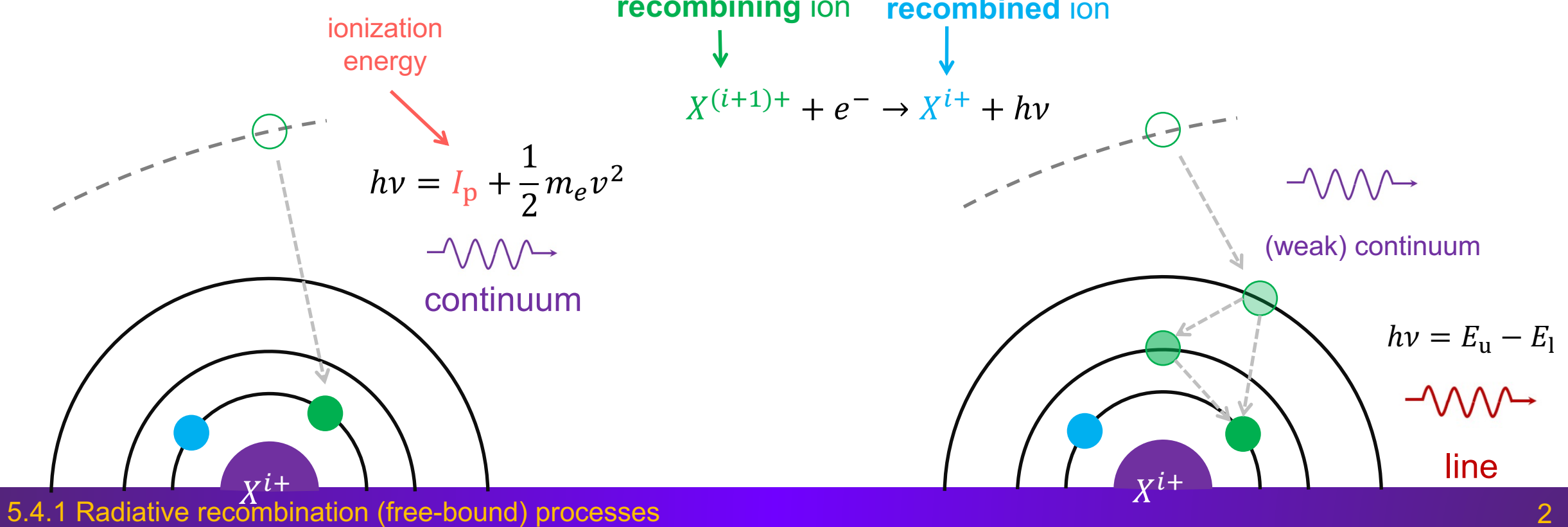
i : ionic charge
(roman numeral – 1)

Emission due to the **capture** of a **free** electron into a **bound** atomic state of an ion

- ✓ a **cooling** process for the electrons
- ✓ **continuum** or **line emission** spectral features

Triply ionized carbon ($Z = 6$): C IV = C^{3+}
Isoelectronic sequence: Li-like (i.e., three bounded electrons)
Ionic charge (used by the atomic physics community): 3

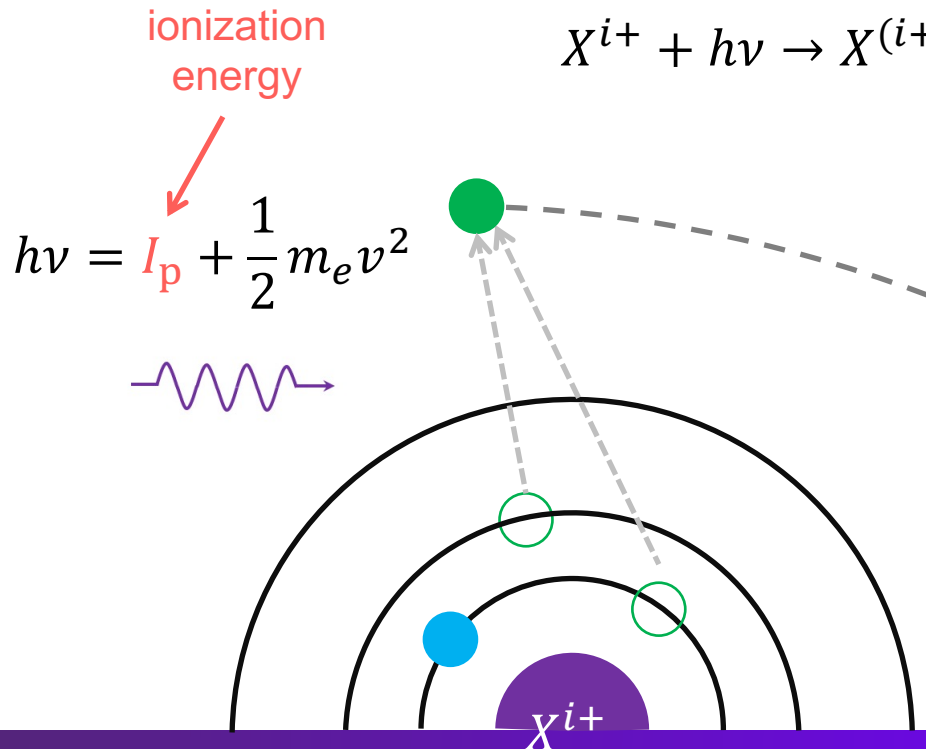
Triply ionized iron ($Z = 26$): Fe XVII = Fe^{16+}
Isoelectronic sequence: Ne-like (i.e., ten bounded electrons)
Ionic charge (used by the atomic physics community): 16



Photoionization (bound-free) process

Photoionization, absorption due to the **ionization** of a **bounded** electron of an ion into the **continuum**, is the reverse process of radiative recombination.

- ✓ a **heating** process for the electrons
- ✓ **continuum** spectral features



5.4.2 Photoionization (bound-free) processes

ASD DATA — INFORMATION —

LiNES LEVELS List of SPECTRA Ground STATES & IonIZATION ENERGIES Bibliography Help

NIST Atomic Spectra Database Ionization Energies Form

<https://physics.nist.gov/PhysRefData/ASD/ionEnergy.html>

This form provides access to NIST critically evaluated data on ground states and ionization energies of atoms and atomic ions.

Spectra: e.g., Fe I or Na or H-Ds I or Mg+ or Al3+ or mg iv,vi-VIII; S V-xii or Fe ne-like-S-like or Ne-Fe I-III or Ni-like or H-like-Ne-like

Default Values Retrieve Data

Units: eV Format output: HTML (formatted) No JavaScript

Ordered by Z Ordered by sequence

Output Data: Atomic number Ground-state electronic shells
 Spectrum name Ground-state configuration
 Ion charge Ground-state level
 Element name Ionized configuration
 Isoelectronic sequence

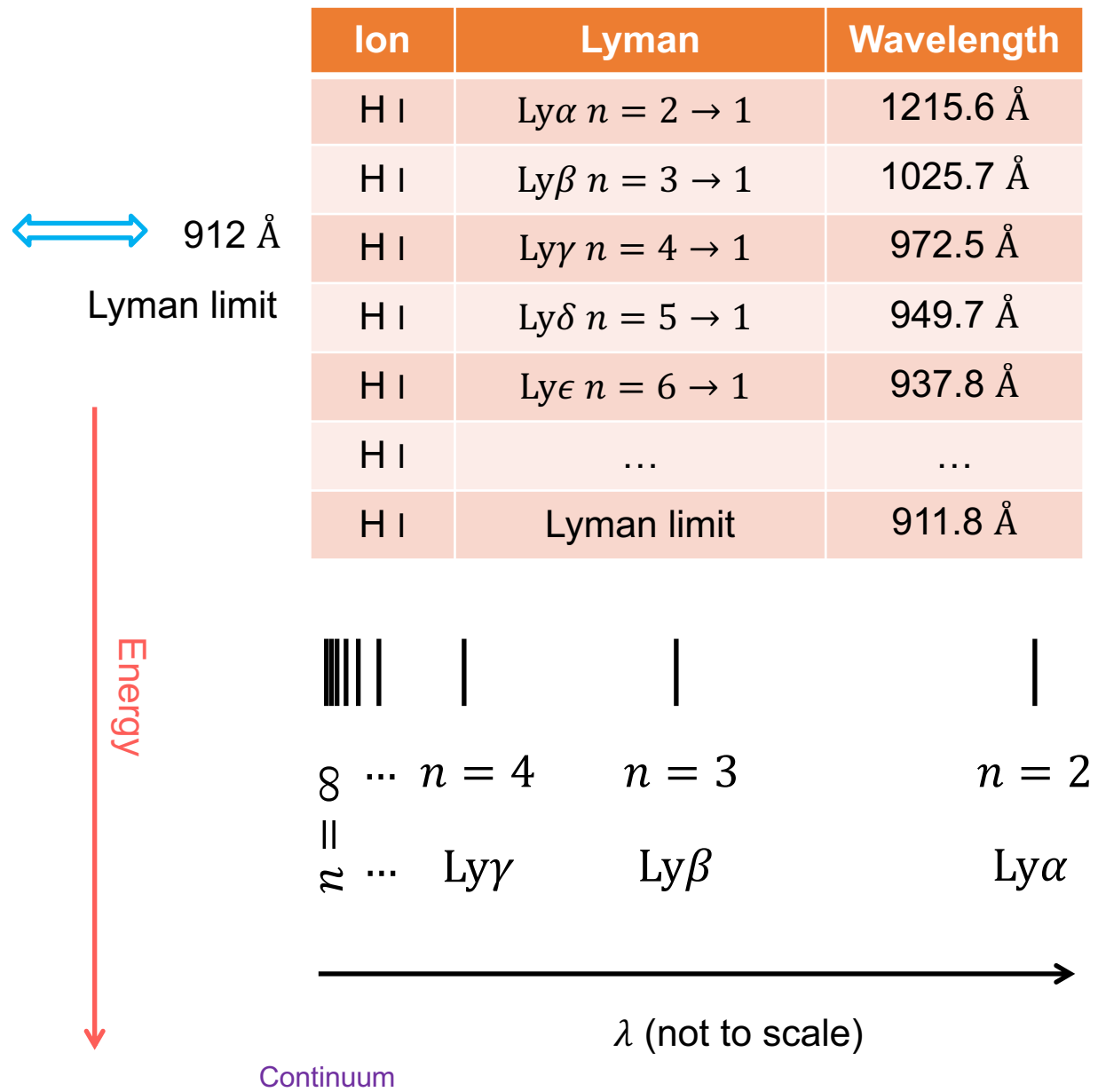
Ionization energy Total binding energy Uncertainty

Bibliographic references:

Default Values Retrieve Data

Ionization energy

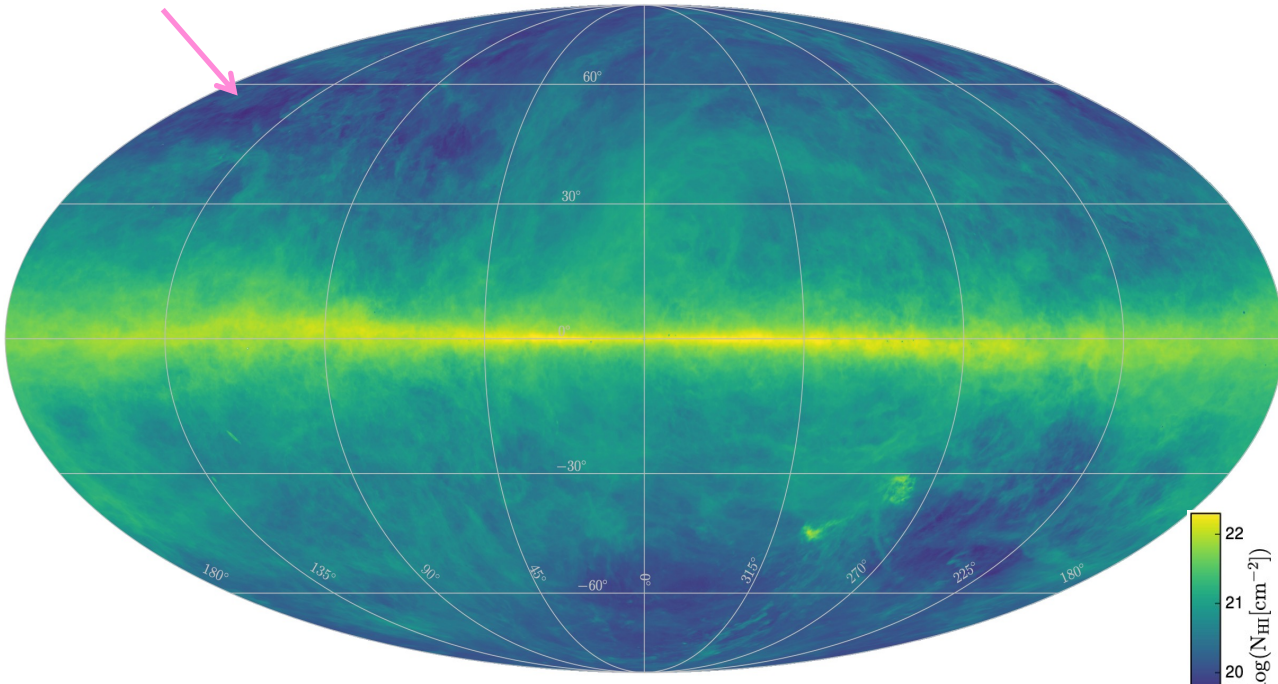
Ion	Ground level	I_p (eV)
H I	$1s\ ^2S_{1/2}$	13.598
He I	$1s^2\ ^2S_0$	24.587
He II	$1s\ ^2S_{1/2}$	54.418
O III	$1s^2 2s^2 2p^2\ ^3P_0$	54.936
O IV	$1s^2 2s^2 2p\ ^2P_{1/2}$	77.414
O V	$1s^2 2s^2\ ^2S_0$	113.899
O VI	$1s^2 2s\ ^2S_{1/2}$	138.119
O VII	$1s^2\ ^2S_0$	739.327
O VIII	$1s\ ^2S_{1/2}$	871.410
Fe XVII	$1s^2 2s^2 2p^6\ ^1S_0$	1262.7
Fe XXV	$1s^2\ ^2S_0$	8828.188
Fe XXVI	$1s\ ^2S_{1/2}$	9277.689



Lyman limit

Lockman hole ($l \sim 150^\circ, b \sim 52^\circ$)
min. Galactic $N_{\text{H I}} \sim 4.5 \times 10^{19} \text{ cm}^{-2}$

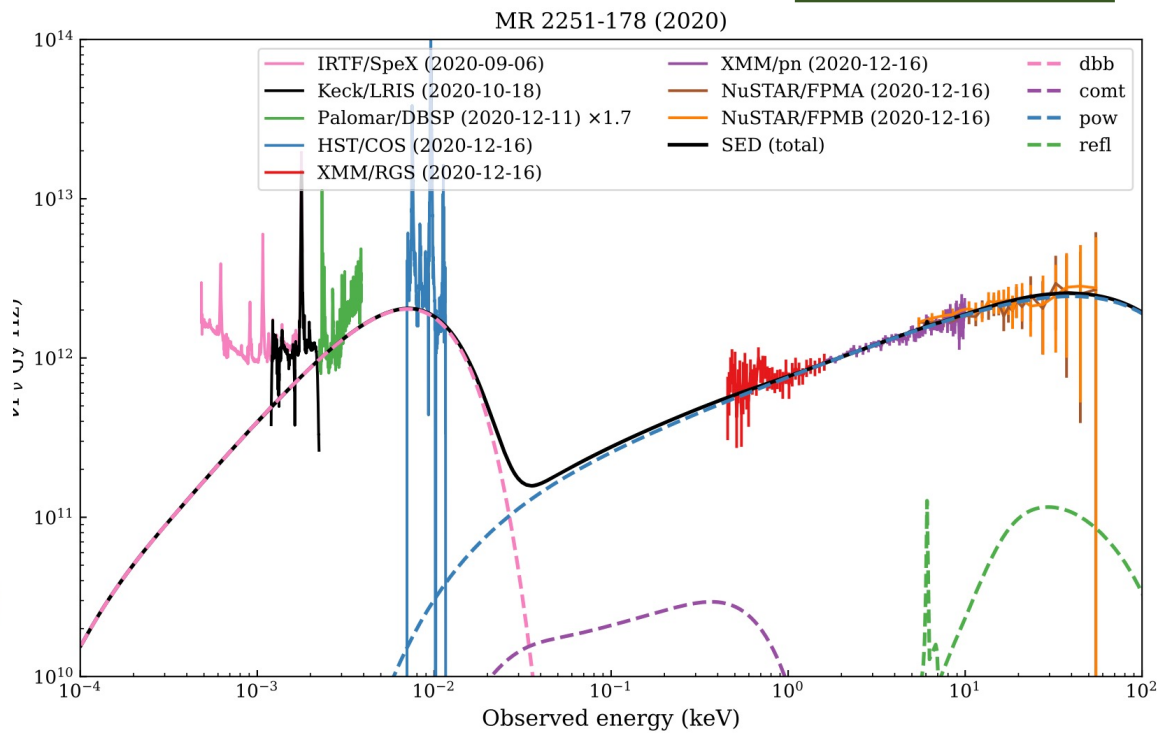
(Lockman et al. 1986)



HI4PI collaboration (2016)

Lyman limit/break

$$912 \text{ \AA} = 13.6 \text{ eV}$$



$$h\nu = 13.6 \text{ eV} + \frac{1}{2}m_e v^2$$



Balmer limit

Ion	Ground level	I_p (eV)
H I	$1s\ ^2S_{1/2}$	13.598
H I	$2p\ ^2P_{1/2}$	3.4

Balmer limit/break/jump/discontinuity

$$3647 \text{ \AA} = 3.4 \text{ eV}$$

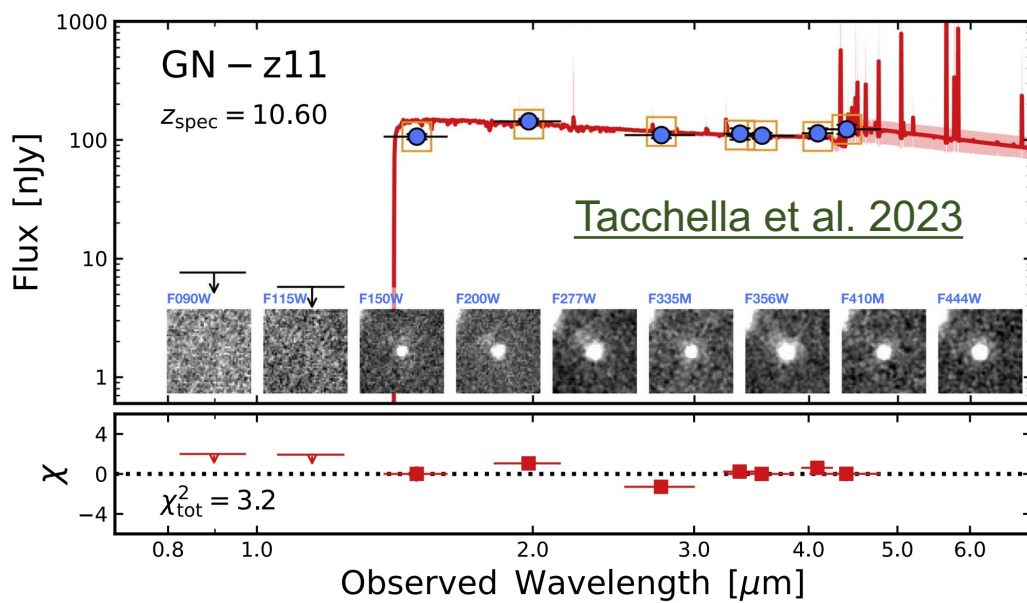
Lyman limit

912 \AA

Balmer limit

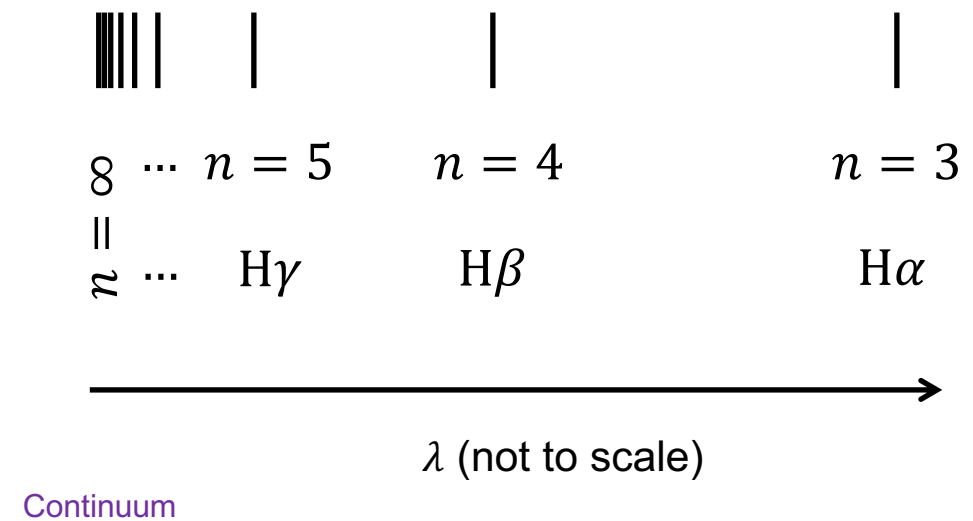
3647 \AA

Ion	Lyman	Wavelength
H I	$H\alpha n = 3 \rightarrow 2$	6562.8 \AA
H I	$H\beta n = 4 \rightarrow 2$	4861.4 \AA
H I	$H\gamma n = 5 \rightarrow 2$	4340.5 \AA
H I	$H\delta n = 6 \rightarrow 2$	4101.7 \AA
H I	$H\epsilon n = 7 \rightarrow 2$	3970.1 \AA
H I
H I	Balmer limit	3646.6 \AA



Balmer limit
@4.23 micron
(redshifted)

Lyman limit
@1.05 micron
(redshifted)



Bohr's radius for hydrogen

The semiclassical Bohr atom consists of a nucleus and electrons moving in circular orbits.

The Bohr radius of the n th shell is n times the De Broglie wavelength of the electron

$$2\pi a_n = n\lambda = n \frac{h}{m_e v}$$

Balancing the Coulomb and centrifugal forces on electrons in circular orbits of hydrogen

$$\frac{e^2}{a_n^2} = \frac{m_e v^2}{a_n}$$

Bohr's radius for hydrogen is

$$a_n = n^2 \frac{h^2}{4\pi^2 m_e e^2} = n^2 5.29 \times 10^{-9} \text{ cm}$$

Bohr radius

$$a_1 = 5.29 \times 10^{-9} \text{ cm}$$

Photoionization cross section (H-like)

The photoionization (bound-free) cross section for H-like ions (e.g., H I, O VIII, Fe XXVI) is ([Kaastra et al. 2008](#))

$$\sigma_n^{\text{PI}} = \frac{64 \pi n \alpha_{\text{fs}} a_1^2}{3\sqrt{3} Z^2} g_{\text{bf}}(E) \left(\frac{I_p}{E}\right)^3$$

$$= 7.90 \times 10^{-18} \frac{n}{Z^2} g_{\text{bf}}(E) \left(\frac{I_p}{E}\right)^3$$

fine structure constant
 $\alpha_{\text{fs}} = \frac{2\pi e^2}{hc} = 7.297 \times 10^{-3} \sim \frac{1}{137}$

principle quantum number
 atomic number

bound-free Gaunt factor
[\(Karzas & Latter 1961\)](#)

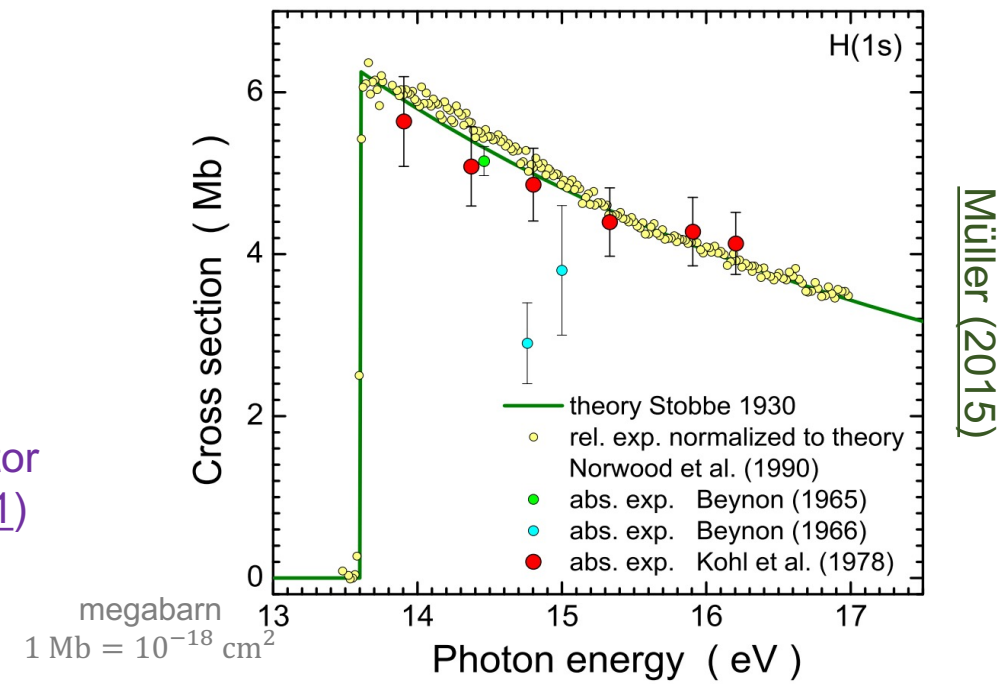
Above the ionization energy ($E > I_p$), the PI cross section decreases with increasing photon energy

classical electron radius

$$r_0 = \frac{e^2}{m_e c^2} = 2.72 \times 10^{-13} \text{ cm}$$

Bohr radius

$$a_1 = 5.29 \times 10^{-9} \text{ cm} = \frac{r_0}{\alpha_{\text{fs}}^2}$$

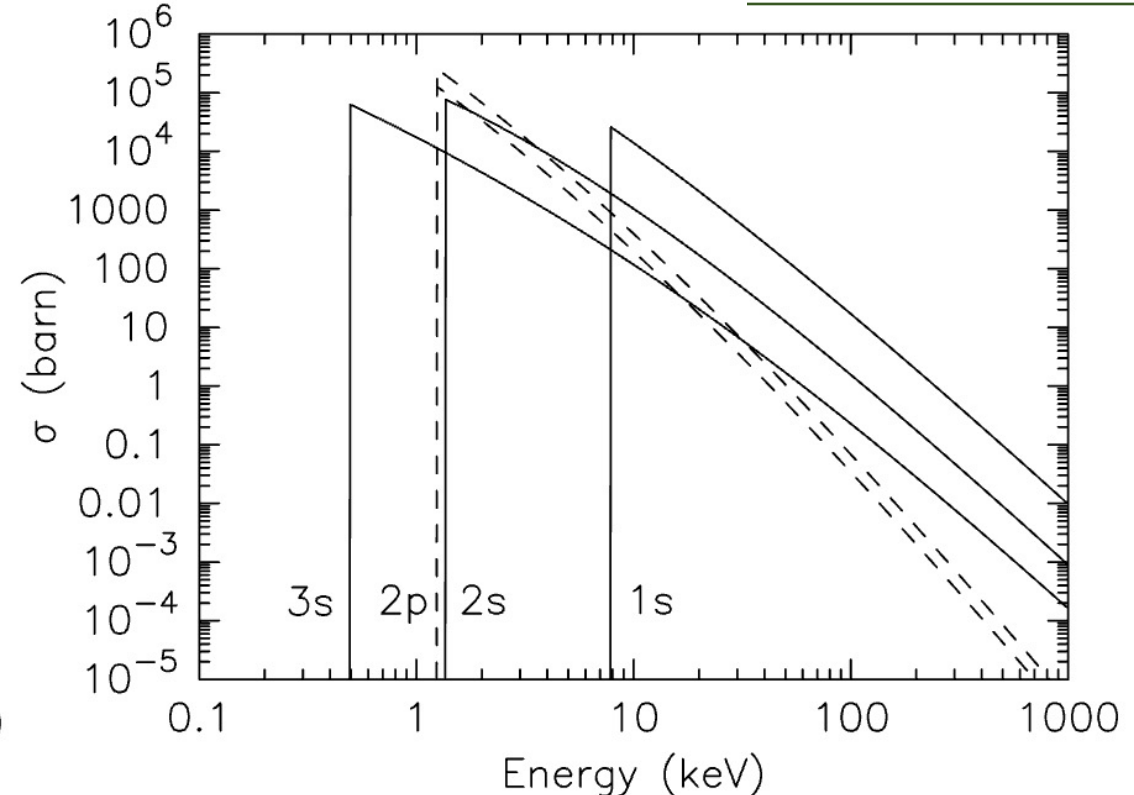
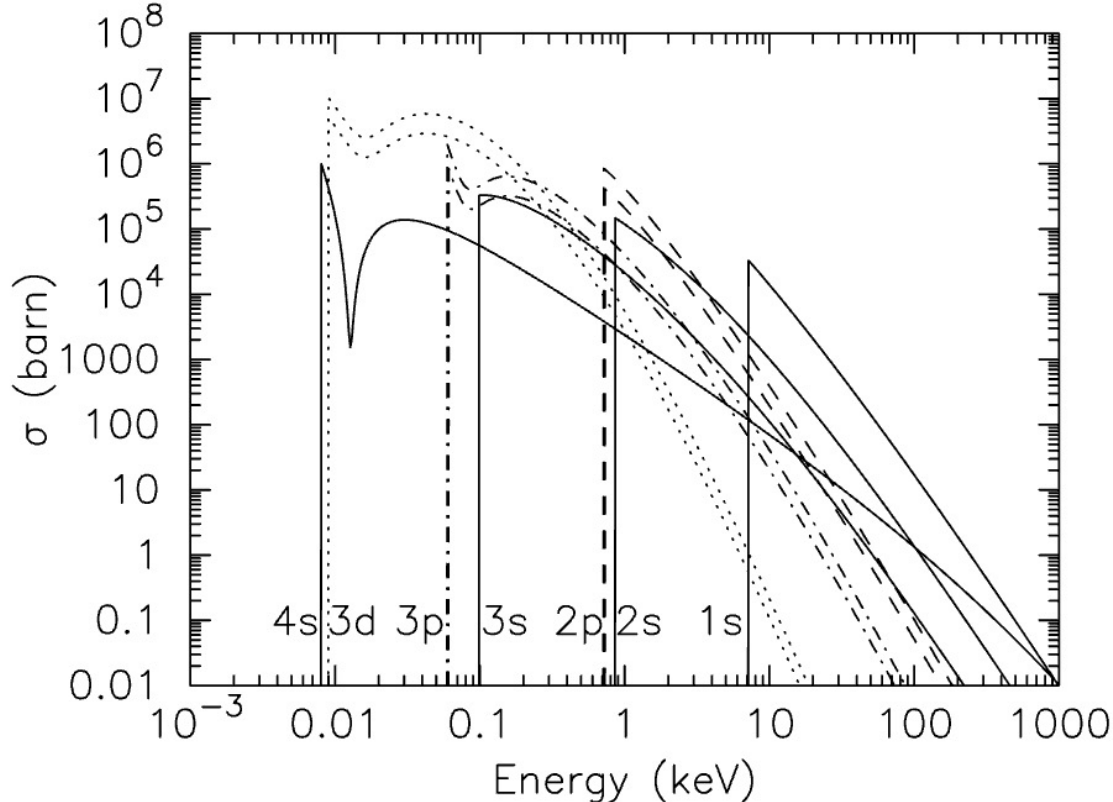


Photoionization cross section (other ions)

The photoionization (bound-free) cross section for other ions might be more complicated than a simple power law (e.g., Fe I in the left and Fe VI in the right).

$$1 \text{ b} = 10^{-24} \text{ cm}^2$$

Kaastra et al. 2008



Generally speaking, above the ionization energy ($E > I_p$), the PI cross section **decreases** with **increasing** photon energy

Saha equation

Previously, we use the Boltzmann distribution to describe the level population of an ion. To determine the distribution of an element among its various ionization degrees, we need the Saha equation for thermodynamic equilibrium plasma

Starting with the generalization of the Boltzmann distribution

$$\frac{dn_{i+1,0}(v)}{dn_{i,0}} = \frac{g_{i+1,0} g_e}{g_{i,0}} \exp\left(-\frac{I_p + \frac{1}{2}m_e v^2}{kT_e}\right)$$

$g_{i+1,0}$ and $g_{i,0}$ statistical weights of the ground states of X^{i+} and X^{i+1} , respectively

$$g_e = \frac{8\pi m_e^3 v^2 dv}{n_e h^3}$$

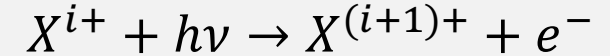
statistical weight of electron

see Sect. 9.5 of the REF book (p260-262) by Rybicki & Lightman

Integrate over all velocity (v)

$$\frac{n_{i+1,0} n_e}{n_{i,0}} = \frac{8\pi m_e^3}{h^3} \frac{g_{i+1,0}}{g_{i,0}} \exp\left(-\frac{I_p}{kT_e}\right) \int_0^\infty \exp\left(-\frac{m_e v^2}{2kT_e}\right) v^2 dv$$

[prev. sl.](#)



Sect. 5.2.2

$$\frac{n_l}{n_u} = \frac{g_l}{g_u} \exp\left(\frac{E_u - E_l}{kT}\right)$$

Saha equation for ground states

prev. sl.

$$\frac{n_{i+1,0} n_e}{n_{i,0}} = \frac{8\pi m_e^3}{h^3} \frac{g_{i+1,0}}{g_{i,0}} \exp\left(-\frac{I_p}{kT_e}\right) \int_0^\infty \exp\left(-\frac{m_e v^2}{2kT_e}\right) v^2 dv$$

$$x^2 = \frac{m_e v^2}{2kT_e}$$

$$\frac{n_{i+1,0} n_e}{n_{i,0}} = \frac{8\pi m_e^3}{h^3} \frac{g_{i+1,0}}{g_{i,0}} \exp\left(-\frac{I_p}{kT_e}\right) \left(\frac{2kT_e}{m_e}\right)^{3/2} \int_0^\infty \exp(-x^2) x^2 dx$$

$$dv = \left(\frac{2kT_e}{m_e}\right)^{1/2} x dx$$

$$\int_0^\infty \exp(-x^2) x^2 dx = \frac{\sqrt{\pi}}{4}$$

Saha equation for the ground states

$$\frac{n_{i+1,0} n_e}{n_{i,0}} = \left(\frac{2\pi m_e k T_e}{h^2}\right)^{3/2} \frac{2g_{i+1,0}}{g_{i,0}} \exp\left(-\frac{I_p}{kT_e}\right)$$

Saha equation

Saha equation for the ground states

$$\frac{n_{i+1,0} n_e}{n_{i,0}} = \left(\frac{2\pi m_e k T_e}{h^2} \right)^{3/2} \frac{2g_{i+1,0}}{g_{i,0}} \exp\left(-\frac{I_p}{k T_e}\right)$$

To obtain the number of ion/atoms in any atomic state via the Boltzmann laws

Saha equation

$$\frac{n_{i+1} n_e}{n_i} = \left(\frac{2\pi m_e k T_e}{h^2} \right)^{3/2} \frac{2U_{i+1}(T_e)}{U_i(T_e)} \exp\left(-\frac{I_p}{k T_e}\right)$$

Boltzmann law: population of level j (with level energy: E_j) for ion X^i

$$n_{i,j} = \frac{n_i}{U_i(T_e)} g_j \exp\left(-\frac{E_j}{k T_e}\right)$$

partition function

$$U(T_e) = \sum_j g_j \exp\left(-\frac{E_j}{k T_e}\right)$$

$$n_i = \sum_j n_{i,j}$$

see Sect. 9.5 of the REF book
(p259-260) by Rybicki & Lightman

$$\frac{n_{i,0}}{n_i} = \frac{g_{i,0}}{U_i(T_e)}$$

$$\frac{n_{i+1,0}}{n_{i+1}} = \frac{g_{i+1,0}}{U_{i+1}(T_e)}$$

Saha equation for hydrogen

Saha equation for the ground states

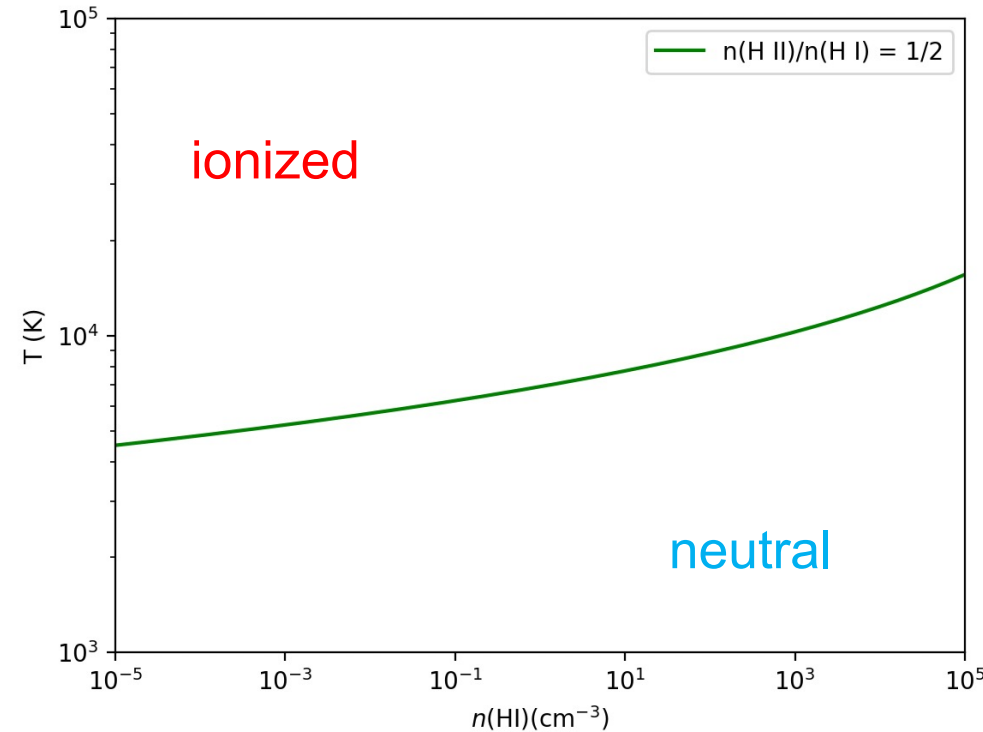
$$\frac{n_{i+1,0} n_e}{n_{i,0}} = \left(\frac{2\pi m_e k T_e}{h^2} \right)^{3/2} \frac{2g_{i+1,0}}{g_{i,0}} \exp \left(-\frac{I_p}{k T_e} \right)$$

For $T \lesssim 10^4$ K, we only need to consider ground states of hydrogen with $I_p = 13.6$ eV

$$n_{i+1,0} = n(\text{H II}) = n_e \quad g_{i+1,0} = g(\text{H II } ^1\text{S}_0) = 1$$

$$n_{i,0} = n(\text{H I}) \quad g_{i,0} = g(\text{H I } ^2\text{S}_{1/2}) = 2$$

$$n(\text{H I}) = 4.83 \times 10^{15} \left(\frac{\text{K}}{T_e} \right)^{3/2} \exp \left(-\frac{1.58 \times 10^5}{(T_e/\text{K})} \right)$$



half-ionization fraction

$$\frac{n(\text{H II})}{n(\text{H I})} = \frac{1}{2}$$

Detailed balance for PI and RR

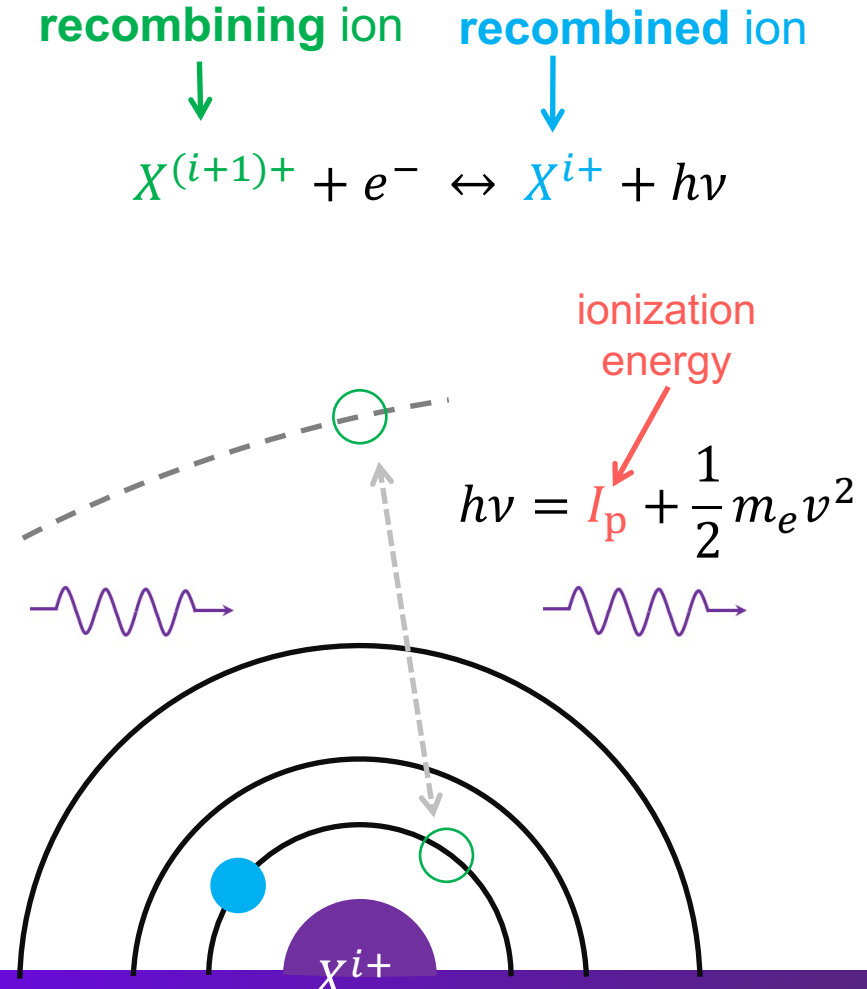
The radiative recombination cross section σ^{RR} can be derived from the photoionization cross section σ^{PI} under the detailed balance principle ([Milne 1924](#))

The rate of recombination to the ground state of X^{i+} in an electron velocity range $d\nu$ per unit volume is

$$n_{i+1,0} n_e \sigma^{\text{RR}}(\nu) f(\nu) d\nu$$

The rate of photoionization from the ground state of X^{i+} in an photon frequency range $d\nu$ for a blackbody radiation field is

$$\frac{4\pi}{h\nu} n_{i,0} \sigma^{\text{PI}}(\nu) \left(1 - \exp\left(-\frac{h\nu}{kT_e}\right)\right) B_\nu(T_e) d\nu$$



Detailed balance for PI and RR (cont.)

Equating the rate of recombination and photoionization

$$n_{i+1,0} n_e \sigma^{\text{RR}}(\nu) \nu f(\nu) d\nu = \frac{4\pi}{h\nu} n_{i,0} \sigma^{\text{PI}}(\nu) \left(1 - \exp\left(-\frac{h\nu}{kT_e}\right)\right) B_\nu(T_e) d\nu$$

$$\frac{\sigma^{\text{PI}}(\nu)}{\sigma^{\text{RR}}(\nu)} = \frac{n_{i+1,0} n_e}{n_{i,0}} \nu f(\nu) \left(\frac{h\nu}{4\pi}\right) \left(1 - \exp\left(-\frac{h\nu}{kT_e}\right)\right)^{-1} B_\nu^{-1} \frac{d\nu}{d\nu}$$

$$\frac{d\nu}{d\nu} = \frac{h}{m_e \nu}$$

$$\begin{aligned} &= \frac{n_{i+1,0} n_e}{n_{i,0}} \exp\left(\frac{h\nu}{kT_e}\right) \frac{f(\nu) \ h c^2}{8\pi m_e \nu^2} \\ &= \frac{n_{i+1,0} n_e}{n_{i,0}} \exp\left(\frac{I_p}{kT_e}\right) \frac{h c^2 \nu^2}{2 m_e \nu^2} \left(\frac{m_e}{2\pi kT_e}\right)^{3/2} \end{aligned}$$

Planck's spectrum

$$B_\nu(T) = \frac{2h\nu^3}{c^2} \left(\exp\left(\frac{h\nu}{kT}\right) - 1 \right)^{-1}$$

Maxwell velocity distribution

$$f(\nu) d\nu = 4\pi \left(\frac{m_e}{2\pi kT_e}\right)^{3/2} \nu^2 \exp\left(-\frac{m_e \nu^2}{2kT_e}\right)$$

Milne relation

prev. sl.

$$\frac{\sigma^{\text{PI}}(\nu)}{\sigma^{\text{RR}}(\nu)} = \frac{n_{i+1,0} n_e}{n_{i,0}} \exp\left(\frac{I_p}{kT_e}\right) \frac{hc^2 \nu^2}{2 m_e \nu^2} \left(\frac{m_e}{2\pi k T_e}\right)^{3/2}$$

prev. sl.

$$\frac{n_{i+1,0} n_e}{n_{i,0}} = \left(\frac{2\pi m_e k T_e}{h^2}\right)^{3/2} \frac{2g_{i+1,0}}{g_{i,0}} \exp\left(-\frac{I_p}{kT_e}\right)$$

$$\frac{\sigma^{\text{PI}}(\nu)}{\sigma^{\text{RR}}(\nu)} = \left(\frac{2\pi m_e k T_e}{h^2}\right)^{3/2} \frac{2g_{i+1,0}}{g_{i,0}} \frac{hc^2 \nu^2}{2 m_e \nu^2} \left(\frac{m_e}{2\pi k T_e}\right)^{3/2}$$

Milne relation

$$\frac{\sigma^{\text{PI}}(\nu)}{\sigma^{\text{RR}}(\nu)} = \frac{g_{i+1,0}}{g_{i,0}} \frac{m_e^2 c^2 \nu^2}{h^2 \nu^2}$$

The radiative recombination cross section can be derived from the photoionization cross section $\sigma^{\text{PI}}(E)$ under the detailed balance principle ([Milne 1924](#))

Radiative recombination data

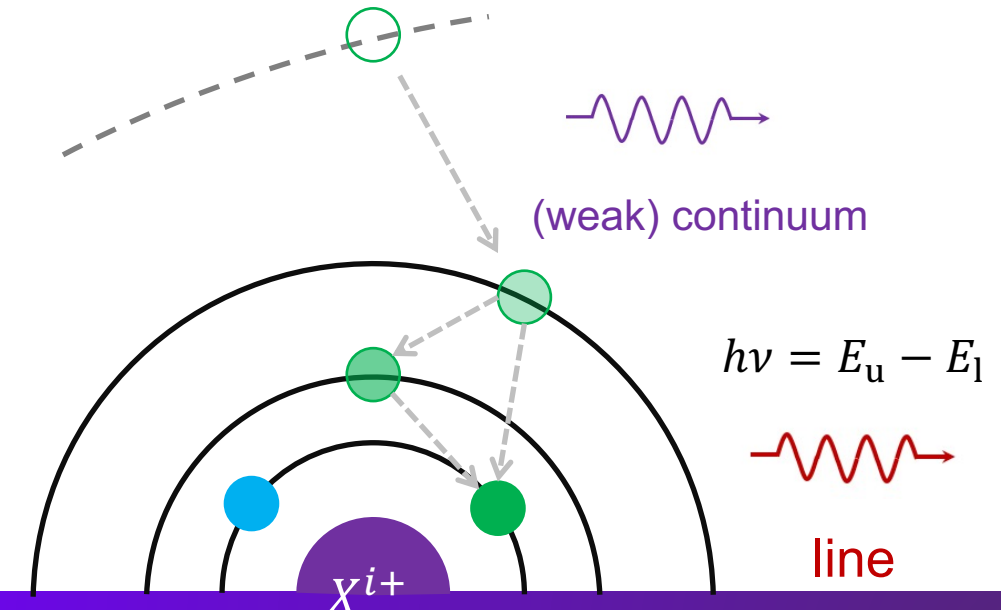
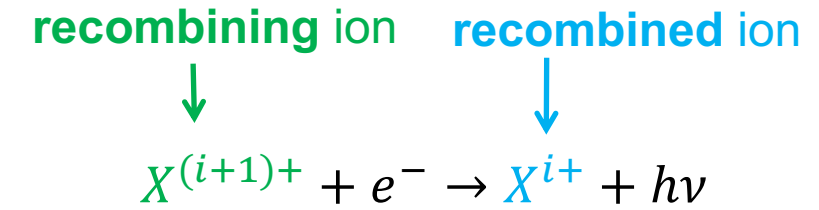
$$\alpha_i = \int_0^\infty \nu f(\nu) \sigma^{\text{RR}}(\nu) d\nu$$

RR rate coefficient of
recombining/recombing ion:
 n –resolved
 nl –resolved
level-resolved for line emission

Total RR rate (per ion) for ionization balance

$$\alpha_i(T_e) = \sum \alpha_i(T_e, n - \text{resolved})$$

RR rate coefficient is in units of $\text{cm}^3 \text{ s}^{-1}$ (cgs)



RR rate coefficient (H-like, n -resolved)

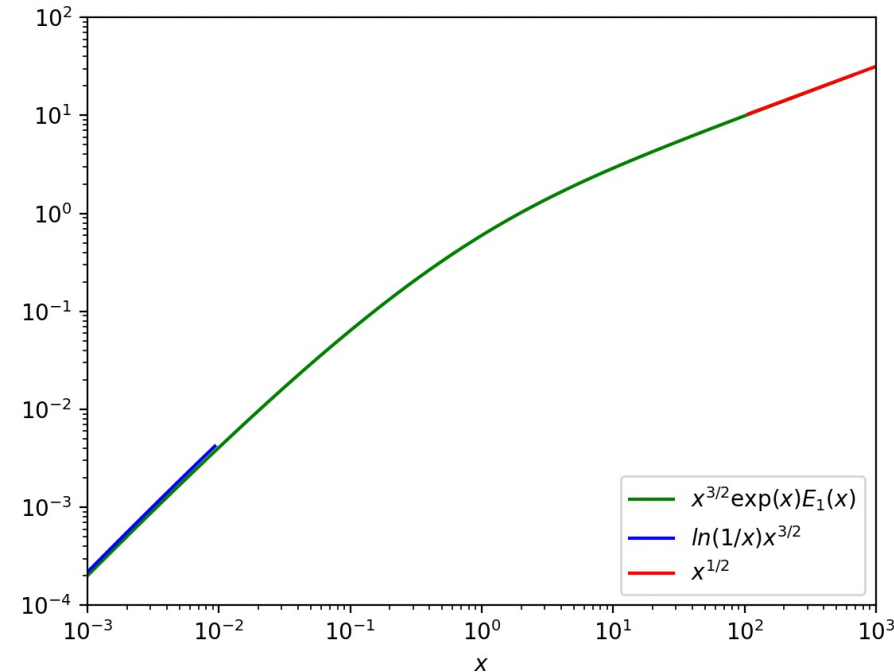
For H-like ions, the n –resolved RR rate coefficient is

$$\alpha_i(n, T_e) = \frac{128 \sqrt{2\pi} n^3 \alpha_{fs} a_1^2 I_p^3 \exp\left(\frac{I_p}{kT_e}\right)}{3\sqrt{3 m_e kT_e} Z^2 kT_e m_e c^3} E_1\left(\frac{I_p}{kT_e}\right)$$

$$= \frac{128 \sqrt{2\pi} n^3 \alpha_{fs} a_1^2 I_p^{3/2}}{3\sqrt{3 m_e} Z^2 m_e c^3} x^{3/2} \exp(x) E_1(x)$$

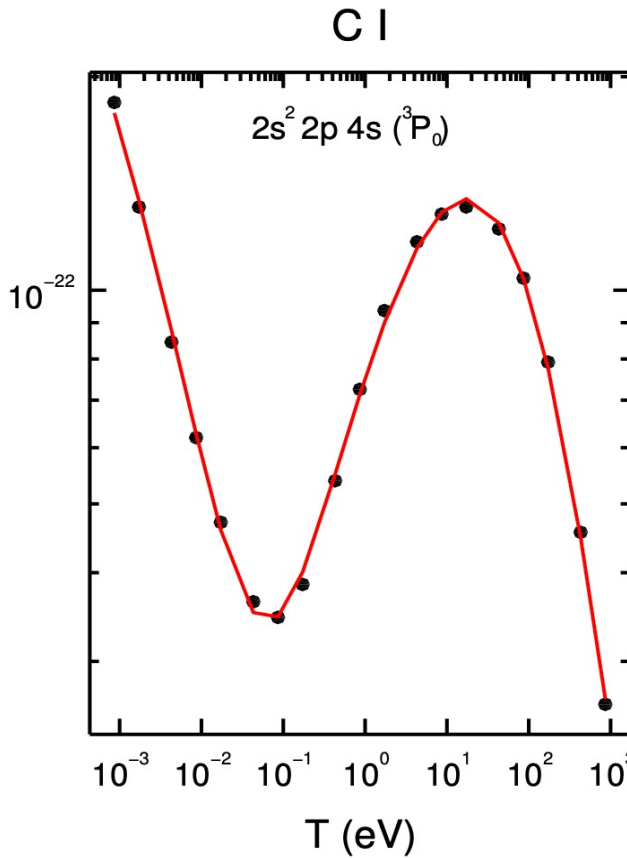
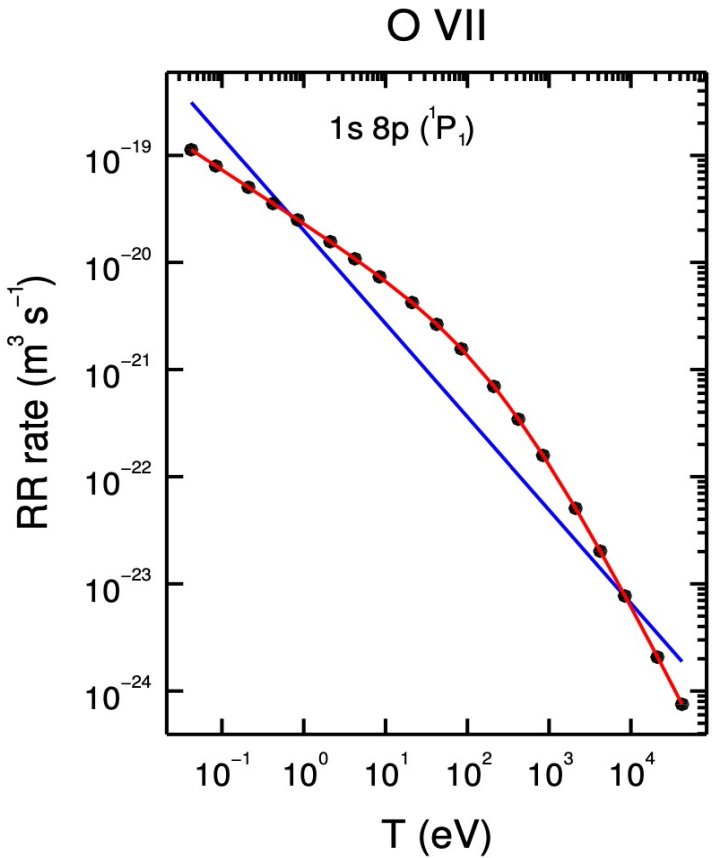
$$E_1(x) = \int_x^\infty \frac{\exp(-t)}{t} dt \quad x = \frac{I_p}{kT_e} \quad \text{Kaastra et al. 2008}$$

see also Sect. 10.5 of the REF book
(p286) by Rybicki & Lightman



- ❖ At low temperatures with $kT_e \ll I_p$ ($x \ll 1$), $\alpha_i \sim T_e^{-\frac{1}{2}}$
- ❖ At high temperatures with $kT_e \gg I_p$ ($x \gg 1$), $\alpha_i \sim \log(kT_e/I_p) T_e^{-3/2}$

RR rate coefficient (level-resolved)



Kaastra et al. 2017, Mao & Kaastra (2016),
Badnell (2006), Mewe (1980)

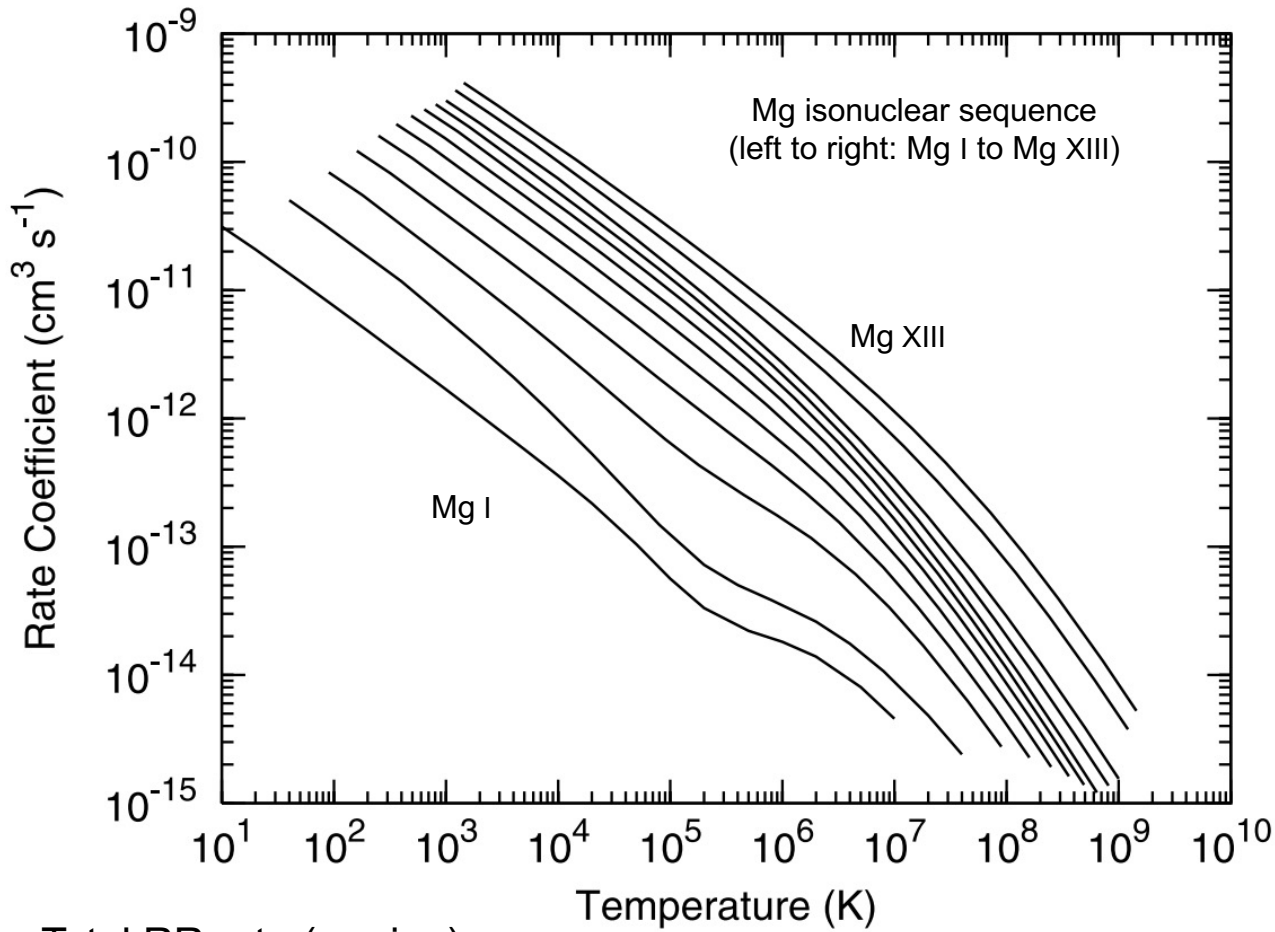
The exact RR rate coefficient is more complicated. The following parameterization can well represent most of the RR rate coefficient (n -resolved and level-resolved) and total rate (per ion):

$$\frac{\alpha(T_e)}{10^{-10} \text{ cm}^3 \text{ s}^{-1}} = a_0 T_e^{-b_0 - c_0 \ln T} \left(\frac{1 + a_2 T_e^{-b_2}}{1 + a_1 T_e^{-b_1}} \right)$$

Mao & Kaastra (2016)

Generally speaking, RR rate coefficients decrease with increasing electron temperature.

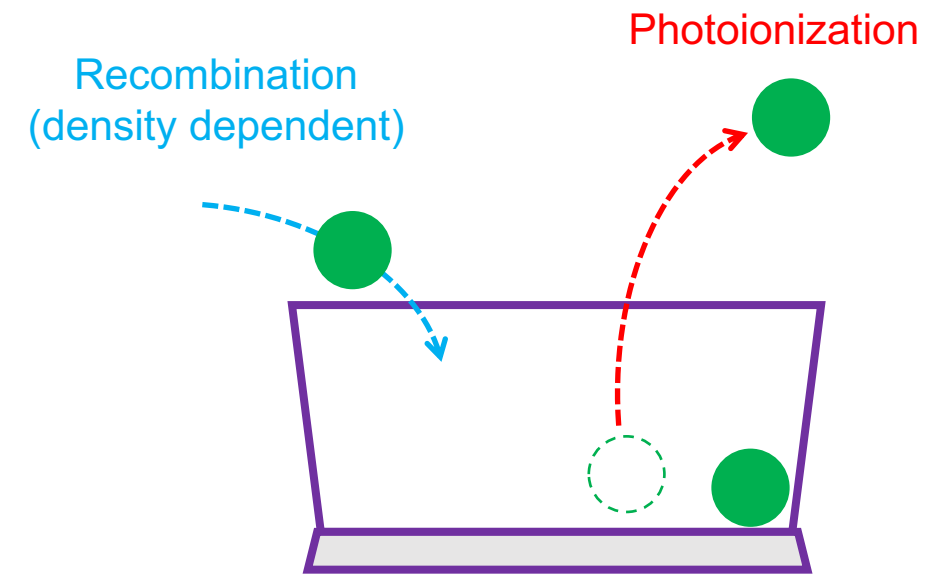
Total RR rate (per ion)



Total RR rate (per ion)

$$\alpha_i(T_e) = \sum_n \alpha_i(T_e, n - \text{resolved})$$

Badnell (2006)



the **higher** the number density,
the **faster** it recombines.

$$t_{\text{rec}} = \frac{1}{n_e \alpha_i(T_e)}$$

Electron energy loss rate due to RR

RR electron energy loss rate coefficient is defined as (Osterbrock & Ferland 2006)

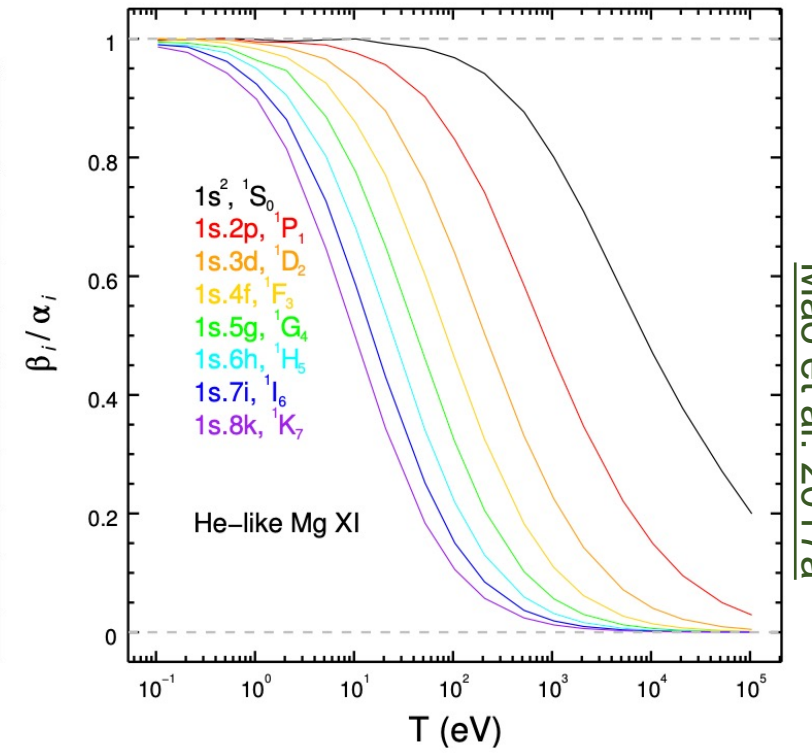
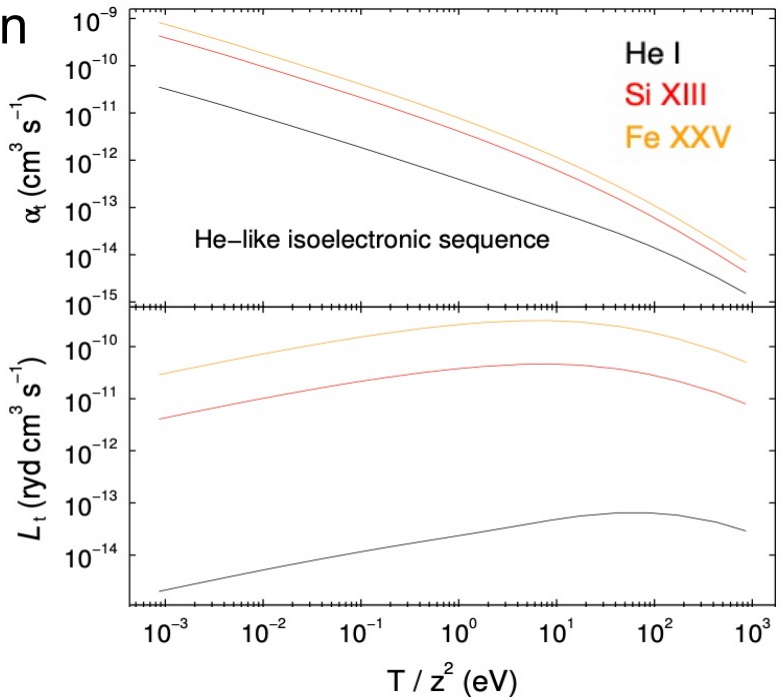
$$\beta_i = \frac{1}{kT_e} \int_0^\infty \frac{1}{2} m_e v^3 f(v) \sigma^{\text{RR}}(v) dv$$

prev. sl.

$$\alpha_i = \int_0^\infty v f(v) \sigma^{\text{RR}}(v) dv$$

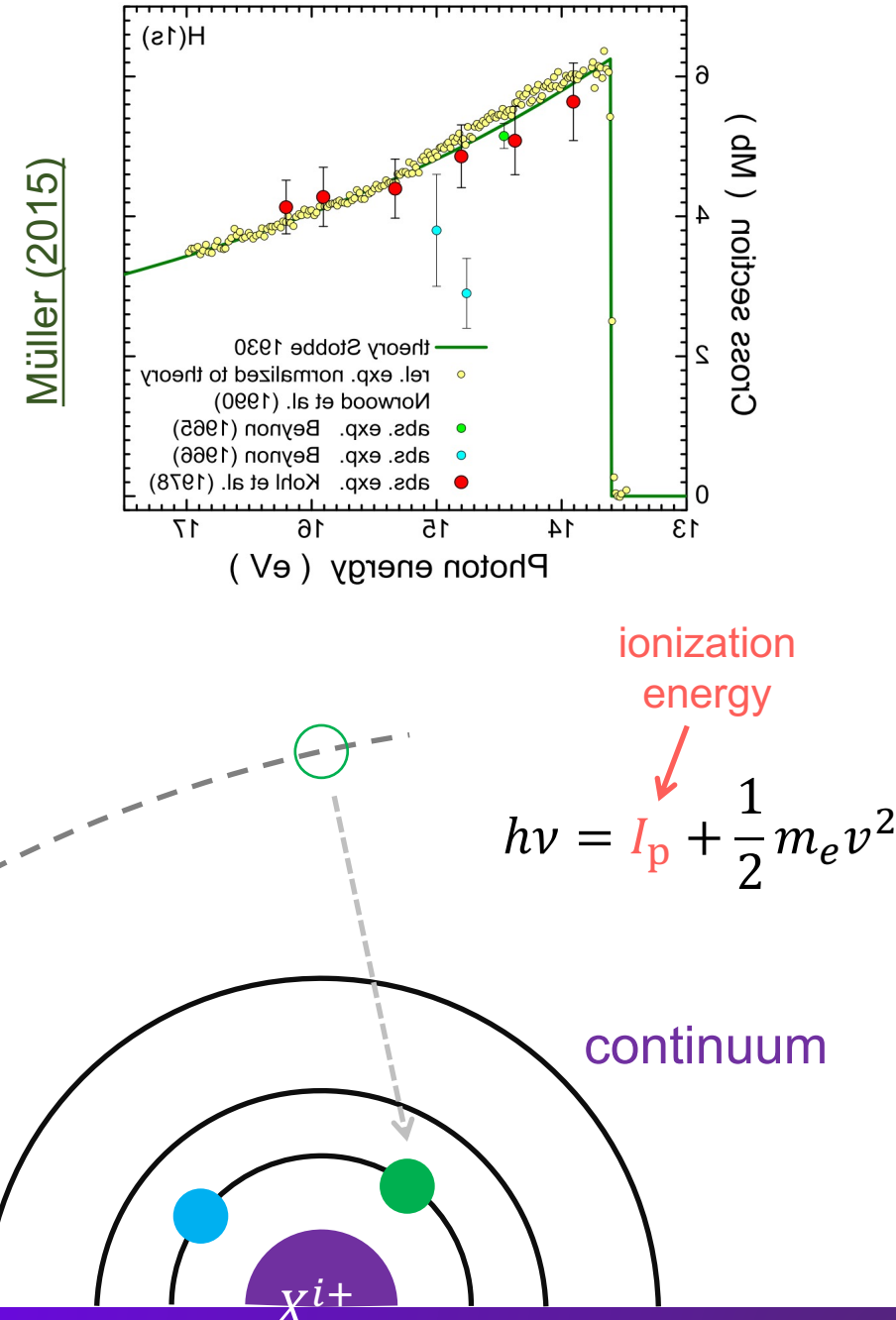
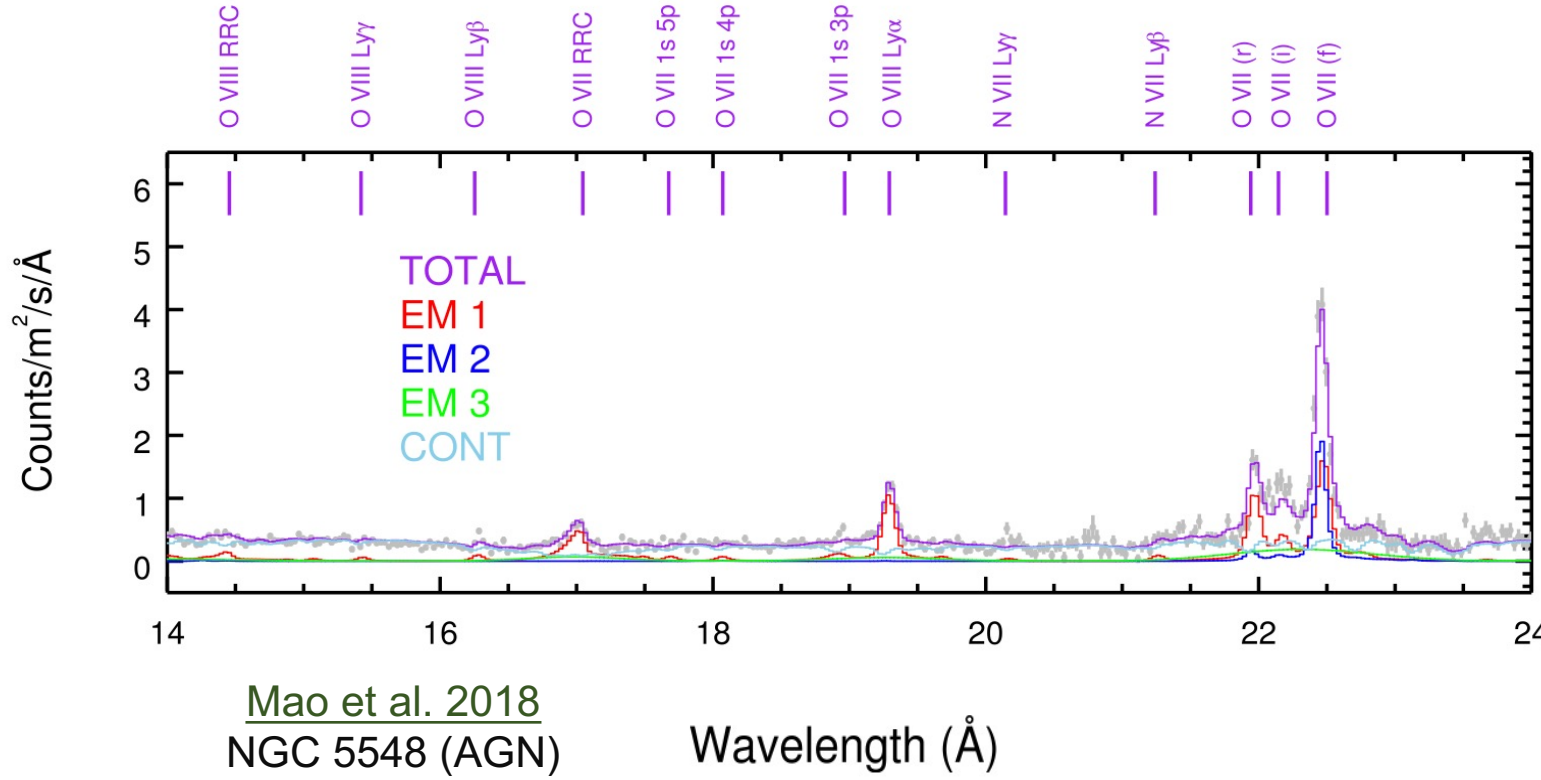
RR electron energy loss rate is then

$$L_i = kT_e \beta_i = kT_e \alpha_i \frac{\beta_i}{\alpha_i}$$



Radiative recombination continuum

Since the kinetic energy of the free electron is not quantized, the emitted photons form a continuous spectrum with sharp edges at the ionization energy of the level that the free electrons are captured into.



RRC spectral shape

RRC radiative power per unit photon energy
is given by ([Smith & Brickhouse 2002](#))

$$\frac{dP(E)}{dE} = n_e n_{i+1} E \sigma^{\text{RR}}(\nu) \nu f(\nu) \frac{d\nu}{dE}$$

$$\frac{d\nu}{dE} = \frac{1}{m_e \nu}$$

$$= n_e n_{i+1} E \frac{g_{i,0}}{g_{i+1,0}} \frac{E^2}{m_e^2 c^2 \nu^2} \sigma^{\text{PI}}(E) \nu 4\pi \left(\frac{m_e}{2\pi k T_e} \right)^{3/2} \nu^2 \exp\left(-\frac{m_e \nu^2}{2k T_e}\right) \frac{1}{m_e \nu}$$

$$= n_e n_{i+1} \frac{g_{i,0}}{g_{i+1,0}} E^3 \sigma^{\text{PI}}(E) \frac{4\pi}{c^2} \left(\frac{1}{2m_e \pi k T_e} \right)^{3/2} \exp\left(-\frac{E - I_p}{k T_e}\right)$$

Maxwell velocity distribution

$$f(\nu) d\nu = 4\pi \left(\frac{m_e}{2\pi k T_e} \right)^{3/2} \nu^2 \exp\left(-\frac{m_e \nu^2}{2k T_e}\right)$$

Milne relation

$$\frac{\sigma^{\text{PI}}(E)}{\sigma^{\text{RR}}(\nu)} = \frac{g_{i+1,0}}{g_{i,0}} \frac{m_e^2 c^2 \nu^2}{E^2}$$

RRC temperature diagnostics

prev. sl.

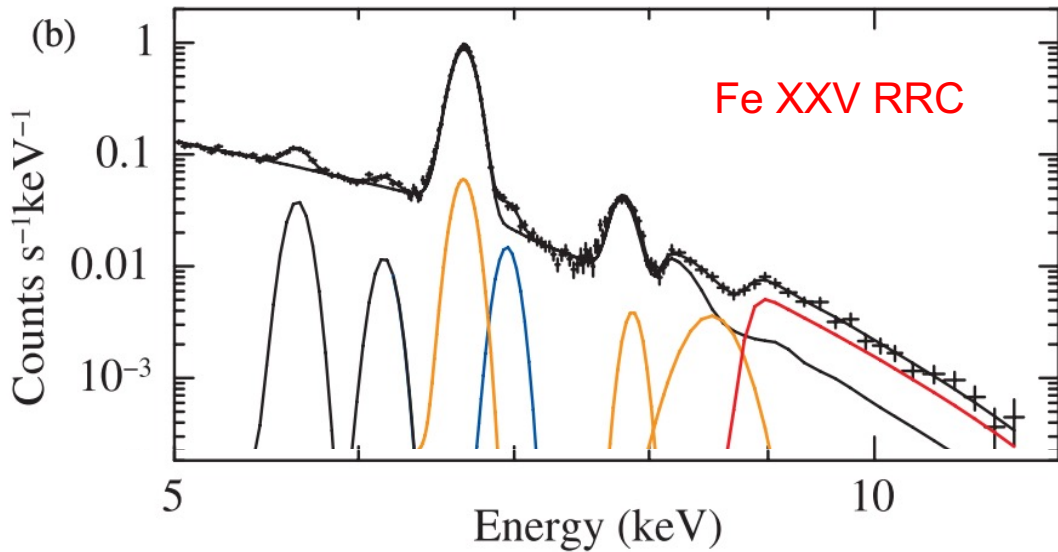
$$\frac{dP(E)}{dE} \propto \exp\left(-\frac{E - I_p}{kT_e}\right)$$

Ion	Ground level	I_p (eV)	λ (Å)
O VII	$1s^2 \ ^2S_0$	739.327	16.77
Fe XXV	$1s^2 \ ^2S_0$	8828.188	1.40

the **broader** the RRC, the **hotter** the electron temperature

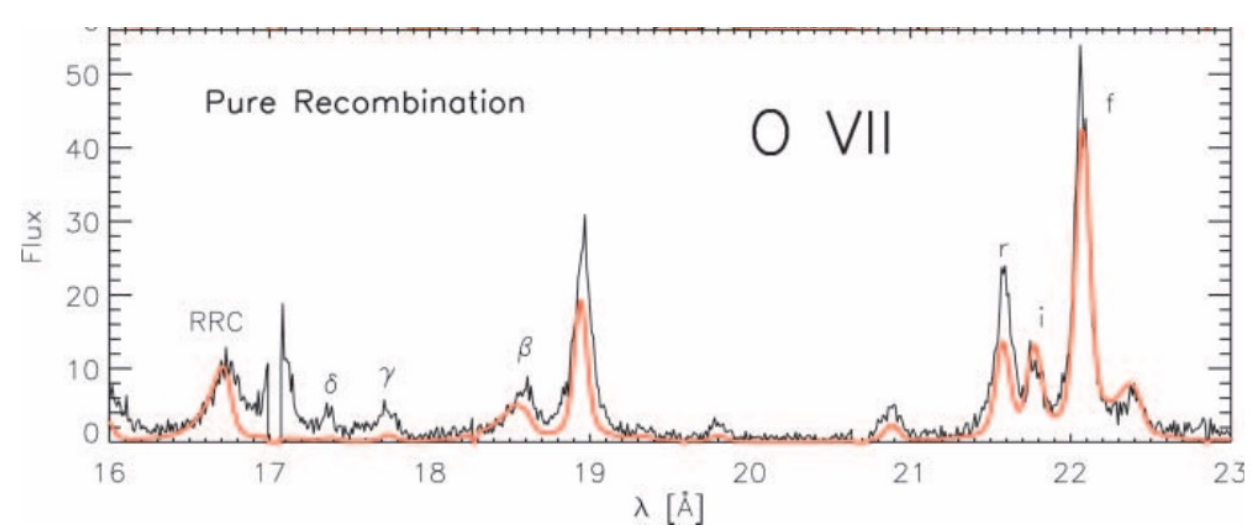
Ozawa et al. 2009

W49B (SNR, $kT_e = 1.52$ keV)



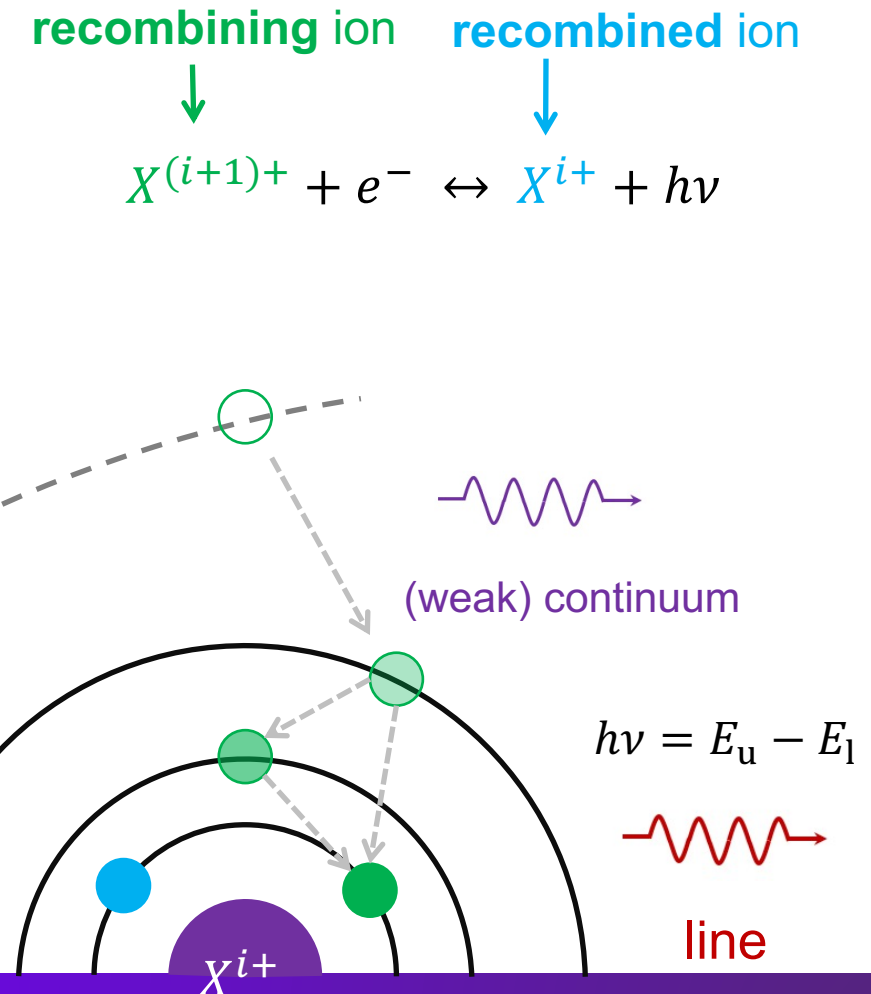
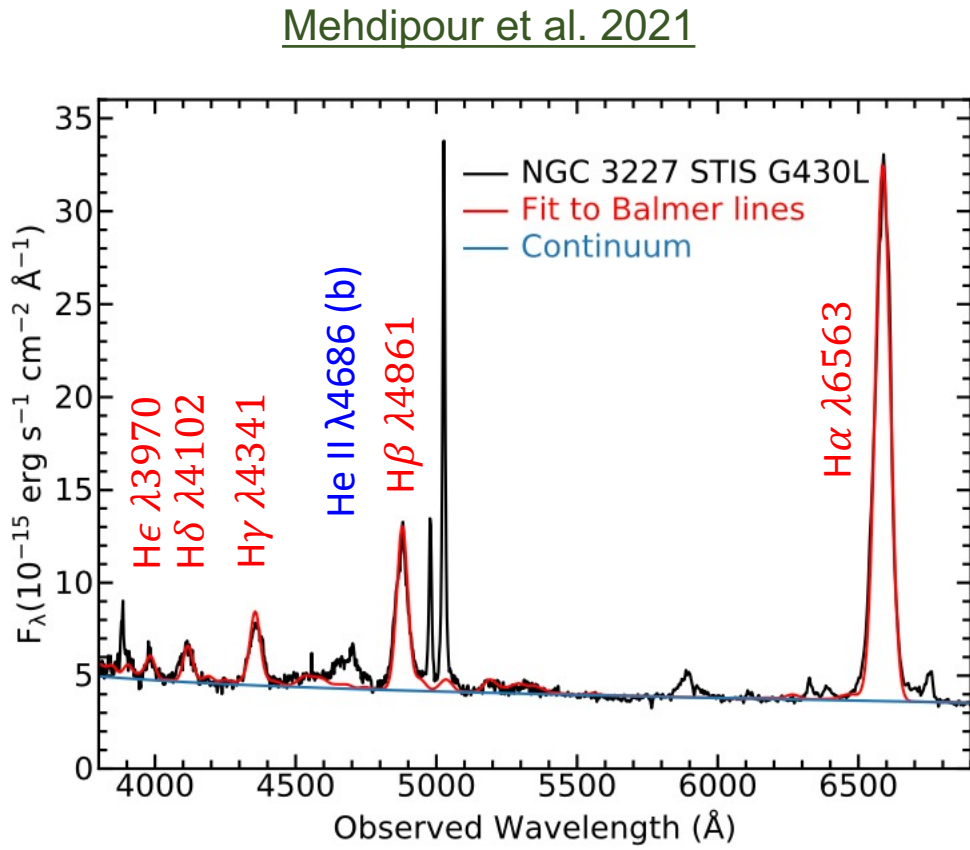
Kinkhabwala et al. 2002

NGC 1068 (AGN, $kT_e = 2.5$ eV)



Recombination lines

After capturing into the excited levels via **radiative recombination**, electrons can **cascade** down to the ground state, giving rise to the so-called **recombination lines** (e.g., Balmer lines)

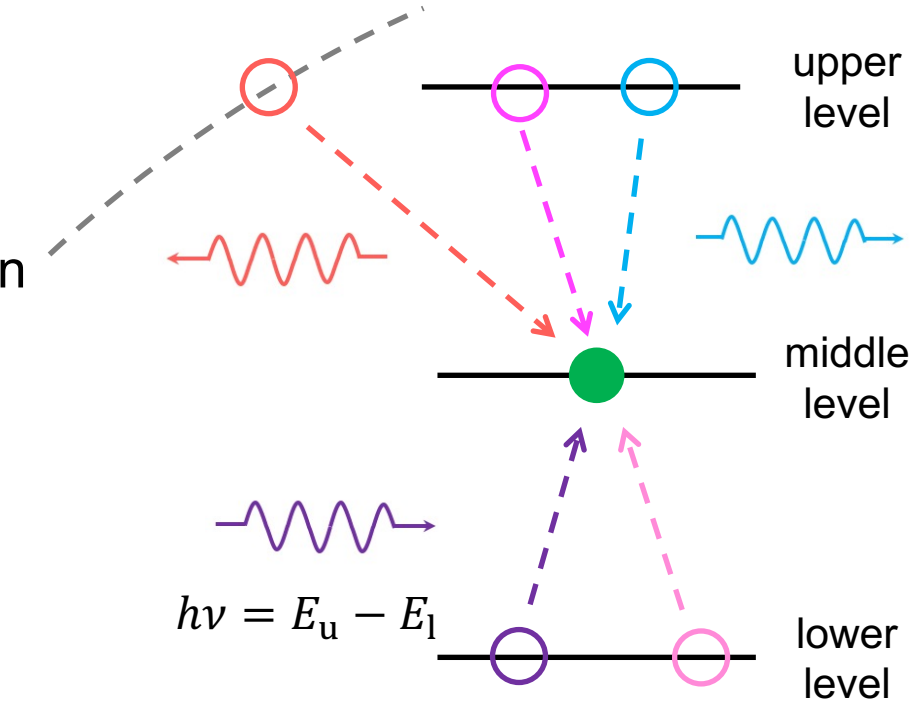


Level population for recombination lines

The middle level of ion X^{i+} is populated via (1) radiative recombination, (2) cascade from upper levels; (3) photo-excitation from lower levels; (4) collisional de-excitation from upper levels, (5) collisional excitation from lower levels, etc.

$$n_e n_{i+1,0} \alpha_{i,m}(T_e) + \sum_{u>m} n_{i,u} A_{um} + \sum_{l<m} n_{i,l} B_{lm} \langle I(v) \rangle \\ + \sum_{u>m} n_e n_{i,u} C_{um} + \sum_{l<m} n_e n_{i,l} C_{lm}$$

To simplify the case, we ignore collisional excitation and de-excitation here



Sect. 5.2.1.2

$$\langle I_\nu \rangle = \int \frac{d\Omega}{4\pi} \int I_\nu \phi(\nu) d\nu$$

Case A and B

Furthermore, in the absence of strong external radiation field, photo-excitation can also be simplified as the following two cases ([Baker et al. 1938](#))

If the medium is **optically thin** to Lyman transitions (**Case A**), the level population balance is reduced to

$$n_e n_{i+1,0} \alpha_{i,m}(T_e) + \sum_{u>m} n_{i,u} A_{um} = \sum_{l<m} n_{i,m} A_{ml}$$

In equilibrium, the level population is balanced out

If the medium is **optically thick** to Lyman transitions (**Case B**), the level population is

$$n_e n_{i+1,0} \alpha_{i,m}(T_e) + \sum_{u>m} n_{i,u} A_{um} + n_{i,0} B_{Ly} \langle I_{Ly} \rangle = \sum_{l<m} n_{i,m} A_{ml}$$

$$n_{i,0} B_{Ly} \langle I_{Ly} \rangle = n_{i,m} A_{m0}$$

$$n_e n_{i+1,0} \alpha_{i,m}(T_e) + \sum_{u>m} n_{i,u} A_{um} = \sum_{1 \leq l < m} n_{i,m} A_{ml}$$

(starting from level #0)

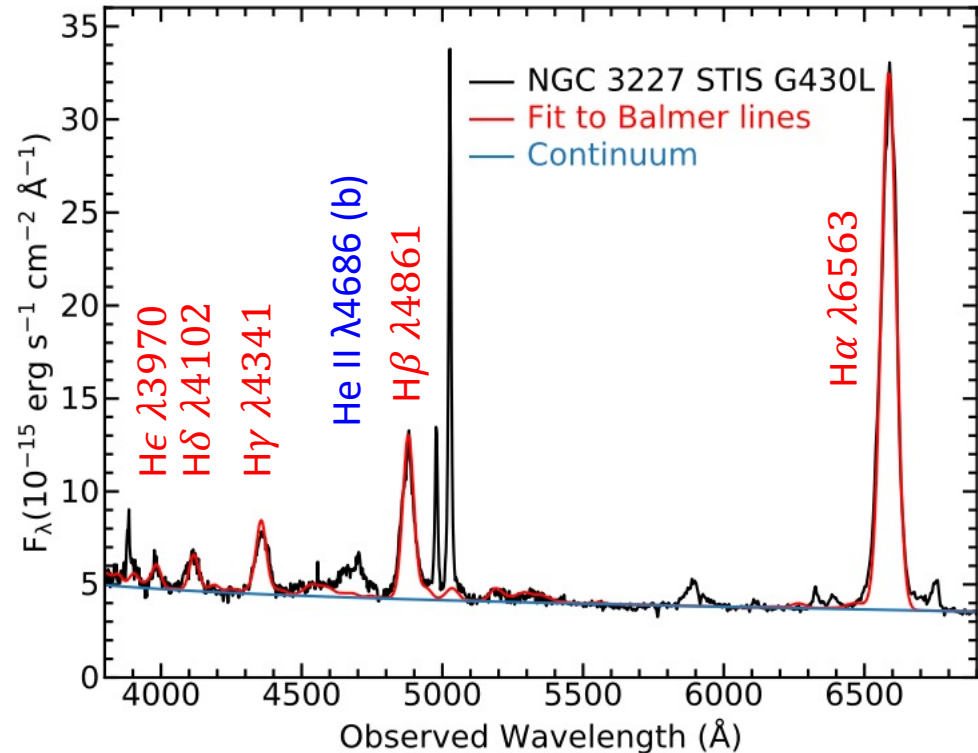
Case A and B

Case A: the medium is optically thin to Lyman transitions

- ✓ no Lyman absorptions
- ✓ rare (ideal)

Case B: the medium is optically thick to Lyman transitions

- ✓ Lyman transition photons are absorbed, scattered, and even destroyed
- ❖ **Balmer decrement:** Balmer line ratios of the same element mainly determined by atomic physics (weakly on T_e)
- ❖ common (practice)



T_e	2500 K	5000 K	10^4 K	2×10^4 K
H α /H β	3.30	3.05	2.87	2.76
H γ /H β	0.444	0.451	0.466	0.474
H δ /H β	0.241	0.249	0.256	0.262
H ϵ /H β	0.147	0.153	0.158	0.162

H I recombination lines in the Case B, low-density limit
(Osterbrock & Ferland 2006)

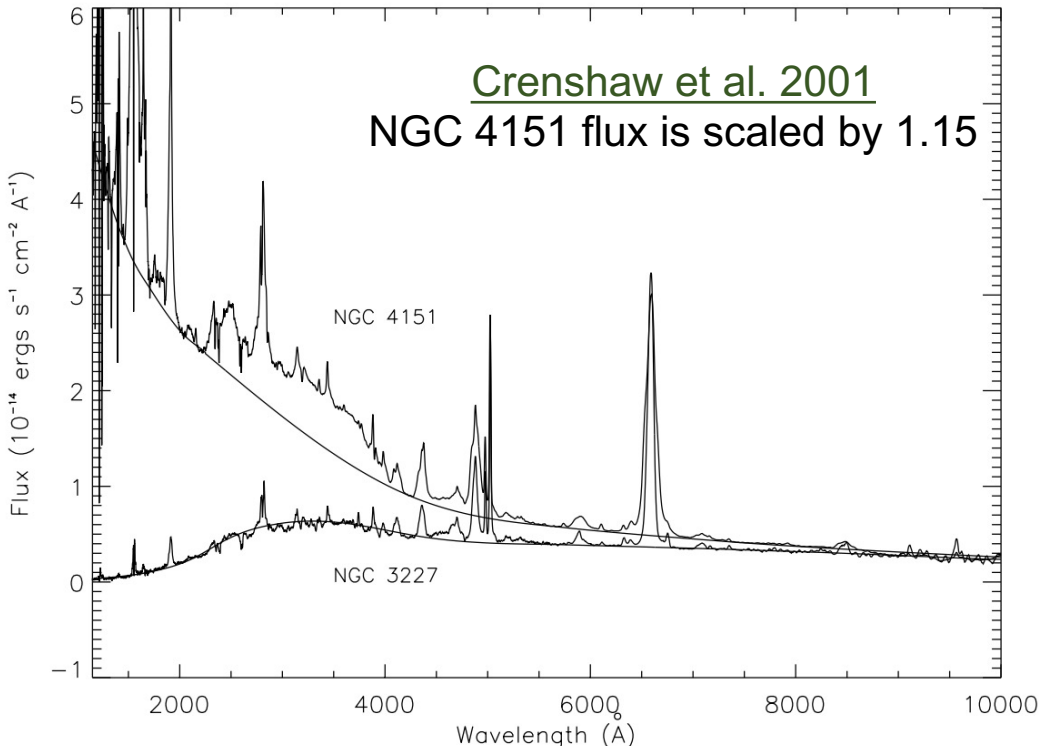
Interstellar reddening

In theory, Balmer line ratios should be roughly the same for targets with the similar T_e .

In practice, the observed the H α /H β ratio might be higher than expected value while the H γ /H β ratio might be lower than expected value. This is due to (line-of-sight) interstellar reddening.

The more the interstellar dust, the larger the discrepancy between theory and observation.

Ion	Transition	λ (Å)	A (s $^{-1}$)
H I	H α $n = 3 \rightarrow 2$	6562.8 Å	4.4×10^7 s $^{-1}$
H I	H β $n = 4 \rightarrow 2$	4861.4 Å	8.4×10^6 s $^{-1}$
H I	H γ $n = 5 \rightarrow 2$	4340.5 Å	2.5×10^6 s $^{-1}$
H I	H δ $n = 6 \rightarrow 2$	4101.7 Å	9.7×10^5 s $^{-1}$
H I	H ϵ $n = 7 \rightarrow 2$	3970.1 Å	4.4×10^5 s $^{-1}$



T_e	2500 K	5000 K	10^4 K	2×10^4 K
H α /H β	3.30	3.05	2.87	2.76
H γ /H β	0.444	0.451	0.466	0.474
H δ /H β	0.241	0.249	0.256	0.262
H ϵ /H β	0.147	0.153	0.158	0.162

H I recombination line ratios in the Case B, low-density limit ([Osterbrock & Ferland 2006](#))

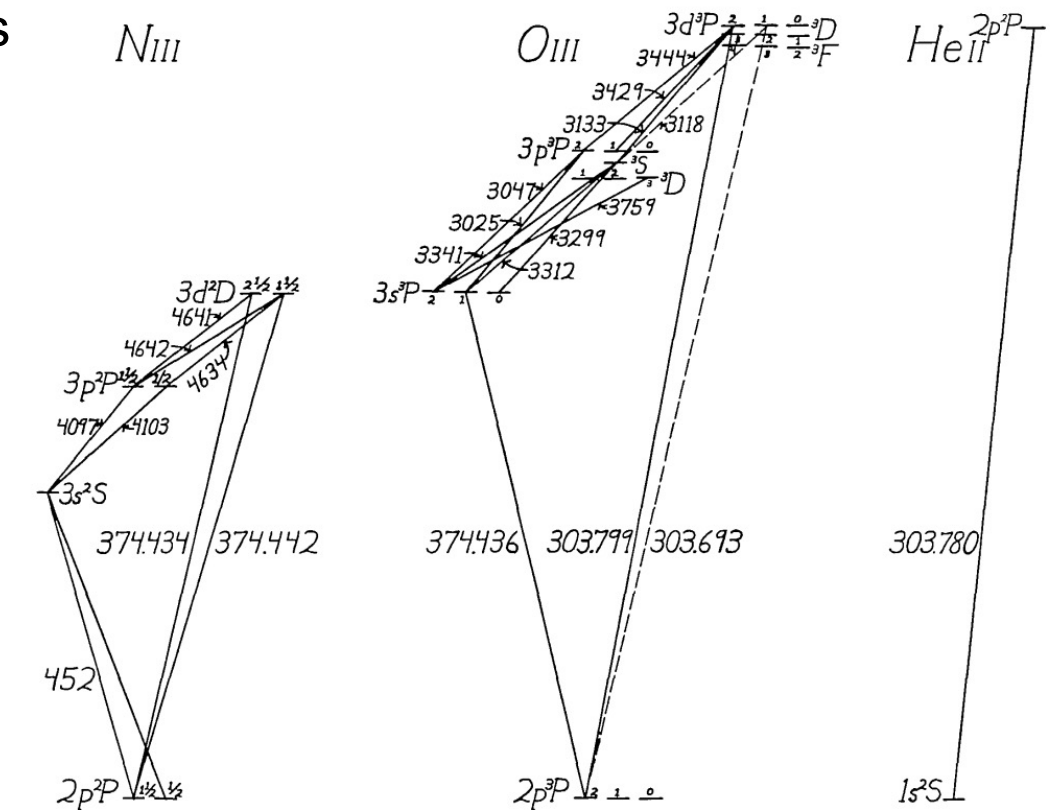
Bowen resonance-fluorescence mechanism

The He II Ly α (recombination) line photons are scattered many times in the medium under case B. A fraction of these He II Ly α transitions are converted to O III $\lambda\lambda 303.80, 303.69$ transitions. By the same token, the O III $\lambda 374.44$ transitions are converted to N III transitions.

Ion	Transition	λ (Å)	A (s $^{-1}$)
He II	$2p\ ^2P_{3/2,1/2} - 1s\ ^2S_{1/2}$	303.78	1.0×10^{10}
O III	$2s^2 2p^2\ ^3P_2 - 2s^2 2p\ 3d\ ^3P_2$	303.80	9.6×10^9
O III	$2s^2 2p^2\ ^3P_2 - 2s^2 2p\ 3d\ ^3P_1$	303.70	5.3×10^9

Ion	Transition	λ (Å)	A (s $^{-1}$)
O III	$2s^2 2p\ ^2P_1 - 2s^2 2p\ 3s\ ^3P_0$	374.33	3.8×10^9
N III	$2s^2 2p\ ^2P_{3/2} - 2s^2 3d\ ^2D_{5/2}$	374.43	1.2×10^{10}
N III	$2s^2 2p\ ^2P_{3/2} - 2s^2 3d\ ^2D_{3/2}$	374.44	2.0×10^9

N_{III}



Bowen (1935)

Bohr atom

After capturing into high-lying excited levels ($n \gg 1$) via **radiative recombination**, electrons can **cascade** down to the neighbouring states ($n - \Delta n$) can give rise to the so-called **radio recombination lines**

The total energy of the electron at n th shell is

$$E_n = \frac{1}{2} m_e v^2 - \frac{e^2}{a_n} = -\frac{e^2}{2a_n} = -\frac{1}{n^2} \frac{2\pi^2 m_e e^4}{h^2}$$

prev. sl.

$$\frac{e^2}{a_n^2} = \frac{m_e v^2}{a_n}$$

$$a_n = n^2 \frac{h^2}{4\pi^2 m_e e^2} = n^2 5.29 \times 10^{-9} \text{ cm}$$

When going from n th to $(n - \Delta n)$ th shell, we have

$$h\nu = \Delta E = \frac{2\pi^2 m_e e^4}{h^2} \left(\frac{1}{n^2} - \frac{1}{(n - \Delta n)^2} \right)$$

$$\nu = \frac{2\pi^2 m_e e^4}{h^3 c} c \left(\frac{1}{n^2} - \frac{1}{(n - \Delta n)^2} \right)$$

Radio recombination line frequency

prev. sl.

$$\nu = \frac{2\pi^2 m_e e^4}{h^3 c} c \left(\frac{1}{n^2} - \frac{1}{(n - \Delta n)^2} \right)$$

$$\nu = R_\infty c \left(\frac{1}{n^2} - \frac{1}{(n - \Delta n)^2} \right)$$

For electrons at high-lying excited levels ($n \gg 1$), the nucleus can be viewed as a H-like ion with an **effective ionic charge** and introducing $R(A)$

$$\nu = \frac{2\pi^2}{h^3 c} \frac{m_e A m_p}{m_e + A m_p} (\textcolor{red}{Z_{\text{eff}}} e)^2 e^2 \left(\frac{1}{n_l^2} - \frac{1}{n_u^2} \right)$$

$$\nu = R(A) c \textcolor{red}{Z_{\text{eff}}^2} \left(\frac{1}{n_l^2} - \frac{1}{n_u^2} \right)$$

$$R(A) = R_\infty \frac{m_e A m_p}{m_e + A m_p} = R_\infty \left(1 + \frac{m_e}{A m_p} \right)^{-1}$$

see Sect. 7.5 of
《天体物理中的
辐射机制》
(p324) by 尤峻汉

Rydberg const.

$$\text{Ry} = R_\infty = \frac{2\pi^2 m_e e^4}{c h^3} = 109737.3 \text{ cm}^{-1}$$

Rydberg frequency

$$R_\infty c = 3.288 \times 10^{15} \text{ Hz}$$

atomic mass number

Element	A	$R(A) \text{ cm}^{-1}$
H	1.007	109678
He	4.00	109722
C	12.00	109733
O	16.00	109733
Si	28.10	109735
Fe	55.85	109736

Radio recombination line (H I)

prev. sl.

$$R(A) = R_\infty \left(1 + \frac{m_e}{A m_p} \right)^{-1}$$

$$\nu = R(A)c Z_{\text{eff}}^2 \left(\frac{1}{n_l^2} - \frac{1}{n_u^2} \right)$$

For H I, $m_e/m_p = 1/1836.15$, $A = 1$, $Z_{\text{eff}} = 1$

$$R(\text{H I})c = 3.288 \times 10^{15} \text{ Hz}$$

$$\nu(\text{H I } 91\alpha) = 3.288 \times 10^{15} \left(\frac{1}{91^2} - \frac{1}{92^2} \right) = 8.585 \times 10^9 \text{ Hz}$$

$n\alpha$ transition: $n + 1 \rightarrow n$

$n\beta$ transition: $n + 2 \rightarrow n$

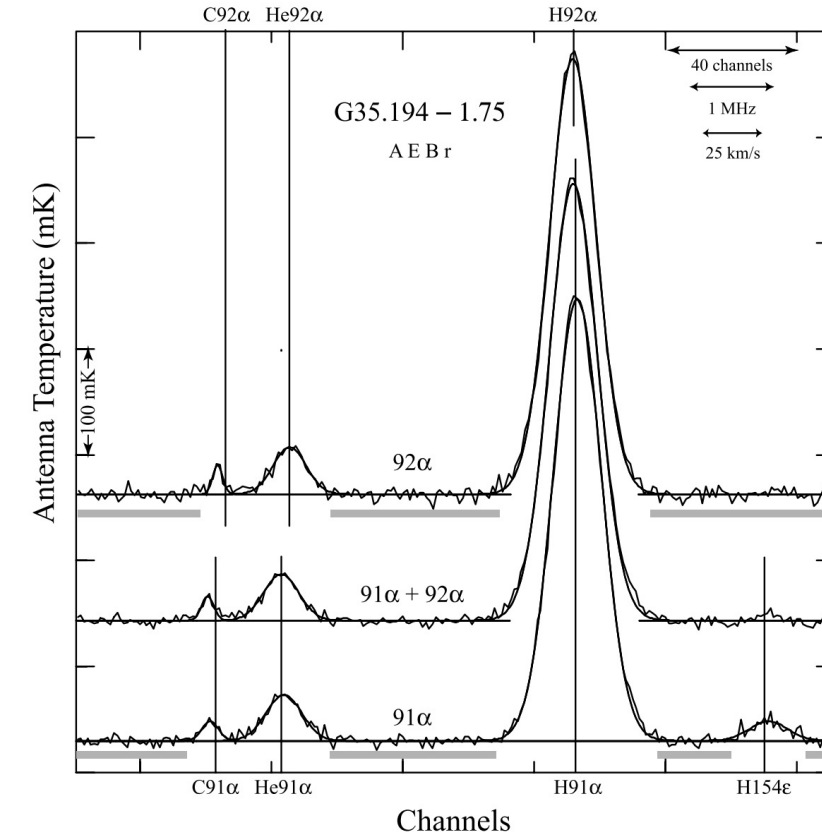
...

Rydberg const.

$$\text{Ry} = R_\infty = \frac{2\pi^2 m_e e^4}{ch^3} = 109737.3 \text{ cm}^{-1}$$

Rydberg frequency

$$R_\infty c = 3.288 \times 10^{15} \text{ Hz}$$



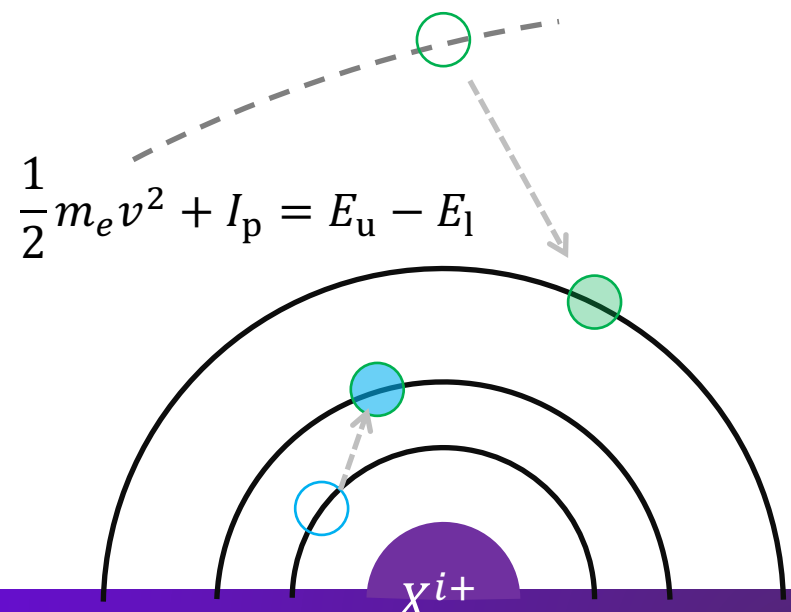
Quiriza et al. 2006

Dielectronic recombination

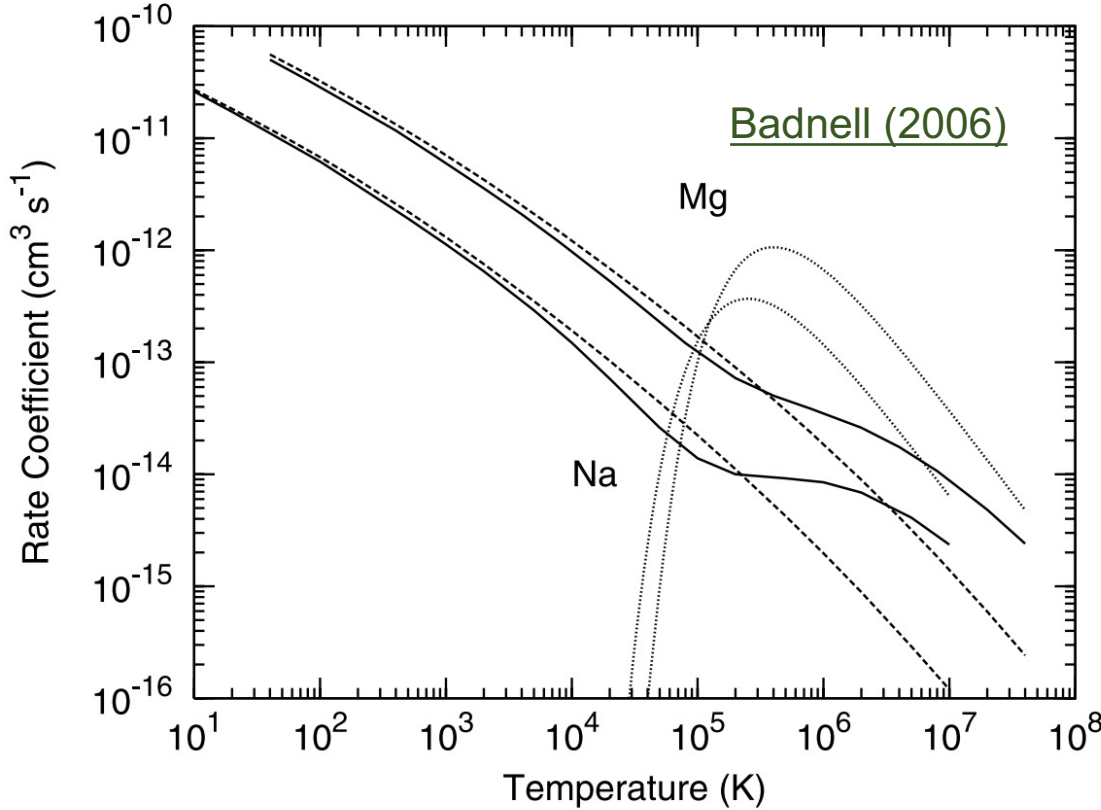
During the DR process, the free electron is captured into one atomic state. Meanwhile, a bound electron (usually in the ground state) is promoted to an excited state. This results in a doubly excited ion

The doubly excited state is not stable. Subsequently, the inverse process auto-ionization (AI) can occur (no photons emitted), or the excited electrons cascade down, giving rise to line emissions (next slide).

- ✓ DR is a **cooling** process for the electrons.
- ✓ AI is a **heating** process for the electrons.
- ❑ DR might produce **line emission** spectral features



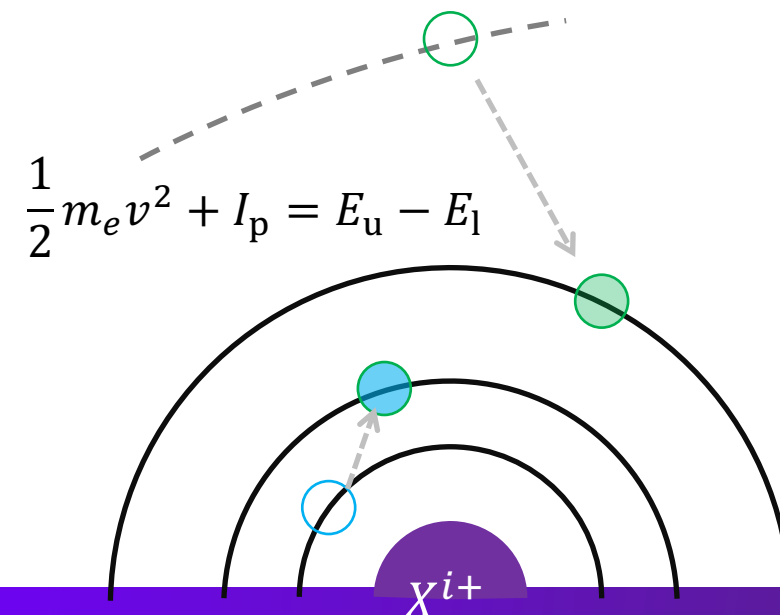
DR rate coefficient (cf. RR rate coefficients)



DR (dotted) and RR (solid and dashed) rate coefficients for Na II and Mg III

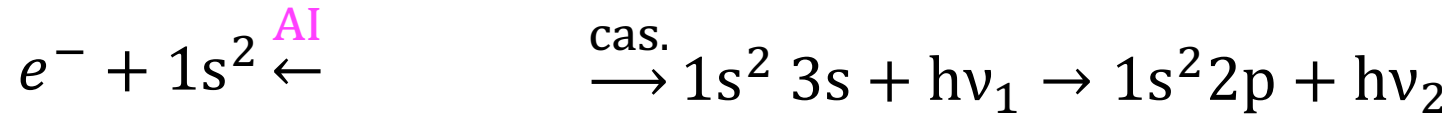
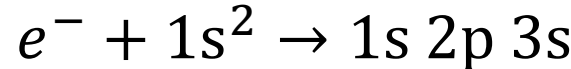
5.4.9.1 DR rate coefficients (cf. RR rate coefficients)

At **relatively low** temperature, DR can be **ignored** as free electrons do not have sufficient energy to excite a bound electron.



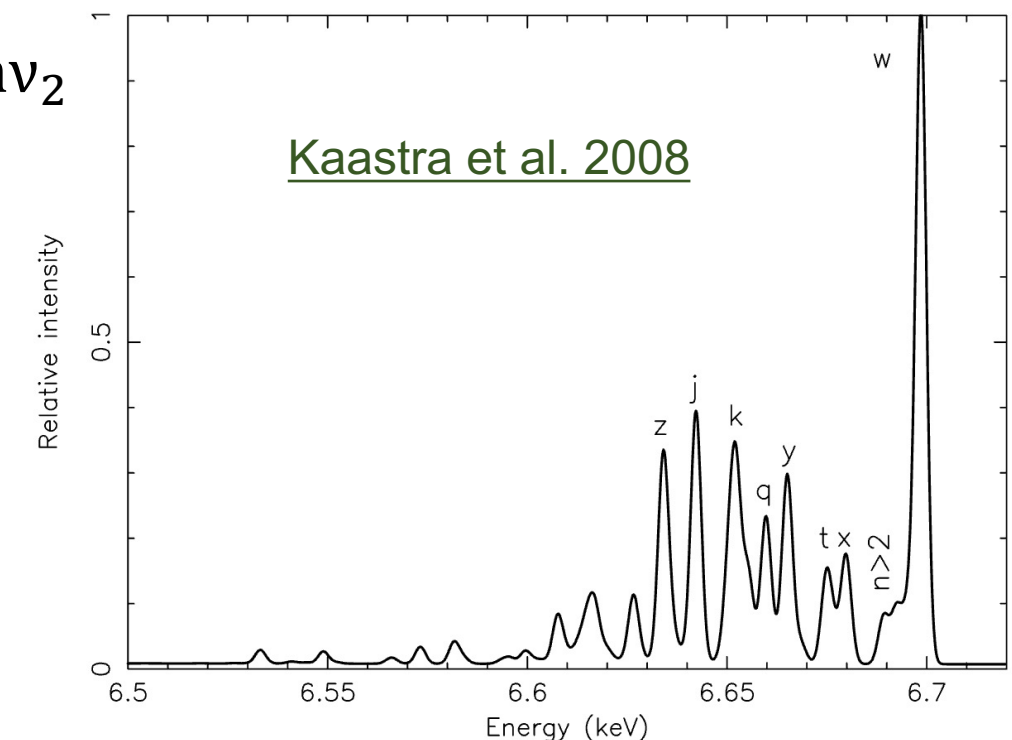
DR satellite lines

Example of DR from a He-like ion to form a Li-like ion



Compared to the regular He-like ($1s\ 2p \rightarrow 1s^2$) transition with photon energy $h\nu_0$, $h\nu_1$ in the above process have a slightly different energy/wavelength due to the presence of the 3s (the atomic state the free electron is captured into). Since there are many states (e.g., 3p, 4s, 4p, ...) the free electron can be captured into, a set of **satellite lines** are formed near the regular He-like ($1s\ 2p \rightarrow 1s^2$) transition.

Ion	Line Energy keV	Upper Level	Lower Level	Emissivity ph cm ⁻³ s ⁻¹	Te peak K	Relative Intensity
Fe XXIV DRsat	6.690	10089	6	1.057e-18	3.981e+07	0.07
Fe XXV	6.682	6	1	8.213e-18	6.310e+07	0.58
Fe XXV	6.668	5	1	9.056e-18	6.310e+07	0.64
Fe XXIV	6.662	48	1	2.897e-18	3.981e+07	0.20
Fe XXIV DRsat	6.658	10242	3	1.168e-18	3.981e+07	0.08
Fe XXIV DRsat	6.655	10247	2	2.821e-18	3.981e+07	0.20
Fe XXIV DRsat	6.645	10248	3	4.202e-18	3.981e+07	0.30
Fe XXV	6.637	2	1	1.423e-17	6.310e+07	1.00



Kappa distribution

Sect. 5.2.7

Non-thermal emission might occur if electrons do not have a Maxwellian velocity distribution

Maxwell energy distribution

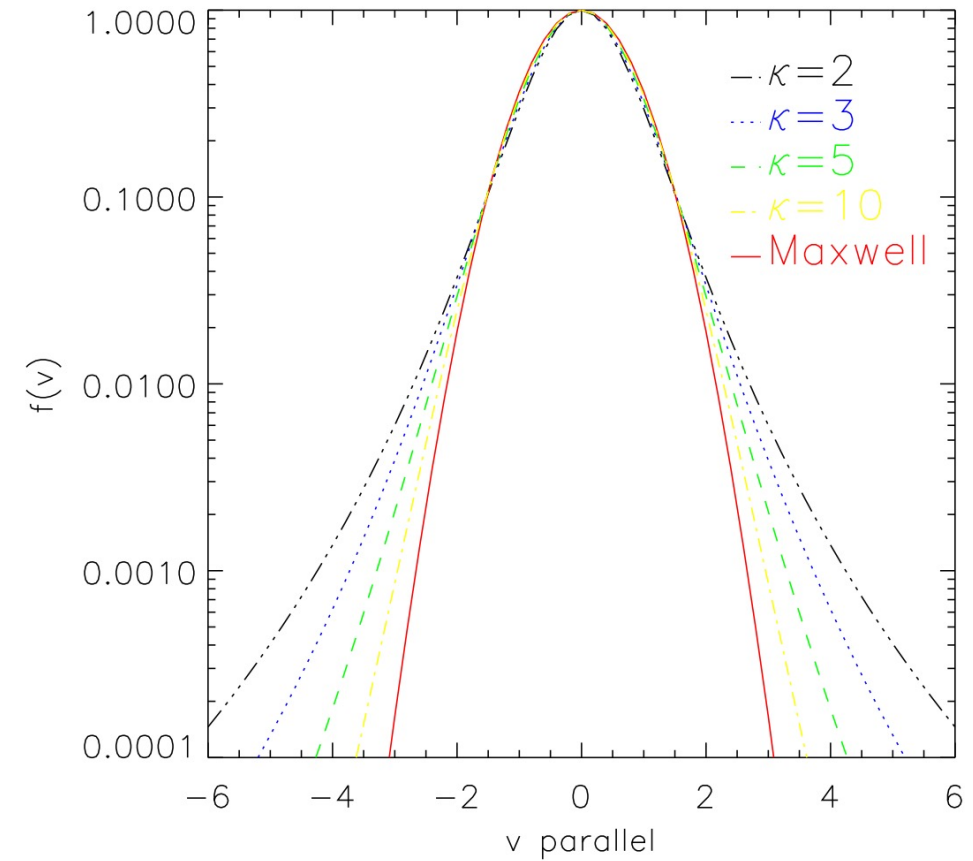
$$f(E)dE = 2 \sqrt{\frac{E}{\pi}} \left(\frac{1}{kT_e}\right)^{3/2} \exp\left(-\frac{E}{kT_e}\right)$$

Kappa energy distribution

$$f_\kappa(E, \kappa)dE = A_\kappa \frac{2}{\sqrt{\pi}} \left(\frac{1}{kT_e}\right)^{3/2} \sqrt{E} \left(1 + \frac{E}{\left(\kappa - \frac{3}{2}\right) kT_e}\right)^{-(\kappa+1)}$$

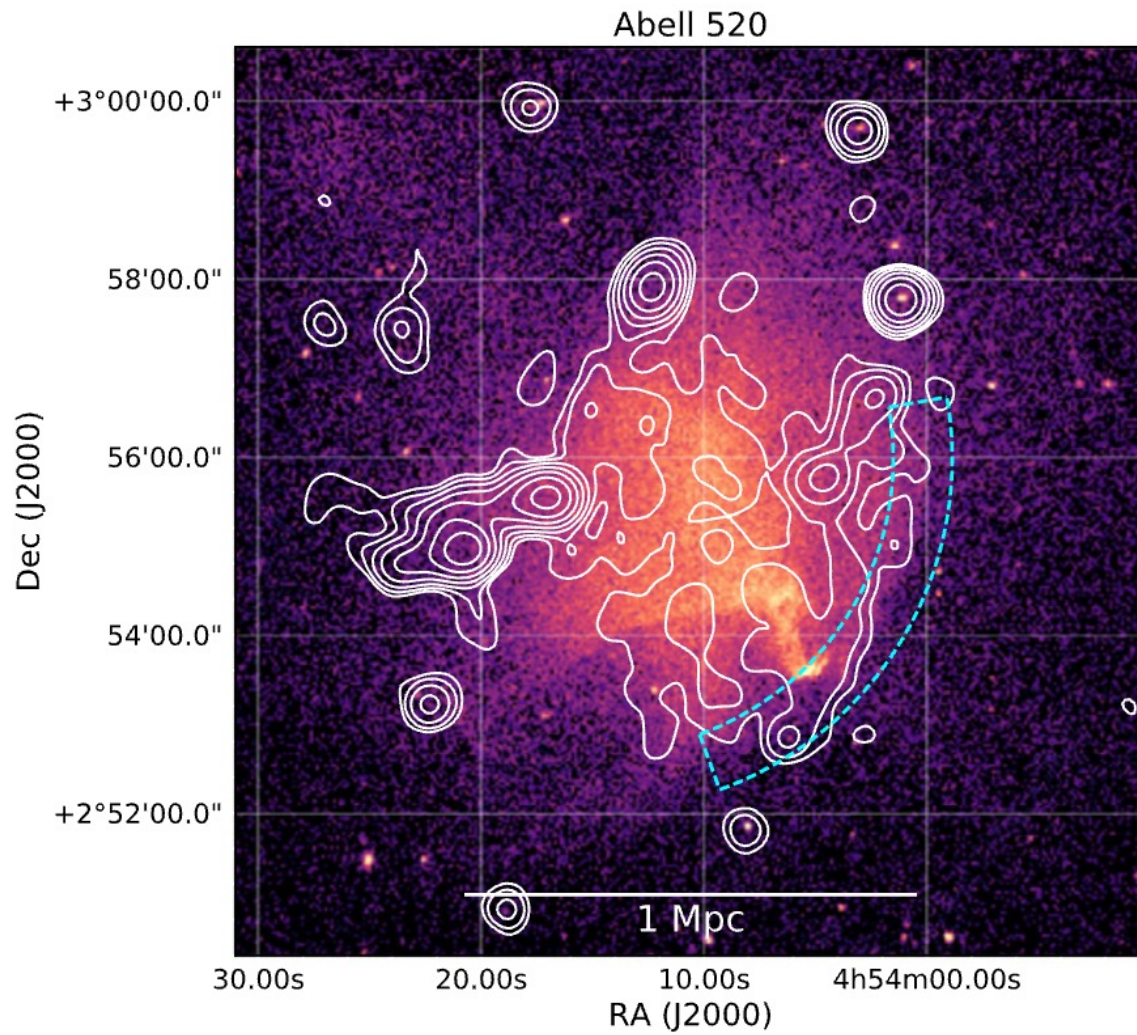
An arbitrary electron distribution (incl. Kappa distribution) can be approximated by the sum of Maxwellian distributions ([Kaastra et al. 2009](#))

Pierrard & Lazar (2010)

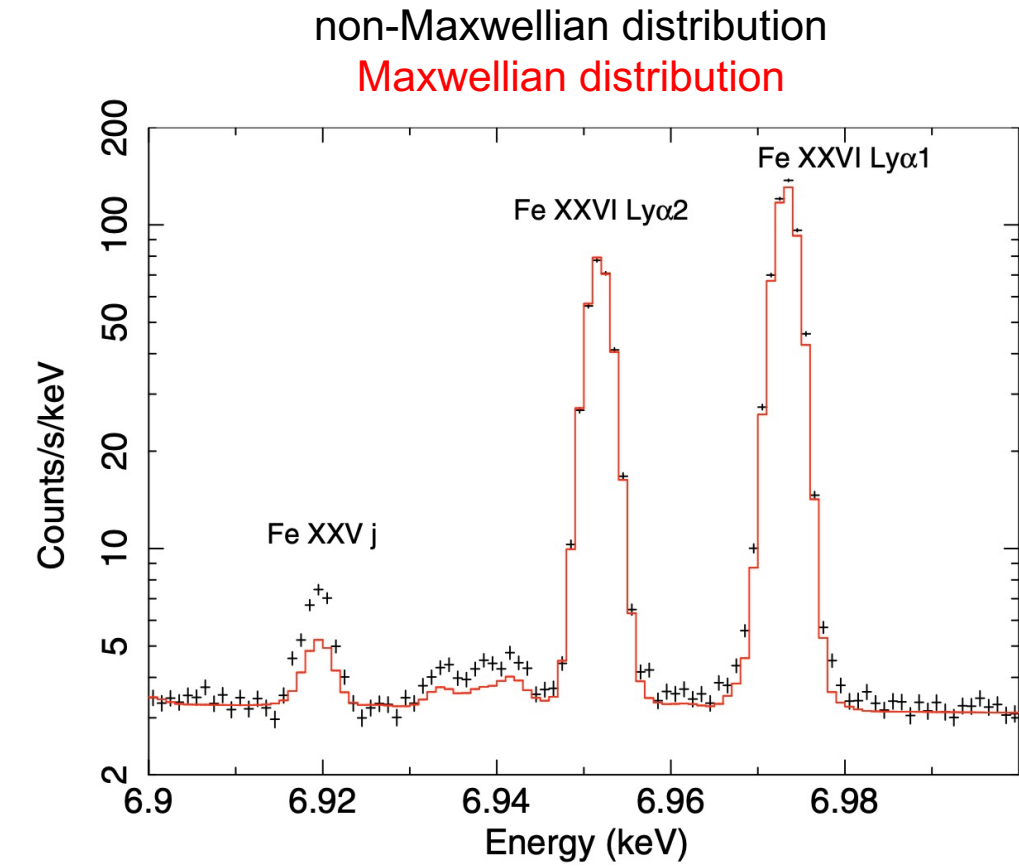


DR satellite non-Maxwellian diagnostics

van Weeren et al. 2019



DR satellite lines are sensitive to the presence of supra-thermal electrons e.g., those behind shocks in merging galaxy clusters (Kaastra et al. 2009).



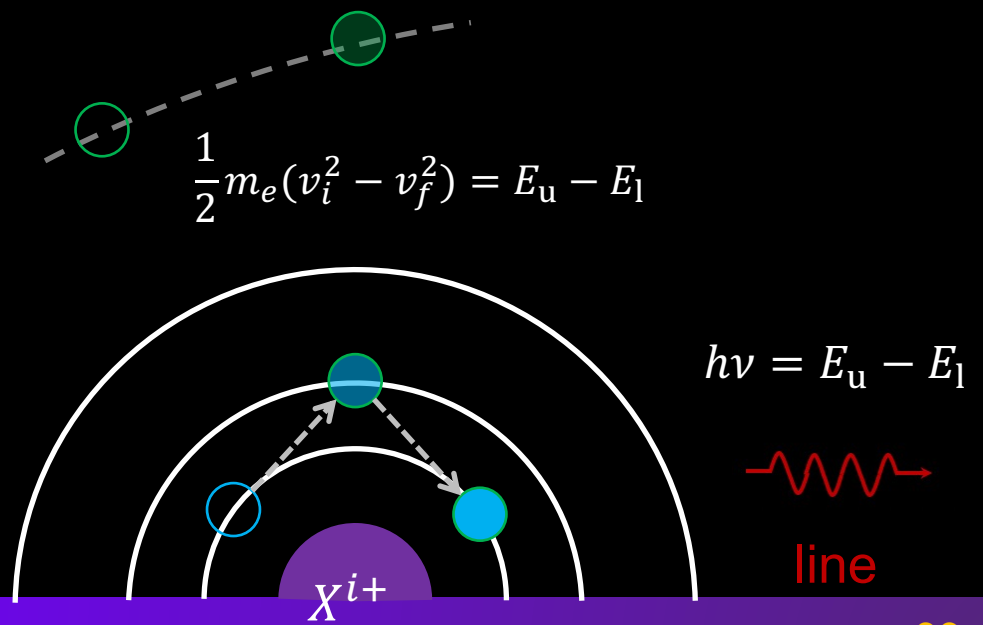
Chpt.5 Atomic processes

5.1 Atomic data for astrophysics
5.2 Two-level system
5.3 Bremsstrahlung
5.4 Recombination and photoionization

5.5 Collisional excitation and de-excitation
5.5.1 More than recombination lines
5.5.2 Allowed, semi-forbidden, and forbidden transitions
5.5.3 Electron-impact excitation and de-excitation
5.5.4 Density and temperature diagnostics

5.6 Other atomic processes
5.7 Astrophysical plasma models

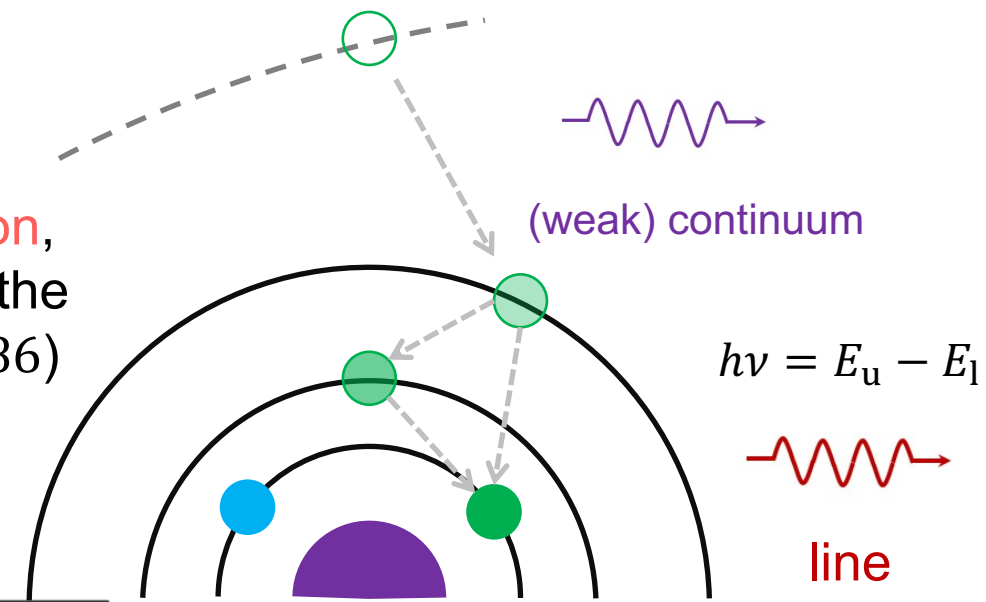
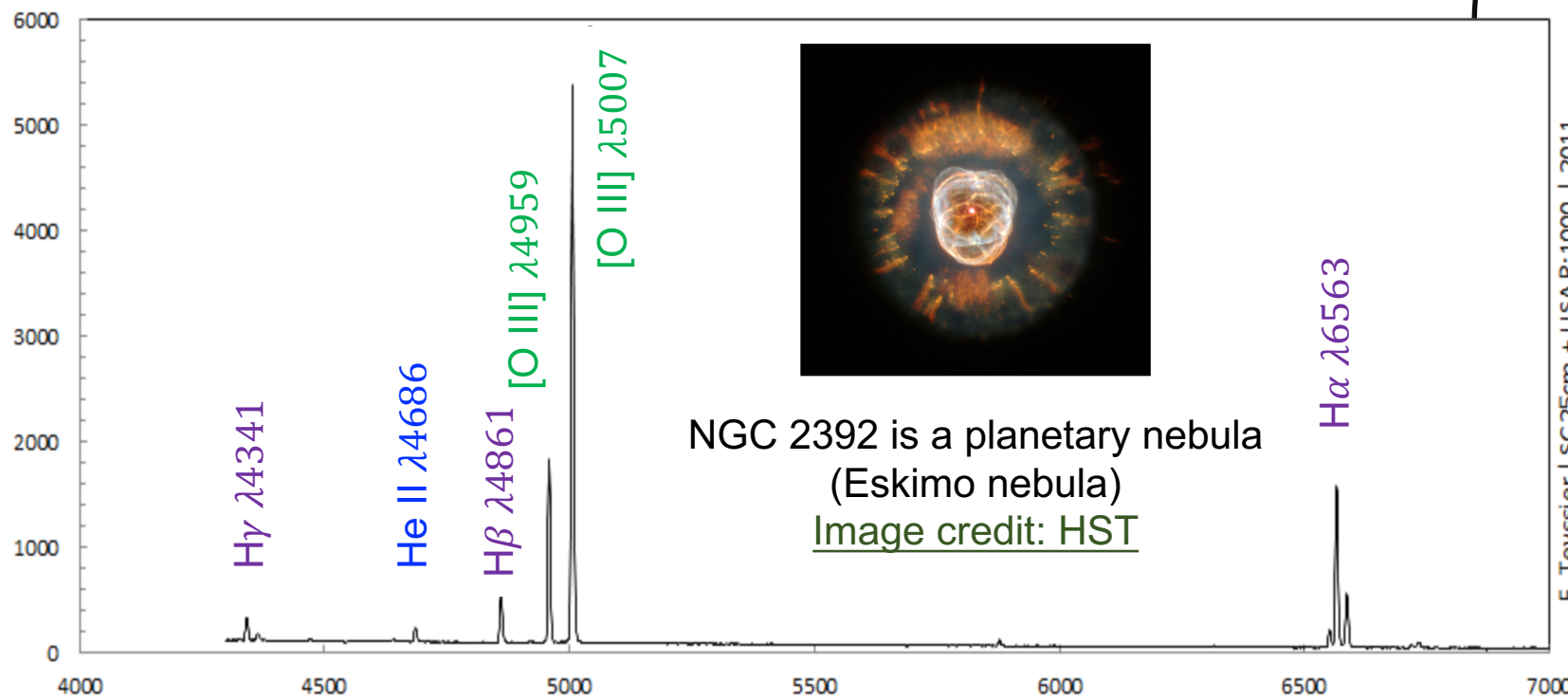
5.5 Collisional excitation and de-excitation



More than recombination lines

After capturing into the excited levels via **radiative recombination**, electrons can **cascade** down to the ground state, giving rise to the so-called **recombination lines** (e.g., Balmer lines and He II $\lambda 4686$)

Spectrum credit: F. Teyssier



The two strong [O III] lines are also seen in AGN, starburst galaxies, etc.

Can these two [O III] lines form via radiative recombination?

Case B

Under the Case B limit, the level population is

Sect. 5.4.7.2

$$n_e n_{i+1,0} \alpha_{i,m}(T_e) + \sum_{u>m} n_{i,u} A_{um} = \sum_{1 \leq l < m} n_{i,m} A_{ml}$$

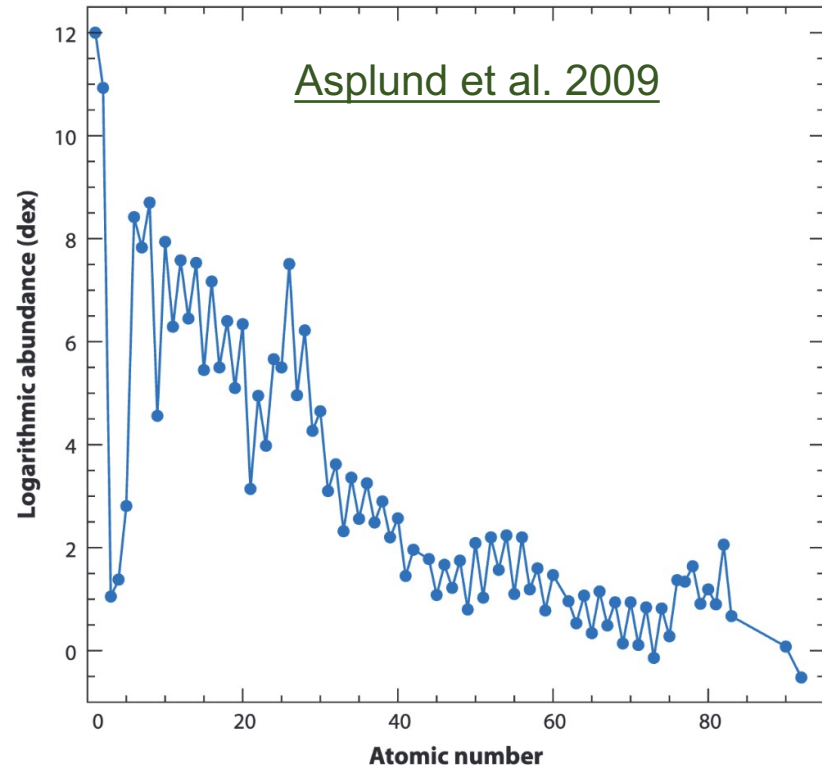
$$n(\text{O IV}) = n_{\text{H}} \frac{N(\text{O})}{N(\text{H})} \frac{N(\text{O IV})}{N(\text{O})}$$

$$n(\text{He III}) = n_{\text{H}} \frac{N(\text{He})}{N(\text{H})} \frac{N(\text{He III})}{N(\text{He})}$$

[O III] $\lambda\lambda 4959, 5007$ vs. He II $\lambda 4686$

Similar ionization energies:

- O III ionization energy: 54.5 eV
- He II ionization energy: 54.2 eV



The cosmic abundance of He is about two orders of magnitude larger than that of O.

OPEN-ADAS

Ion	Transition	λ (Å)	E (eV)	A (s^{-1})
He II	$3d\ ^2D_{5/2} - 4f\ ^2F_{7/2}$	4685.8	2.69	2.2×10^8
O III	$2p^2\ ^3P_1 - 2p^2\ ^1D_2$	4958.9	2.50	6.2×10^{-3}
O III	$2p^2\ ^3P_2 - 2p^2\ ^1D_2$	5006.8	2.48	1.8×10^{-2}

$$T_e = \frac{E}{k} \sim \frac{2.50 \text{ eV}}{8.62 \times 10^{-5} \text{ eV/K}}$$

$\sim 29000 \text{ K}$

Sect. 5.4.7.2

$$n_e n_{i+1,0} \alpha_{i,m}(T_e) + \sum_{u>m} n_{i,u} A_{um} = \sum_{1 \leq l < m} n_{i,m} A_{ml}$$

The two level populations need to differ by ~ 10 orders of magnitude.

With $kT_e \sim 29000 \text{ K}$, what is the radiative recombination rate coefficient for He I and O III?

OPEN-ADAS (RR data)

<https://open.adas.ac.uk/adf48>

OPEN-ADAS

Atomic Data and Analysis Structure | Ra II (4533.1Å)



DATA CLASSES

FUNDAMENTAL

ADF01

ADF04

ADF07

ADF08

ADF09

ADF38

ADF39

ADF48

DERIVED

ADF11

ADF12

ADF13

ADF15

ADF21

ADF22

ADF
48

Radiative recombination rate coefficients

ADF48 files contain partial final-state resolved radiative recombination rate coefficients from both ground and metastable levels.

Search ADF48 files

atomic number: e.g., 2 for He

Ion

Element

2

Charge

2

Coupling Scheme

LS

IC

Search

ionic charge: 2 for 2+

Number of files: 900 Total size: 404.4 MB

1 ADF48 files found

Ion

Year

Coupling

File Details

He²⁺

05

IC

ADF 48 nrb05##_he2ic.dat

data file

nrb05##_he2ic.dat

Radiative Recombination Rate Coefficients

Ion He²⁺

Temperature Range 40.00 eV → 4.000 × 10⁷ eV

Download data

Filename: nrb05##_he2ic.dat

Full Path: adf48/nrb05##/nrb05##_he2ic.dat

• Documentation • Software libraries

Parents

Recombined

Comments

Origins

Parent states

hash(0x1ece9d0) ¹S_{0.0}

Note: Search for the recombining ion

RR rate coefficient for He II

Ion	Transition	λ (Å)	E (eV)	A (s^{-1})
He II	$3d\ ^2D_{5/2} - 4f\ ^2F_{7/2}$	4685.8	2.69	2.2×10^8
O III	$2p\ ^2P_1 - 2p\ ^2P_2$	4958.9	2.50	6.2×10^{-3}
O III	$2p\ ^2P_2 - 2p\ ^2P_3$	5006.8	2.48	1.8×10^{-2}

$$T_e = \frac{E}{k} \sim \frac{2.50 \text{ eV}}{8.62 \times 10^{-5} \text{ eV/K}}$$

$\sim 29000 \text{ K}$

```

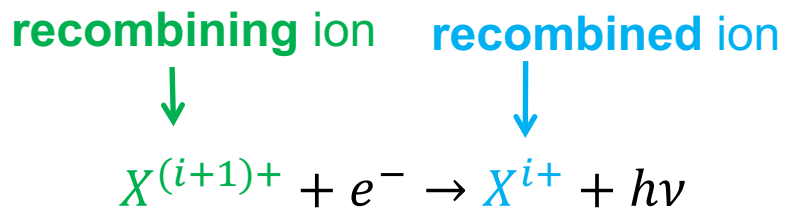
SEQ='H'      NUCCHG= 2

PARENT LEVEL INDEXING          /IC/
-----                         /IC/
INDP   CODE        BWNP=    0.0   NPRNTI= 1   NPRNTF= 1
-----   -----        S L   WI       WNP
-----   -----        --- --- --- -----
1      ---        (1)0( 0.0)     0.0

IC RESOLVED LEVEL INDEXING
-----                         /IC/
-----                         /IC/
INDX  INDP   CODE        BWRN=  438949.6   NLVL= 64
-----   -----   -----        S L   WJ       WNR
-----   -----   -----        --- --- --- -----
1      1      1S1        (1)*( 0.5)     0.0
2      1      2S1        (1)*( 0.5)   329212.2
3      1      2P1        (1)*( 0.5)   329212.2
4      1      2P1        (1)*( 1.5)   329212.2
5      1      3S1        (1)*( 0.5)   390177.4
6      1      3P1        (1)*( 0.5)   390177.4
7      1      3P1        (1)*( 1.5)   390177.4
8      1      3D1        (1)*( 1.5)   390177.4
9      1      3D1        (1)*( 2.5)   390177.4
10     1      4S1        (1)*( 0.5)   411515.3
11     1      4P1        (1)*( 0.5)   411515.3
12     1      4P1        (1)*( 1.5)   411515.3
13     1      4D1        (1)*( 1.5)   411515.3
14     1      4D1        (1)*( 2.5)   411515.3
15     1      4F1        (1)*( 2.5)   411515.3
16     1      4F1        (1)*( 3.5)   411515.3

```

Badnell (2006)



RR rate coefficient for He II (cont.)

PRTI= 1 LVLVRT= (1S 0.0)

INDX	TE=	4.00E+01	8.00E+01	2.00E+02	4.00E+02	8.00E+02	2.00E+03	4.00E+03	8.00E+03	2.00E+04	4.00E+04
---	---	8.00E+04	2.00E+05	4.00E+05	8.00E+05	2.00E+06	4.00E+06	8.00E+06	2.00E+07	4.00E+07	4.00E+07
1	1.04E-11	7.36E-12	4.66E-12	3.29E-12	2.33E-12	1.47E-12	1.04E-12	7.30E-13	4.56E-13	3.16E-13	
	2.16E-13	1.24E-13	7.76E-14	4.56E-14	2.03E-14	1.01E-14	4.72E-15	1.58E-15	6.53E-16		
2	1.53E-12	1.08E-12	6.82E-13	4.82E-13	3.41E-13	2.16E-13	1.52E-13	1.07E-13	6.73E-14	4.68E-14	
	3.20E-14	1.83E-14	1.13E-14	6.55E-15	2.85E-15	1.40E-15	6.43E-16	2.12E-16	8.72E-17		
3	1.40E-12	9.88E-13	6.25E-13	4.41E-13	3.11E-13	1.95E-13	1.36E-13	9.40E-14	5.56E-14	3.57E-14	
	2.16E-14	9.92E-15	4.99E-15	2.31E-15	7.46E-16	2.97E-16	1.14E-16	3.05E-17	1.11E-17		

Badnell (2006)

$T_e \sim 29000$ K

skipping many rows											
15	3.69E-13	2.60E-13	1.64E-13	1.15E-13	7.97E-14	4.80E-14	3.15E-14	1.96E-14	9.31E-15	4.75E-15	
16	2.20E-15	6.98E-16	2.72E-16	1.02E-16	2.68E-17	9.61E-18	3.42E-18	8.69E-19	3.08E-19		
	4.92E-13	3.47E-13	2.18E-13	1.53E-13	1.06E-13	6.40E-14	4.20E-14	2.62E-14	1.24E-14	6.33E-15	
	2.93E-15	9.30E-16	3.63E-16	1.36E-16	3.57E-17	1.28E-17	4.56E-18	1.16E-18	4.10E-19		

Atomic process	Rate coefficient @ $T_e \sim 3 \times 10^4$ K
He III – He II $4f^2 F_{7/2}$	$\alpha^{RR} \sim (0.6 - 1.2) \times 10^{-14} \text{ cm}^3 \text{ s}^{-1}$
O IV $2p^2 P_{1/2}$ – O III $2p^2 ^1D_2$	

RR rate coefficient for O III

Ion	Transition	λ (Å)	E (eV)	A (s^{-1})
He II	$3d\ ^2D_{5/2} - 4f\ ^2F_{7/2}$	4685.8	2.69	2.2×10^8
O III	$2p^2\ ^3P_1 - 2p^2\ ^1D_2$	4958.9	2.50	6.2×10^{-3}
O III	$2p^2\ ^3P_2 - 2p^2\ ^1D_2$	5006.8	2.48	1.8×10^{-2}

```

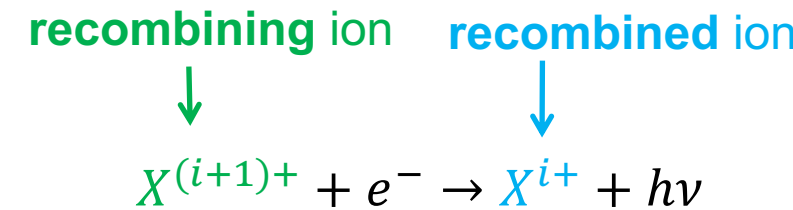
SEQ='C'      NUCCHG= 8                                /IC/
PARENT LEVEL INDEXING          BNWP= 15629588.6   NPRNTI= 5   NPRNTF=10
-----          S L   WI          WNP
INDP      CODE
-----          --- --- -----
→ 1        2S2 2P1    (2)1( 0.5)      0.0
              2        2S2 2P1    (2)1( 1.5)      347.7
  
```

```

IC RESOLVED LEVEL INDEXING          BNWR= 16064389.3   NLVL=1021
-----          S L   WI          WNR
INDX  INDP  CODE
-----          --- --- -----
1    9999  2S2 2P2    (3)1( 0.0)      0.0
2    9999  2S2 2P2    (3)1( 1.0)     110.1
3    9999  2S2 2P2    (3)1( 2.0)     324.6
→ 4    9999  2S2 2P2    (1)2( 2.0)    20520.5
5    9999  2S2 2P2    (1)0( 0.0)    43497.8
  
```

$$T_e = \frac{E}{k} \sim \frac{2.50 \text{ eV}}{8.62 \times 10^{-5} \text{ eV/K}}$$

~29000 K



Badnell (2006)

OPEN-ADAS
Atomic Data and Analysis Structure

RR rate coefficient for O III (cont.)

Badnell (2006)

OPEN-ADAS
Atomic Data and Analysis Structure

PRTI= 1 LVLVRT= (2P 0.5)

$T_e \sim 29000$ K

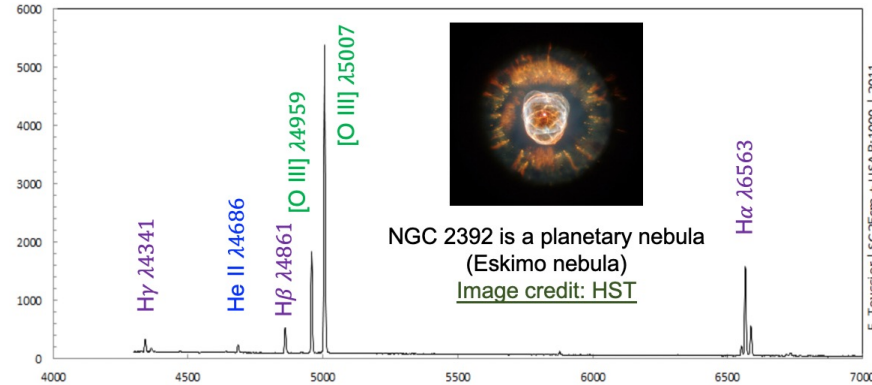
INDX	TE=	9.00E+01	1.80E+02	4.50E+02	9.00E+02	1.80E+03	4.50E+03	9.00E+03	1.80E+04	4.50E+04	9.00E+04
---	---	1.80E+05	4.50E+05	9.00E+05	1.80E+06	4.50E+06	9.00E+06	1.80E+07	4.50E+07	9.00E+07	
1		3.27E-12	2.31E-12	1.46E-12	1.03E-12	7.31E-13	4.62E-13	3.27E-13	2.31E-13	1.45E-13	1.01E-13
		6.95E-14	3.96E-14	2.39E-14	1.32E-14	5.23E-15	2.34E-15	9.80E-16	2.85E-16	1.08E-16	
2		7.27E-12	5.14E-12	3.25E-12	2.30E-12	1.63E-12	1.03E-12	7.27E-13	5.13E-13	3.23E-13	2.26E-13
		1.55E-13	8.81E-14	5.33E-14	2.95E-14	1.16E-14	5.22E-15	2.18E-15	6.35E-16	2.39E-16	
3		4.12E-12	2.91E-12	1.84E-12	1.30E-12	9.21E-13	5.83E-13	4.12E-13	2.91E-13	1.83E-13	1.28E-13
		8.77E-14	5.00E-14	3.02E-14	1.67E-14	6.61E-15	2.96E-15	1.24E-15	3.60E-16	1.36E-16	
4		6.94E-12	4.91E-12	3.10E-12	2.19E-12	1.55E-12	9.82E-13	6.95E-13	4.92E-13	3.11E-13	2.19E-13
		1.51E-13	8.79E-14	5.39E-14	3.02E-14	1.21E-14	5.45E-15	2.29E-15	6.70E-16	2.53E-16	
5		1.23E-12	8.67E-13	5.49E-13	3.88E-13	2.74E-13	1.74E-13	1.23E-13	8.73E-14	5.56E-14	3.94E-14
		2.76E-14	1.64E-14	1.02E-14	5.82E-15	2.37E-15	1.08E-15	4.55E-16	1.34E-16	5.06E-17	

Atomic process	Rate coefficient @ $T_e \sim 3 \times 10^4$ K
He III – He II $4f\ ^2F_{7/2}$	$\alpha^{RR} \sim (0.6 - 1.2) \times 10^{-14} \text{ cm}^3 \text{ s}^{-1}$
O IV $2p\ ^2P_{1/2}$ – O III $2p\ ^2D_2$	$\alpha^{RR} \sim (3.1 - 4.9) \times 10^{-13} \text{ cm}^3 \text{ s}^{-1}$

More than recombination lines

Sect. 5.4.7.2

$$n_e n_{i+1,0} \alpha_{i,m}(T_e) + \sum_{u>m} n_{i,u} A_{um} = \sum_{1 \leq l < m} n_{i,m} A_{ml}$$



Ion	Transition	λ (Å)	E (eV)	A (s^{-1})
He II	$3d\ ^2D_{5/2} - 4f\ ^2F_{7/2}$	4685.8	2.69	2.2×10^8
O III	$2p^2\ ^3P_1 - 2p^2\ ^1D_2$	4958.9	2.50	6.2×10^{-3}
O III	$2p^2\ ^3P_2 - 2p^2\ ^1D_2$	5006.8	2.48	1.8×10^{-2}

The two strong [O III] lines are also seen in AGN, starburst galaxies, etc.

Atomic process	Rate coefficient @ $T_e \sim 3 \times 10^4$ K
He III – He II $4f\ ^2F_{7/2}$	$\alpha^{RR} \sim (0.6 - 1.2) \times 10^{-14} \text{ cm}^3 \text{ s}^{-1}$
O IV $2p\ ^2P_{1/2} - O\ III\ 2p^2\ ^1D_2$	$\alpha^{RR} \sim (3.1 - 4.9) \times 10^{-13} \text{ cm}^3 \text{ s}^{-1}$

Selection rule

The following selection rules must be satisfied for **allowed** transition

- ✓ Parity must change
- ✓ One electron jump with $|\Delta n| \geq 1$ and $\Delta l = \pm 1$
- ✓ $\Delta S = 0$
- ✓ $\Delta L = 0, \pm 1$
- ✓ $\Delta J = 0, \pm 1$ but not $\Delta J = 0 \rightarrow 0$

Semi-forbidden transitions (denoted with **]**) satisfy all but

- ✓ $\Delta S = 0$

Forbidden transitions (denoted with **[]**) violates more than one selection rules

Ion	Transition	$\lambda (\text{\AA})$	$A (\text{s}^{-1})$
He II	$1s^2 S_{1/2} - 2p^2 P_{3/2,1/2}^o$	303.78	1.0×10^{10}
He II	$3d^2 D_{5/2} - 4f^2 F_{7/2}^o$	4685.8	2.2×10^8
O III	$2s^2 2p^2 ^3P_2 - 2s^2 2p 3d ^3P_2^o$	303.80	9.6×10^9
O III	$2s^2 2p^2 ^3P_2 - 2s^2 2p 3d ^3P_1^o$	303.70	5.3×10^9

Ion	Transition	$\lambda (\text{\AA})$	$A (\text{s}^{-1})$
C III]	$2s^2 ^1S_0 - 2s 2p ^3P_1^o$	1908.7	1.1×10^2
N IV]	$2s^2 ^1S_0 - 2s 2p ^3P_1^o$	1486.5	5.9×10^2
N III]	$2s^2 2p ^2P_{3/2}^o - 2s 2p ^2 ^4P_{5/2}$	1749.7	3.1×10^2

Ion	Transition	$\lambda (\text{\AA})$	$A (\text{s}^{-1})$
[O III]	$2p^2 ^3P_1 - 2p^2 ^1D_2$	4958.9	6.2×10^{-3}
[O III]	$2p^2 ^3P_2 - 2p^2 ^1D_2$	5006.8	1.8×10^{-2}

Oscillator strength for allowed transition

Allowed transitions have large A-values and f-values

$$f_{lu} = \frac{m_e c}{8 \pi^2 e^2} \frac{g_u}{g_l} \lambda^2 A_{ul} = 1.499 \times 10^{-16} \frac{g_u}{g_l} \left(\frac{\lambda}{\text{\AA}} \right)^2 \left(\frac{A_{ul}}{\text{s}^{-1}} \right)$$

$$g_{u/l} = 2j + 1$$



e.g. [Mao et al. 2020a](#)

(absorption) oscillator strength

CHIANTI

H I

An Atomic Database for Spectroscopic Diagnostics of Astrophysical Plasmas.

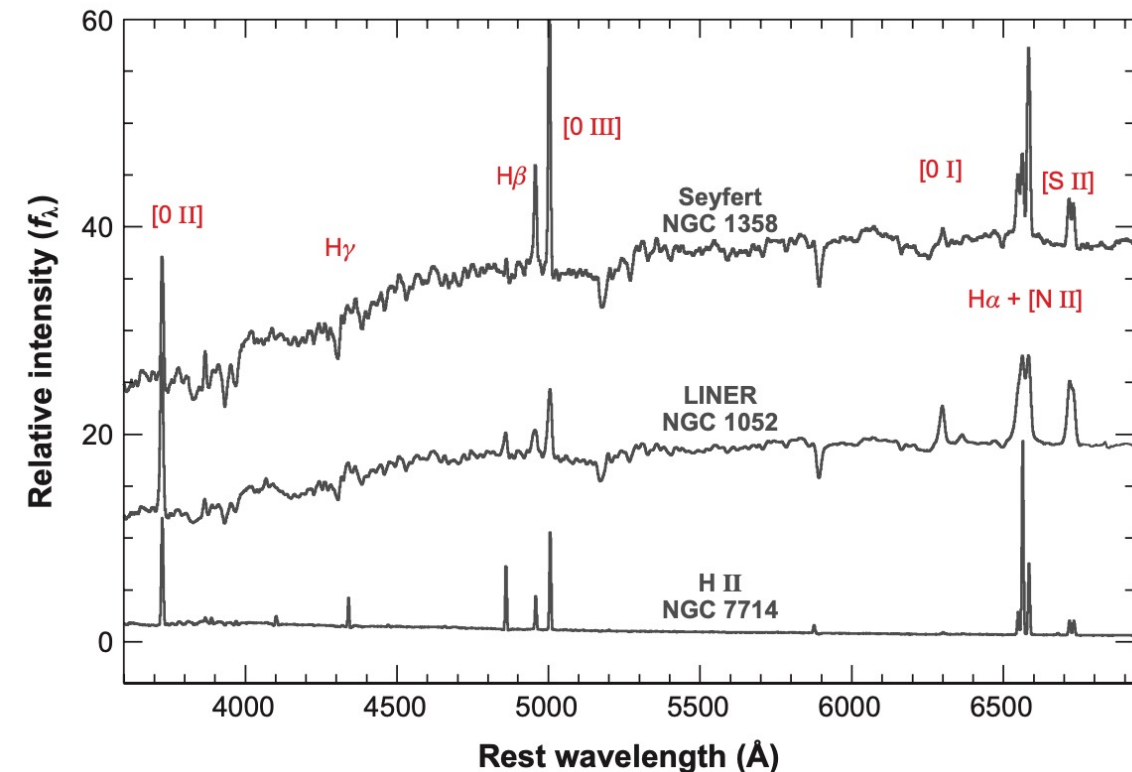
$\lambda (\text{\AA})$	gf	$A (\text{s}^{-1})$	Transition
1215.674	2.780e-01	6.260e+08	1s 2S1/2 - 2p 2P1/2
1215.668	5.550e-01	6.260e+08	1s 2S1/2 - 2p 2P3/2
6564.564	2.720e-02	2.100e+06	2p 2P1/2 - 3s 2S1/2
6564.722	5.440e-02	4.210e+06	2p 2P3/2 - 3s 2S1/2

$$gf = g_l f_{lu} = g_u f_{ul}$$
$$\log(gf) = \log(g_l f_{lu})$$

Forbidden transitions

Ho 2008

Ion	Transition	λ (Å)	A (s^{-1})
[O II]	$3p^3\ ^4S_{3/2}^0 - 3p^3\ ^2D_{3/2}^0$	3726.0	1.6×10^{-4}
[O II]	$3p^3\ ^4S_{3/2}^0 - 3p^3\ ^2D_{5/2}^0$	3728.8	2.9×10^{-5}
[O III]	$2p^2\ ^3P_1 - 2p^2\ ^1D_2$	4958.9	6.2×10^{-3}
[O III]	$2p^2\ ^3P_2 - 2p^2\ ^1D_2$	5006.8	1.8×10^{-2}
[N II]	$2p^2\ ^3P_1 - 2p^2\ ^1D_2$	5006.8	9.8×10^{-4}
[N II]	$2p^2\ ^3P_2 - 2p^2\ ^1D_2$	5006.8	2.9×10^{-3}
[S II]	$3p^3\ ^4S_{3/2}^0 - 3p^3\ ^2D_{5/2}^0$	6716.4	1.9×10^{-4}
[S II]	$3p^3\ ^4S_{3/2}^0 - 3p^3\ ^2D_{3/2}^0$	6730.8	1.2×10^{-4}



Tip: Forbidden transitions are forbidden in terms of electric dipole transitions (i.e., allowed transitions) but possible via magnetic dipole and electric quadrupole.

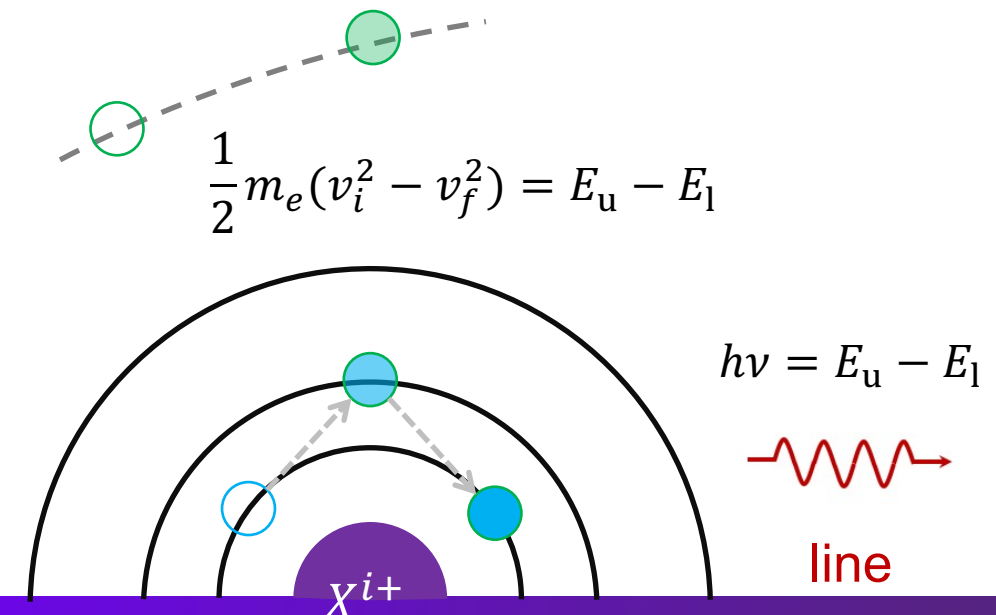
Collisional excitation process

Two types of collisional excitation: **electron-impact excitation (EIE)** and proton-impact excitation.

During the **EIE** process, the free electron transfers part of its kinetic energy to promote a bound electron of an ion into an excited atomic state.

The excited state is not stable. Subsequently, the inverse process electron-impact de-excitation (Elde) can occur, or the excited electron cascade down, giving rise to **line emissions**.

- ✓ EIE is a **cooling** process for the electrons
- ✓ Elde is a **heating** process for the electrons
- ✓ **line emission** spectral features for EIE



EIE rate coefficient

prev. sl.

$$\alpha = \int_{v_0}^{\infty} v f(v) \sigma^{\text{RR}}(v) dv$$

$$q_{\text{lu}} = \int_{v_0}^{\infty} v f(v) \sigma_{\text{lu}}^{\text{EIE}}(v) dv$$

$$v \geq v_0 = \left(\frac{2(E_u - E_l)}{m_e} \right)^{1/2}$$

Sect. 8.6 of 《天体物理中的辐射机制》(p349-352) by 尤峻汉

$$\sigma_{\text{lu}}^{\text{EIE}}(v) = \frac{h^2}{4\pi m_e^2 v^2} \frac{1}{g_l} \Omega_{\text{lu}}(v)$$

ordinary collisional strength (dimensionless)

Maxwell velocity distribution

$$f(v) dv = 4\pi \left(\frac{m_e}{2\pi k T_e} \right)^{3/2} v^2 \exp\left(-\frac{m_e v^2}{2k T_e}\right) dv$$

$$q_{\text{lu}} = \int_{v_0}^{\infty} v 4\pi \left(\frac{m_e}{2\pi k T_e} \right)^{3/2} v^2 \exp\left(-\frac{m_e v^2}{2k T_e}\right) \frac{h^2}{4\pi m_e^2 v^2} \frac{1}{g_l} \Omega_{\text{lu}} dv$$

$$= \int_{E_0}^{\infty} \frac{h^2}{m_e^3} \left(\frac{m_e}{2\pi k T_e} \right)^{3/2} \frac{1}{g_l} \Omega_{\text{lu}} \exp\left(-\frac{E}{k T_e}\right) dE$$

$$E = \frac{1}{2} m_e v^2, E_0 = E_u - E_l$$

$$= \int_{x_0}^{\infty} \frac{h^2 k}{(2\pi m_e k)^{3/2}} \frac{1}{g_l} \left(\frac{1}{T} \right)^{1/2} \Omega_{\text{lu}} \exp(-x) dx$$

$$x = \frac{E}{k T_e}, x_0 = \frac{E_u - E_l}{k T_e}$$

Effective collision strength

prev. sl.

$$q_{lu} = \int_{x_0}^{\infty} \frac{h^2 k}{(2\pi m_e k)^{\frac{3}{2}}} \frac{1}{g_l} \left(\frac{1}{T}\right)^{1/2} \Omega_{lu} \exp(-x) dx$$

ordinary collisional strength

$$\frac{q_{lu}}{\text{cm}^3 \text{s}^{-1}} = 8.629 \times 10^{-6} \frac{1}{g_l} \left(\frac{1}{T}\right)^{1/2} \int_{x_0}^{\infty} \Omega_{lu} \exp(-x) dx$$

Introducing the **effective collisional strength (dimensionless)**

Sect. 8.6 of 《天体物理中的辐射机制》(p349-352) by 尤峻汉

$$\Upsilon_{lu} = \frac{\int_{x_0}^{\infty} \Omega_{lu} \exp(-x) dx}{\int_{x_0}^{\infty} \exp(-x) dx} = \frac{1}{\exp(-x_0)} \int_{x_0}^{\infty} \Omega_{lu} \exp(-x) dx$$

$$\int_{x_0}^{\infty} \exp(-x) dx = \exp(-x_0)$$

$$x_0 = \frac{E_u - E_l}{kT_e}$$

$$\frac{q_{lu}}{\text{cm}^3 \text{s}^{-1}} = 8.629 \times 10^{-6} \frac{1}{g_l} \left(\frac{T}{K}\right)^{-1/2} \Upsilon_{lu} \exp\left(-\frac{E_u - E_l}{kT_e}\right)$$

cf. RR and EIE rate coefficients

prev. sl.

$$\frac{q_{lu}}{\text{cm}^3 \text{ s}^{-1}} = 8.629 \times 10^{-6} \frac{1}{g_l} \left(\frac{T}{K} \right)^{-1/2} \gamma_{lu} \exp \left(-\frac{E_u - E_l}{kT_e} \right)$$

effective collisional strength

Ion	Transition	$\lambda (\text{\AA})$	$E (\text{eV})$	$A (\text{s}^{-1})$
He II	$3d \ ^2D_{5/2} - 4f \ ^2F_{7/2}$	4685.8	2.69	2.2×10^8
O III	$2p^2 \ ^3P_1 - 2p^2 \ ^1D_2$	4958.9	2.50	6.2×10^{-3}
O III	$2p^2 \ ^3P_2 - 2p^2 \ ^1D_2$	5006.8	2.48	1.8×10^{-2}

Atomic process	Rate coefficient @ $T_e \sim 3 \times 10^4 \text{ K}$
He III – He II $4f \ ^2F_{7/2}$	$\alpha^{\text{RR}} \sim (0.6 - 1.2) \times 10^{-14} \text{ cm}^3 \text{ s}^{-1}$
O IV $2p \ ^2P_{1/2} - O \text{ III } 2p^2 \ ^1D_2$	$\alpha^{\text{RR}} \sim (3.1 - 4.9) \times 10^{-13} \text{ cm}^3 \text{ s}^{-1}$
O III $2p^2 \ ^3P_1 - O \text{ III } 2p^2 \ ^1D_2$?
O III $2p^2 \ ^3P_2 - O \text{ III } 2p^2 \ ^1D_2$?

Literature EIE data

Tayal & Zatsarinny (2017)

prev. sl.

$$\frac{q_{lu}}{\text{cm}^3 \text{ s}^{-1}} = 8.629 \times 10^{-6} \frac{1}{g_l} \left(\frac{T}{K}\right)^{-1/2} \Upsilon_{lu} \exp\left(-\frac{E_u - E_l}{kT_e}\right)$$

Index	Configuration	LSJ π	Exp ^a (eV)
1	$2s^2 2p^2$	3P_0	0.000
2	$2s^2 2p^2$	3P_1	0.014
3	$2s^2 2p^2$	3P_2	0.038
4	$2s^2 2p^2$	1D_2	2.514
5	$2s^2 2p^2$	1S_0	5.354
6	$2s 2p^3$	$^5S_2^o$	7.479
7	$2s 2p^3$	$^3D_3^o$	14.881
8	$2s 2p^3$	$^3D_2^o$	14.885
9	$2s 2p^3$	$^3D_1^o$	14.885
10	$2s 2p^3$	$^3P_2^o$	17.653

→ → →

$$g_l = 3$$

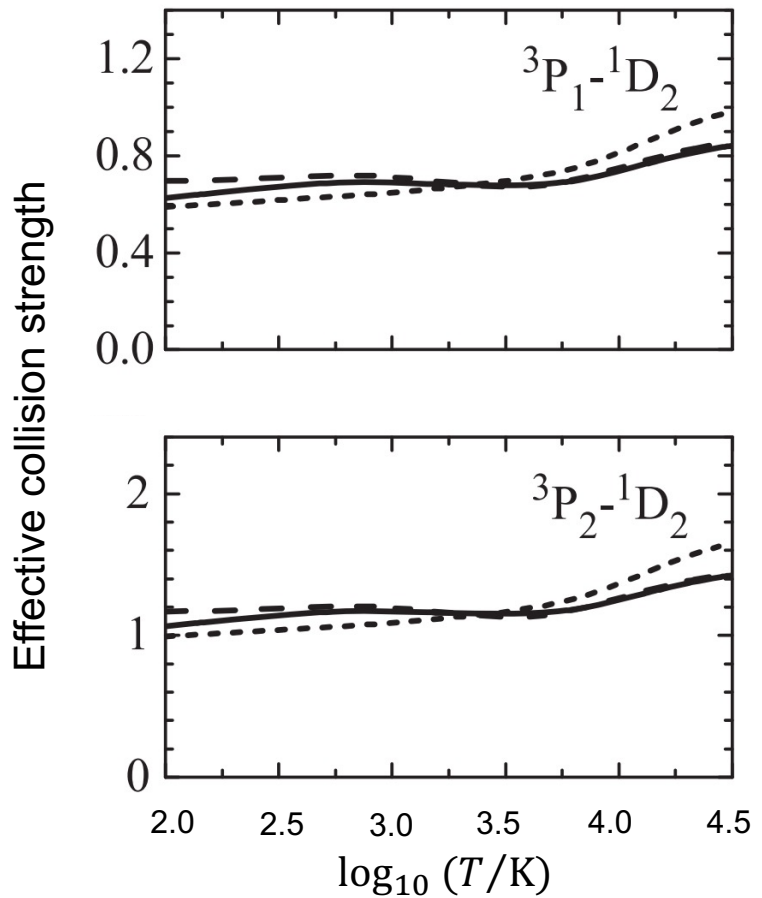
$$\log_{10}(T/\text{K}) \sim 4.48$$

$$\Upsilon(2 \rightarrow 4) \sim 0.83$$

$$\Upsilon(3 \rightarrow 4) \sim 1.4$$

Atomic process	Rate coefficient @ $T_e \sim 3 \times 10^4 \text{ K}$
He III – He II $4f \ ^2F_{7/2}$	$\alpha^{\text{RR}} \sim (0.6 - 1.2) \times 10^{-14} \text{ cm}^3 \text{ s}^{-1}$
O IV $2p \ ^2P_{1/2}$ – O III $2p^2 \ ^1D_2$	$\alpha^{\text{RR}} \sim (3.1 - 4.9) \times 10^{-13} \text{ cm}^3 \text{ s}^{-1}$
O III $2p^2 \ ^3P_1$ – O III $2p^2 \ ^1D_2$	$q^{\text{EIE}} \sim 5.2 \times 10^{-9} \text{ cm}^3 \text{ s}^{-1}$
O III $2p^2 \ ^3P_2$ – O III $2p^2 \ ^1D_2$	$q^{\text{EIE}} \sim 8.9 \times 10^{-9} \text{ cm}^3 \text{ s}^{-1}$

solid: [Tayal & Zatsarinny \(2017\)](#),
short-dashed: [Palay 2012](#)
long-dashed: [Storey et al. 2014](#)



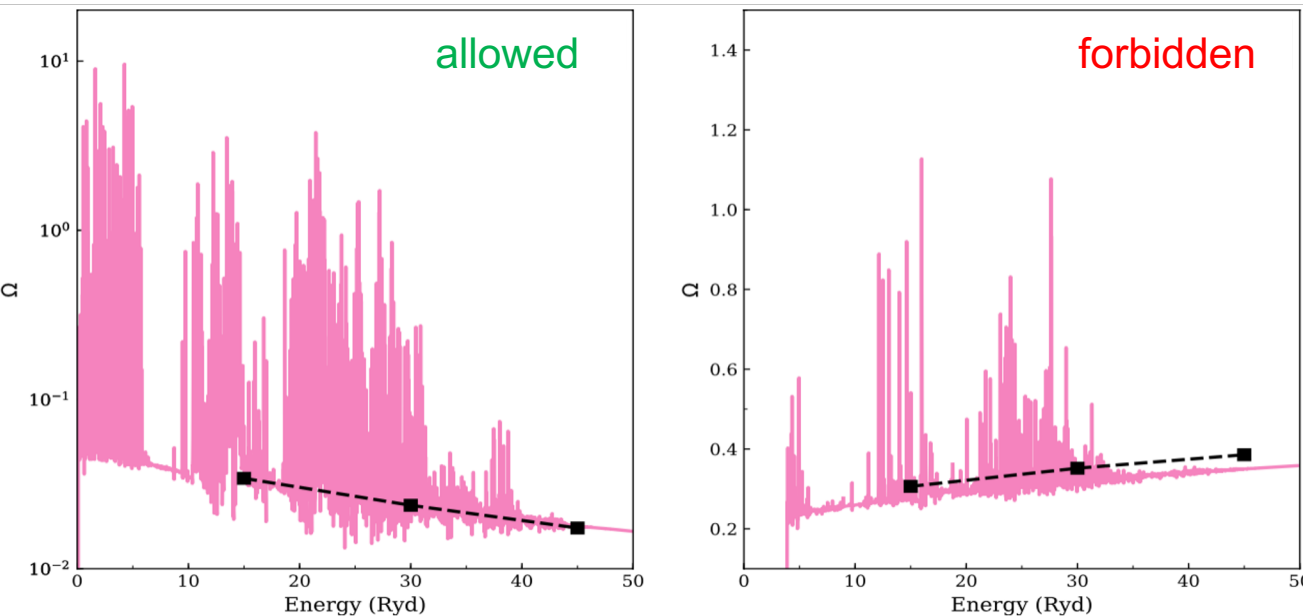
cf. ordinary collision strength

prev. sl.

$$q_{lu} = \int_{x_0}^{\infty} \frac{h^2 k}{(2\pi m_e k)^{\frac{3}{2}}} \frac{1}{g_l} \left(\frac{1}{T}\right)^{1/2} \Omega_{lu} \exp(-x) dx$$

ordinary collisional strength

— R-matrix: [Mao et al. 2020a](#)
 ■ - ■ Distorted wave (DW): [Dere et al. 1979](#)



A-values taken from [Mao et al. 2020a](#) as they are not available in NIST

Ion	Transition	$\lambda (\text{\AA})$	$A (\text{s}^{-1})$
Ar XIII	$2s^2 2p^2 {}^3P_0 - 2s^2 2p^2 {}^3P_1$	236.3	3.0×10^9
Ar XIII	$2s^2 2p^2 {}^3P_0 - 2s 2p^3 {}^3D_1$	10149	1.9×10^1

For **allowed** (**forbidden**) transitions,
ordinary collision strengths **decrease** (**increase**) with increasing energy

cf. effective collision strength

ordinary collisional strength

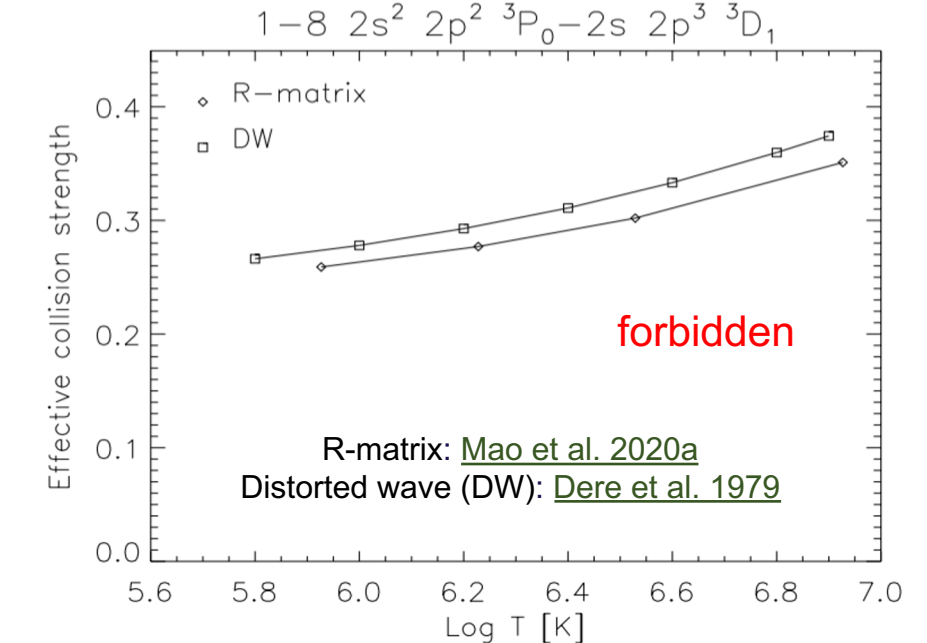
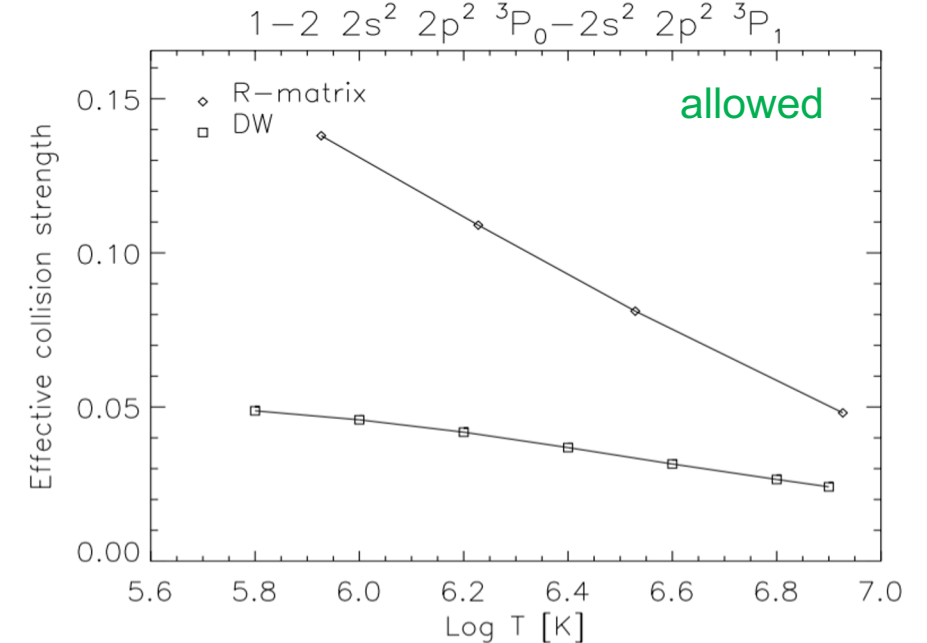
$$\gamma_{lu} = \frac{1}{\exp(-x_0)} \int_{x_0}^{\infty} \Omega_{lu} \exp(-x) dx$$

prev. sl.

effective collisional strength

Ion	Transition	$\lambda (\text{\AA})$	$A (s^{-1})$
Ar XIII	$2s^2 2p^2 {}^3P_0 - 2s^2 2p^2 {}^3P_1$	236.3	3.0×10^9
Ar XIII	$2s^2 2p^2 {}^3P_0 - 2s 2p^3 {}^3D_1$	10149	1.9×10^1

For allowed (forbidden) transitions, effective collision strengths decrease (increase) with increasing energy



EIdE rate coefficient

The electron-impact de-excitation rate coefficient can be derived under the detailed balance principle

prev. sl.

$$\frac{q_{lu}}{\text{cm}^3 \text{s}^{-1}} = 8.629 \times 10^{-6} \frac{1}{g_l} \left(\frac{T}{K}\right)^{-1/2} \gamma_{lu} \exp\left(-\frac{E_u - E_l}{kT_e}\right)$$

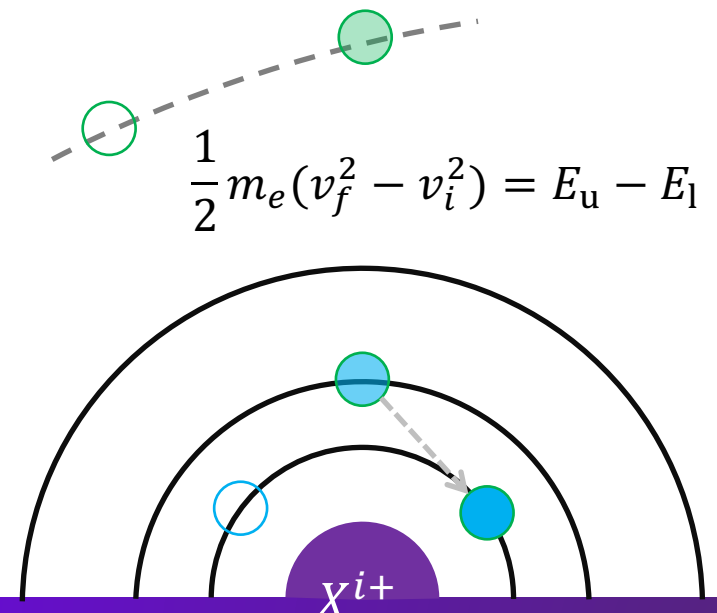
prev. sl.

$$\frac{q_{ul}}{q_{lu}} = \frac{n_l}{n_u} = \frac{g_l}{g_u} \exp\left(\frac{E_u - E_l}{kT}\right)$$

$$q_{ul} = q_{lu} \frac{g_l}{g_u} \exp\left(\frac{E_u - E_l}{kT}\right)$$

$$\frac{q_{ul}}{\text{cm}^3 \text{s}^{-1}} = 8.629 \times 10^{-6} \frac{1}{g_u} \left(\frac{T}{K}\right)^{-1/2} \gamma_{lu}$$

no line emission/absorption
(**heating** for the electrons)



Critical density

In the absence of external emission (i.e., $I_\nu = 0$), for a two-level system,

Sect. 5.2.6

$$n_u(A_{ul} + n_e C_{ul}) = n_l n_e C_{lu}$$

Critical density

$$n_e^{\text{crit}} = \frac{A_{ul}}{C_{ul}}$$

$$C_{ul} = q_{ul} = 8.629 \times 10^{-6} \frac{1}{g_u} \left(\frac{T}{K}\right)^{-1/2} \gamma_{lu}$$

prev. sl.

$$\frac{q_{ul}}{\text{cm}^3 \text{s}^{-1}} = 8.629 \times 10^{-6} \frac{1}{g_u} \left(\frac{T}{K}\right)^{-1/2} \gamma_{lu}$$

Table 3.15

Critical densities for collisional deexcitation

Ion	Level	n_e (cm ⁻³)	Ion	Level	n_e (cm ⁻³)
C II	$^2P_{3/2}^o$	5.0×10^1	O III	1D_2	6.8×10^5
C III	$^3P_2^o$	5.1×10^5	O III	3P_2	3.6×10^3
N II	1D_2	6.6×10^4	O III	3P_1	5.1×10^2
N II	3P_2	3.1×10^2	Ne II	$^2P_{1/2}^o$	7.1×10^5
N II	3P_1	8.0×10^1	Ne III	1D_2	9.5×10^6
N III	$^2P_{3/2}^o$	1.5×10^3	Ne III	3P_0	3.1×10^4
N IV	$^3P_2^o$	1.1×10^6	Ne III	3P_1	2.1×10^5
O II	$^2D_{3/2}^o$	1.5×10^4	Ne V	1D_2	1.3×10^7
O II	$^2D_{5/2}^o$	3.4×10^3	Ne V	3P_2	3.5×10^4
			Ne V	3P_1	6.2×10^3

NOTE: All values are calculated for $T = 10,000$ K.

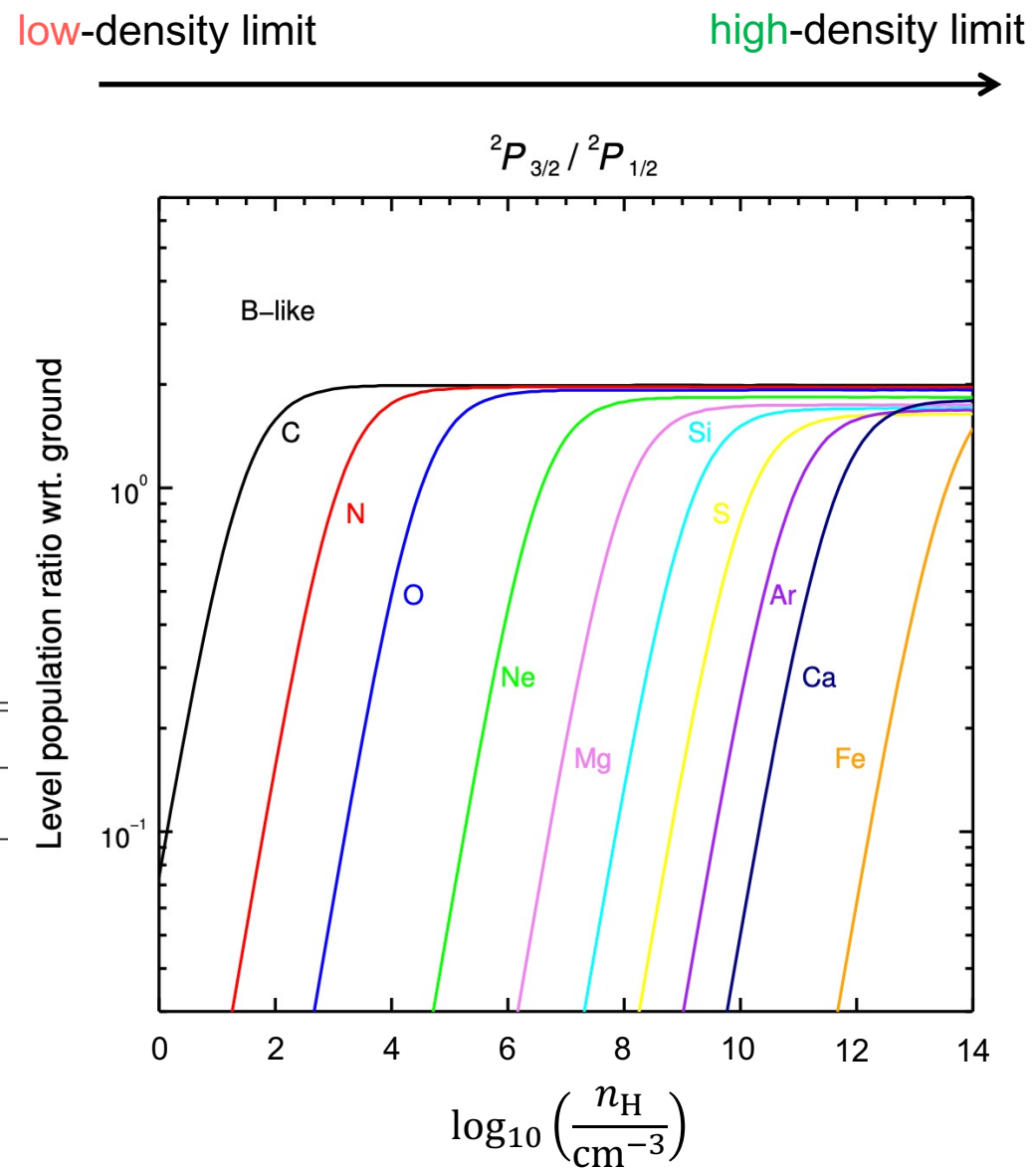
Osterbrock & Ferland 2006

Metastable levels

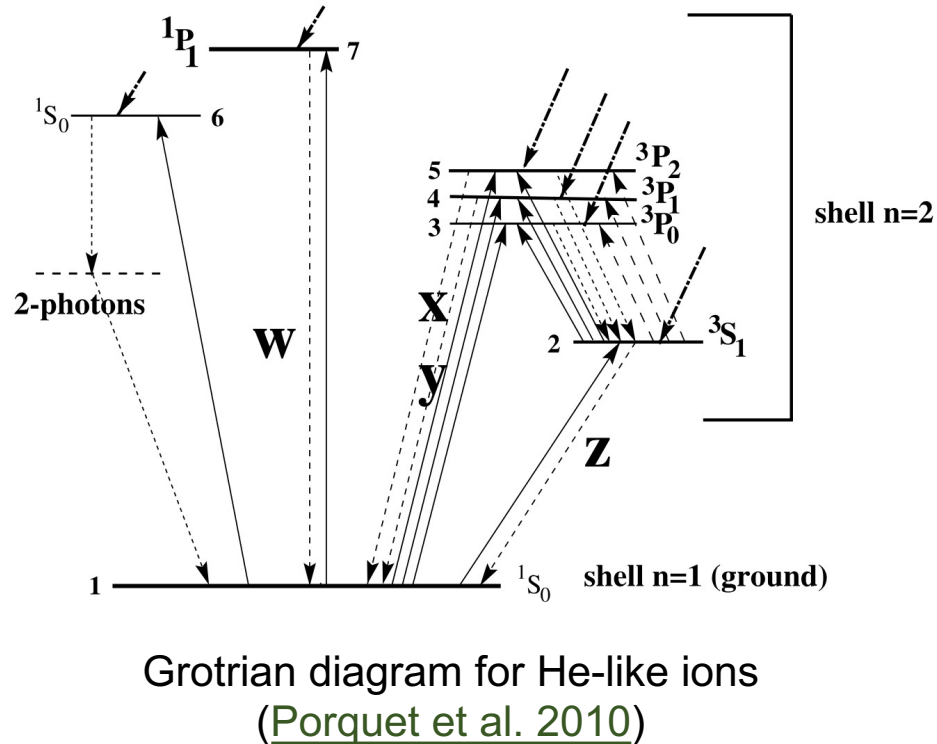
- In the **low-density limit** ($n_e \ll n_e^{\text{crit}}$), the ground level population is almost unity
- In the **high-density limit** ($n_e \gg n_e^{\text{crit}}$), the level population follows **Boltzmann** distribution
- ✓ Metastable levels are relatively **long-lived** excited levels (small A-value for the downward transition to the ground)

Mao et al. 2017b

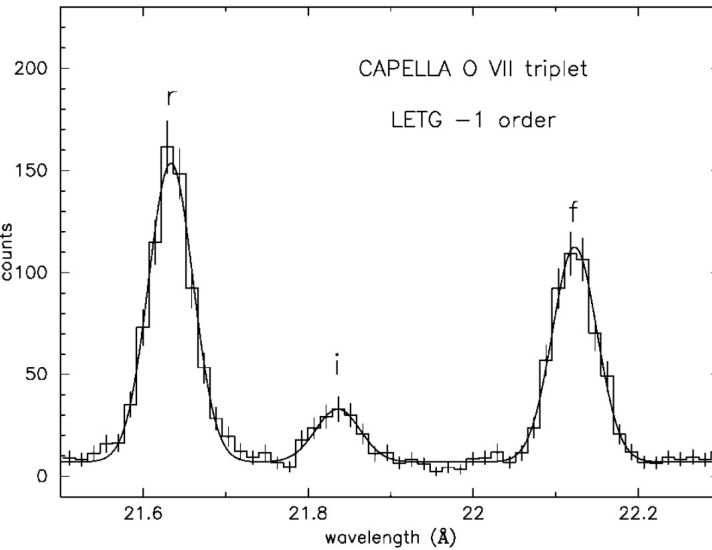
Index	1	2	3	4				
Sequence	Conf.	$^{2S+1}L_J$	Conf.	$^{2S+1}L_J$	Conf.	$^{2S+1}L_J$	Conf.	$^{2S+1}L_J$
Be-like	$2s^2$	1S_0	$2s2p$	3P_0	$2s2p$	3P_1	$2s2p$	3P_2
B-like	$2s^22p$	$^2P_{1/2}$	$2s^22p$	$^2P_{3/2}$	—	—	—	—
C-like	$2s^22p^2$	3P_0	$2s^22p^2$	3P_1	$2s^22p^2$	3P_2	$2s^22p^2$	1D_2
N-like (Fe)	$2s^22p^3$	$^4S_{3/2}$	$2s^22p^3$	$^2D_{3/2}$	$2s^22p^3$	$^2D_{5/2}$	$2s^22p^3$	$^2P_{1/2}$
O-like (Fe)	$2s^22p^4$	3P_2	$2s^22p^4$	3P_0	$2s^22p^4$	3P_1	$2s^22p^4$	1D_2
F-like (Fe)	$2s^22p^5$	$^2P_{3/2}$	$2s^22p^5$	$^2P_{1/2}$	—	—	—	—



He-like triplets



Transition	label	aka
$1s^2 \ 1S_0 - 1s \ 2p \ ^1P_1^0$	w (R)	resonance
$1s^2 \ 1S_0 - 1s \ 2p \ ^3P_2^0$	x (I)	inter-combination
$1s^2 \ 1S_0 - 1s \ 2p \ ^3P_1^0$	y (I)	inter-combination
$1s^2 \ 1S_0 - 1s \ 2p \ ^3S_1$	z (F)	forbidden



Brinkman et al. 2001

There are 4 key $n = 2 \rightarrow 1$ transitions in total. With insufficient spectral resolution, the x and y lines cannot be distinguished.

NIST Atomic Spectra Database Levels Data

Configuration	Term	J	Level (eV)
$1s^2$	1S	0	0.0000
$1s2s$	3S	1	560.98386
$1s2p$	$^3P^o$	0	568.54442
		1	568.55186
		2	568.62005
$1s2s$	1S	0	568.88662
$1s2p$	$^1P^o$	1	573.94778

Ritz Wavelength Vac (Å)	Rel. Int. (?)	A_{ki} (s ⁻¹)	Acc.	E_i (cm ⁻¹)	E_k (cm ⁻¹)	Lower Level Conf., Term, J	Upper Level Conf., Term, J
21.6020		3.309e+12	AA	0	- 4 629 201.0	$1s^2$ 1S 0	$1s2p$ $^1P^o$ 1
21.8044		3.31e+05	A	0	- 4 586 230.0	$1s^2$ 1S 0	$1s2p$ $^3P^o$ 2
21.8070				0	- 4 585 680.0	$1s^2$ 1S 0	$1s2p$ $^3P^o$ 1
22.1012		1.04e+03	AA	0	- 4 524 640.0	$1s^2$ 1S 0	$1s2s$ 3S 1

He-like triplets wavelengths

Porquet et al. 2010

	C V	N VI	O VII	Ne IX	Mg XI	Si XIII	S XV	Ca XIX	Fe XXV
w	40.2674 (0.3079)	28.7870 (0.4307)	21.6015 (0.5740)	13.4473 (0.9220)	9.1688 (1.3522)	6.6479 (1.8650)	5.0387 (2.4606)	3.1772 (3.9024)	1.8504 (6.7004)
x	40.7280 (0.3044)	29.0819 (0.4263)	21.8010 (0.5687)	13.5503 (0.9150)	9.2282 (1.3431)	6.6850 (1.8547)	5.0631 (2.4488)	3.1891 (3.8878)	1.8554 (6.6823)
y	40.7302 (0.3044)	29.0843 (0.4263)	21.8036 (0.5686)	13.5531 (0.9148)	9.2312 (1.3431)	6.6882 (1.8538)	5.0665 (2.4471)	3.1927 (3.8833)	1.8595 (6.6676)
z	41.4715 (0.2990)	29.5347 (0.4198)	22.0977 (0.5611)	13.6990 (0.9051)	9.3143 (1.3311)	6.7403 (1.8394)	5.1015 (2.4303)	3.2110 (3.8612)	1.8682 (6.6366)

Label	Lower Level	Upper Level	Ion	ID	λ (Å)	
He α -w (He-like)	$1s^2 \ ^1S_0$	$1s\ 2p\ ^1P_1$	C V	He α -z	41.472	
He α -x (He-like)	$1s^2 \ ^1S_0$	$1s\ 2p\ ^3P_2$	C V	He α -y	40.731	more He-like transitions
He α -y (He-like)	$1s^2 \ ^1S_0$	$1s\ 2p\ ^3P_1$	C V	He α -x	40.728	(e.g., Al XII, Ar XVII) can
He α -z (He-like)	$1s^2 \ ^1S_0$	$1s\ 2s\ ^3S_1$	C V	He α -w	40.268	be found in
He β -w (He-like)	$1s^2 \ ^1S_0$	$1s\ 3p\ ^1P_1$	C V	He β -w	34.973	Mao et al. 2022c
He γ -w (He-like)	$1s^2 \ ^1S_0$	$1s\ 4p\ ^1P_1$	C V	He γ -w	33.426	
He δ -w (He-like)	$1s^2 \ ^1S_0$	$1s\ 5p\ ^1P_1$	C V	He δ -w	32.754	

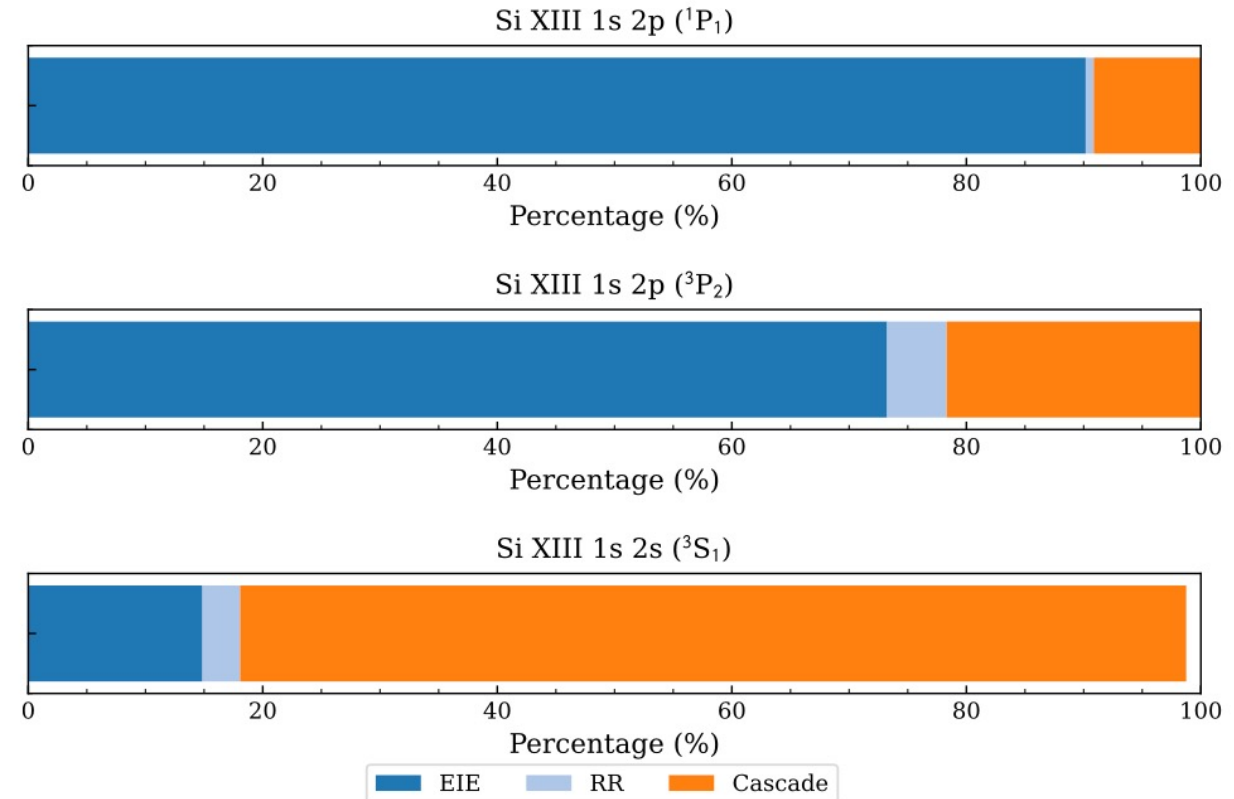
G-ratio

Gabriel & Jordan (1969b)

$$G(T_e) \equiv \frac{z + (x + y)}{w} \quad \left(\text{or } \equiv \frac{F + I}{R} \right)$$

- For **high** temperature collisional-dominated plasmas (e.g., stellar coronae), collisional excitation (EIE) favors the population of $1s\ 2p\ ^1P_1$, leading to stronger w (or R) line and $G \sim 1$
- For **low** temperature photoionized plasmas (e.g., NLR in AGN), recombination (RR) favors the population of $1s\ 2p\ ^3P_{2,1}$ and $1s\ 2s\ ^3S_1$, leading to stronger $z + x + y$ (or $F + I$) line and $G \sim 4$

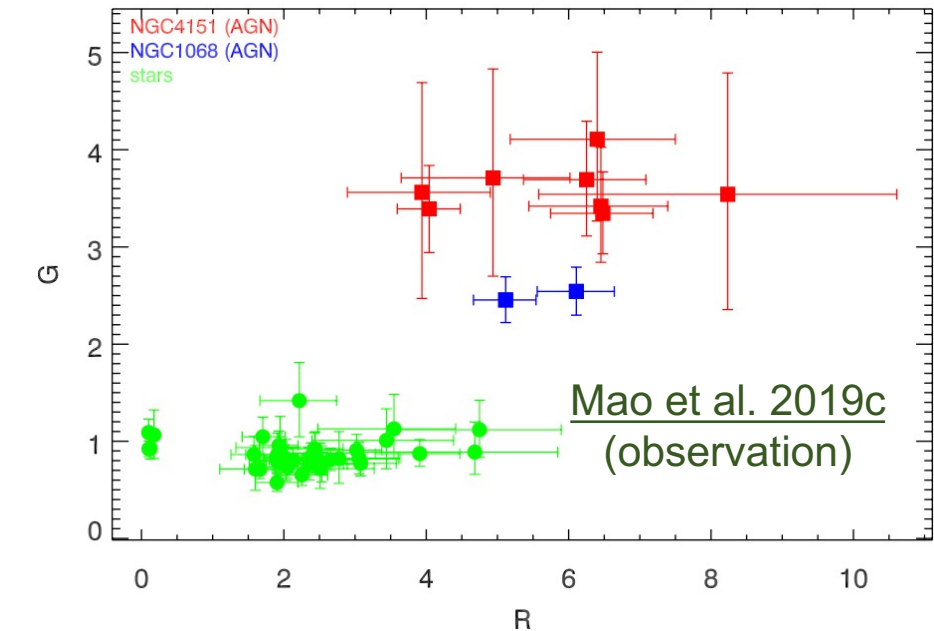
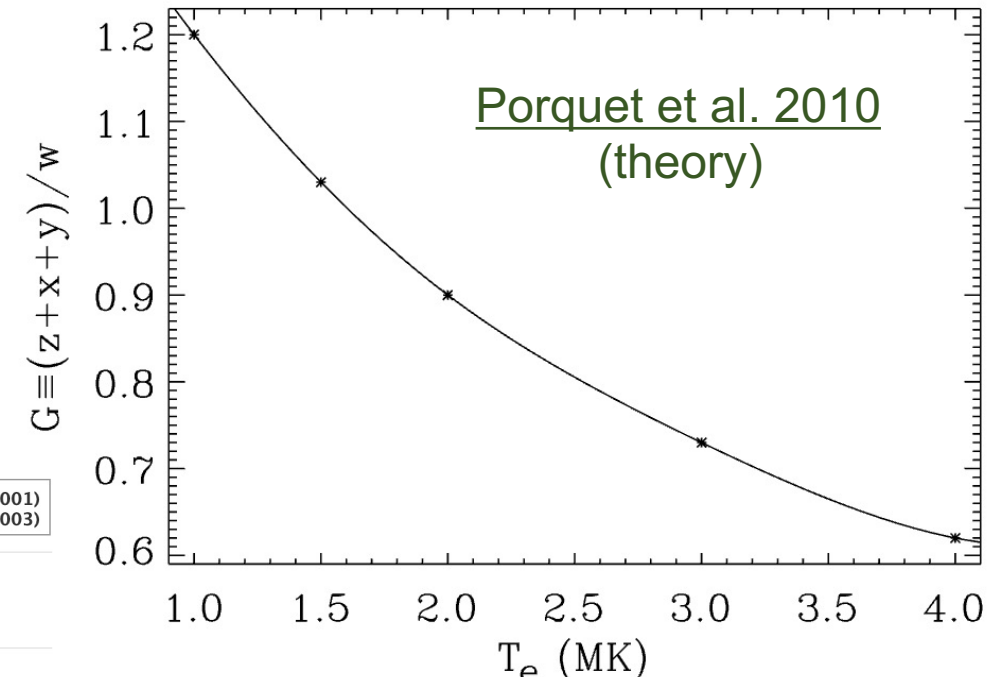
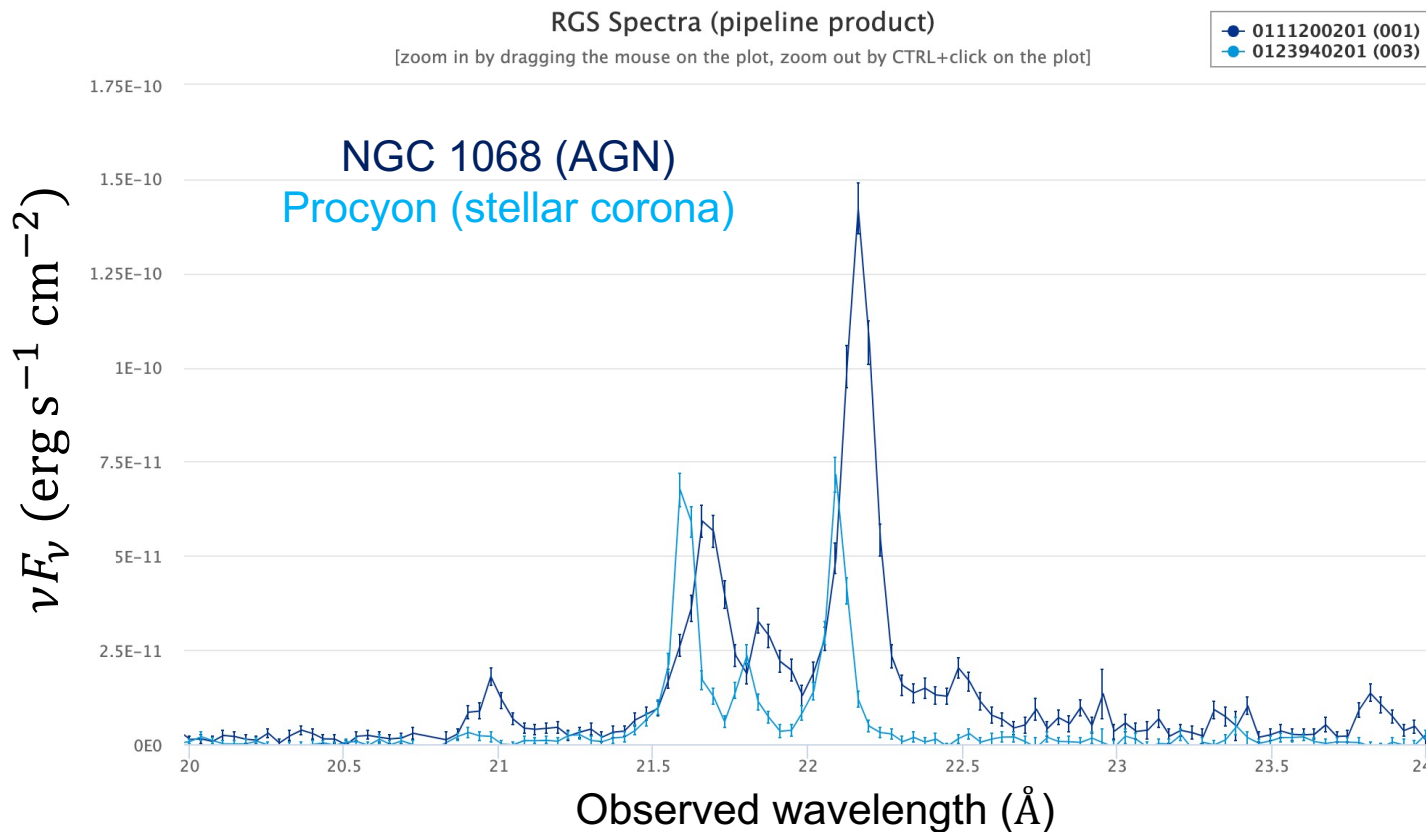
Mao et al. 2022c
for **high** temperature plasmas (e.g., stellar coronae, ICM of CIG)



G-ratio (theory vs. observation)

Gabriel & Jordan (1969b)

$$G(T_e) \equiv \frac{z + (x + y)}{w} \quad \left(\text{or } \equiv \frac{F + I}{R} \right)$$

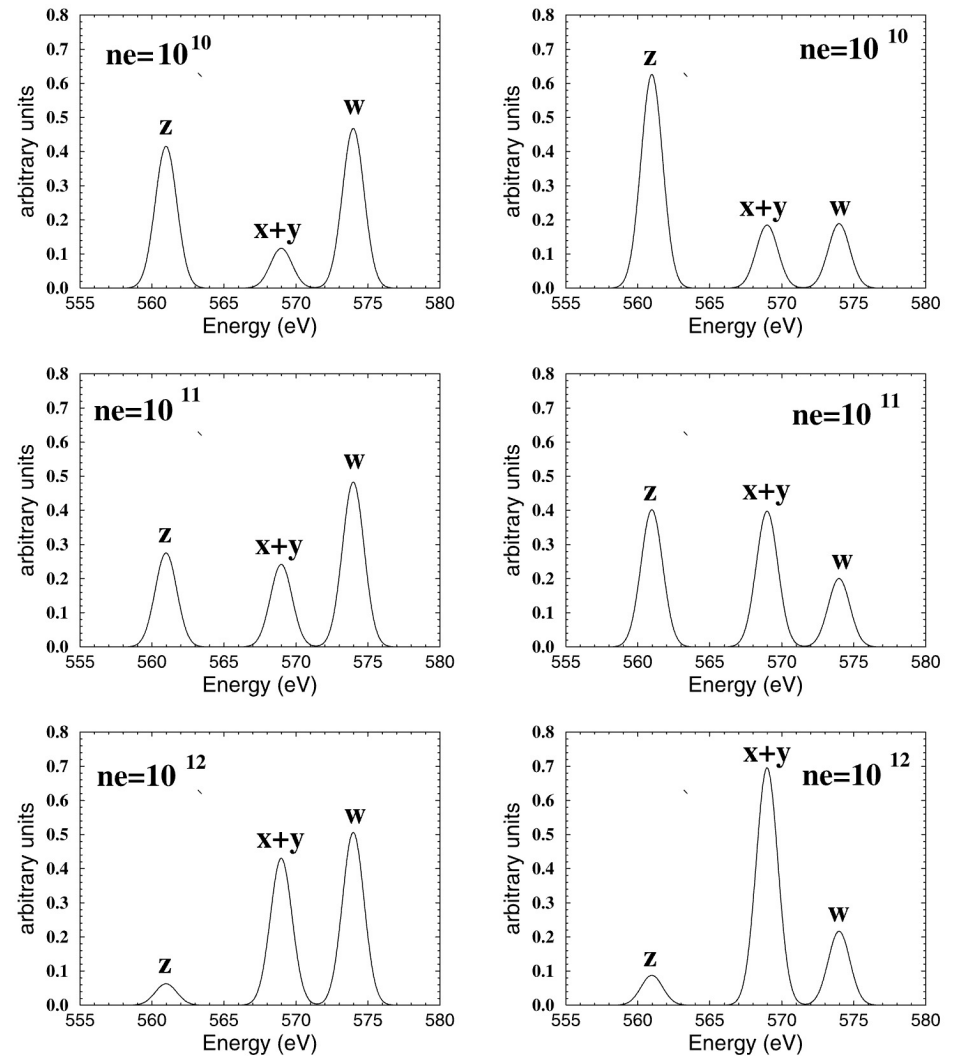


R-ratio

Gabriel & Jordan (1969b)

$$\mathcal{R}(n_e) \equiv \frac{z}{x+y} \quad \left(\text{or } \equiv \frac{F}{I} \right)$$

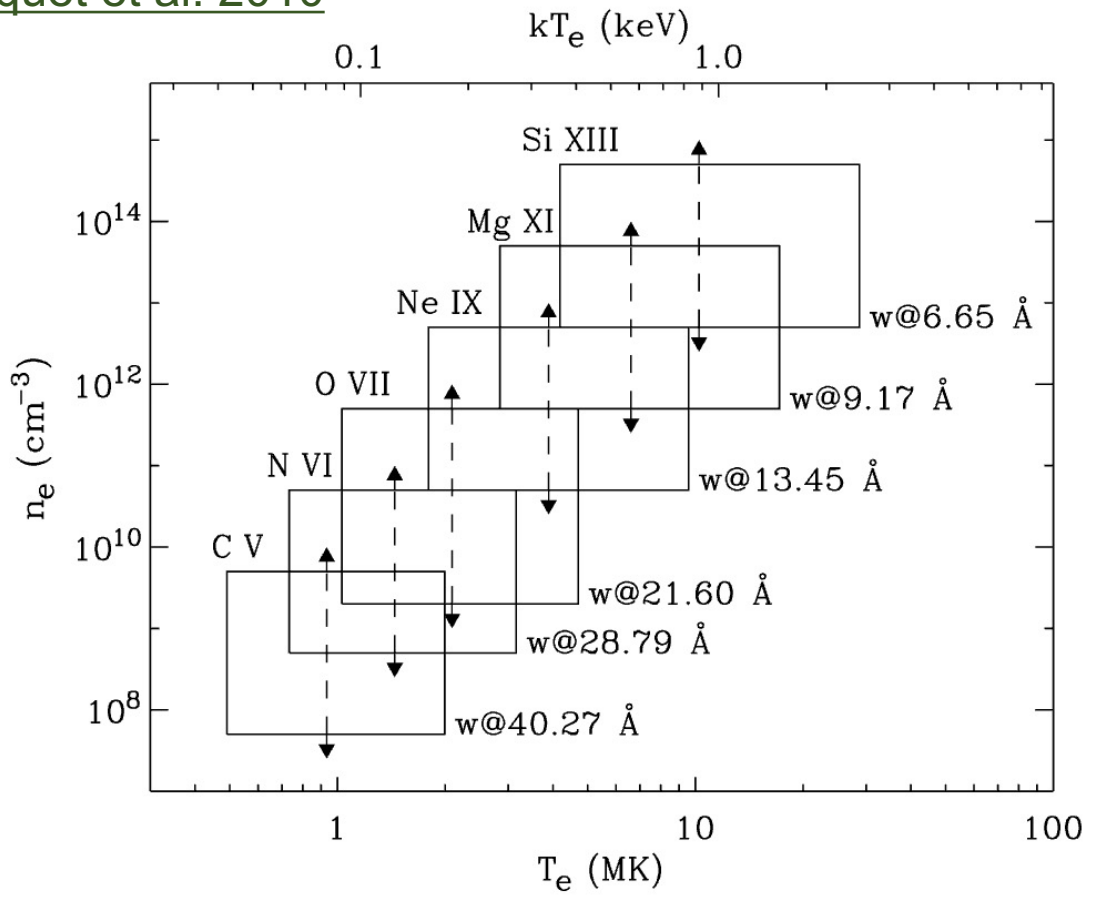
For collisional-dominated or photoionized plasmas, at high number densities, collisional excitation excite the upper level (metastable) of the z line to the upper level of $x + y$ line



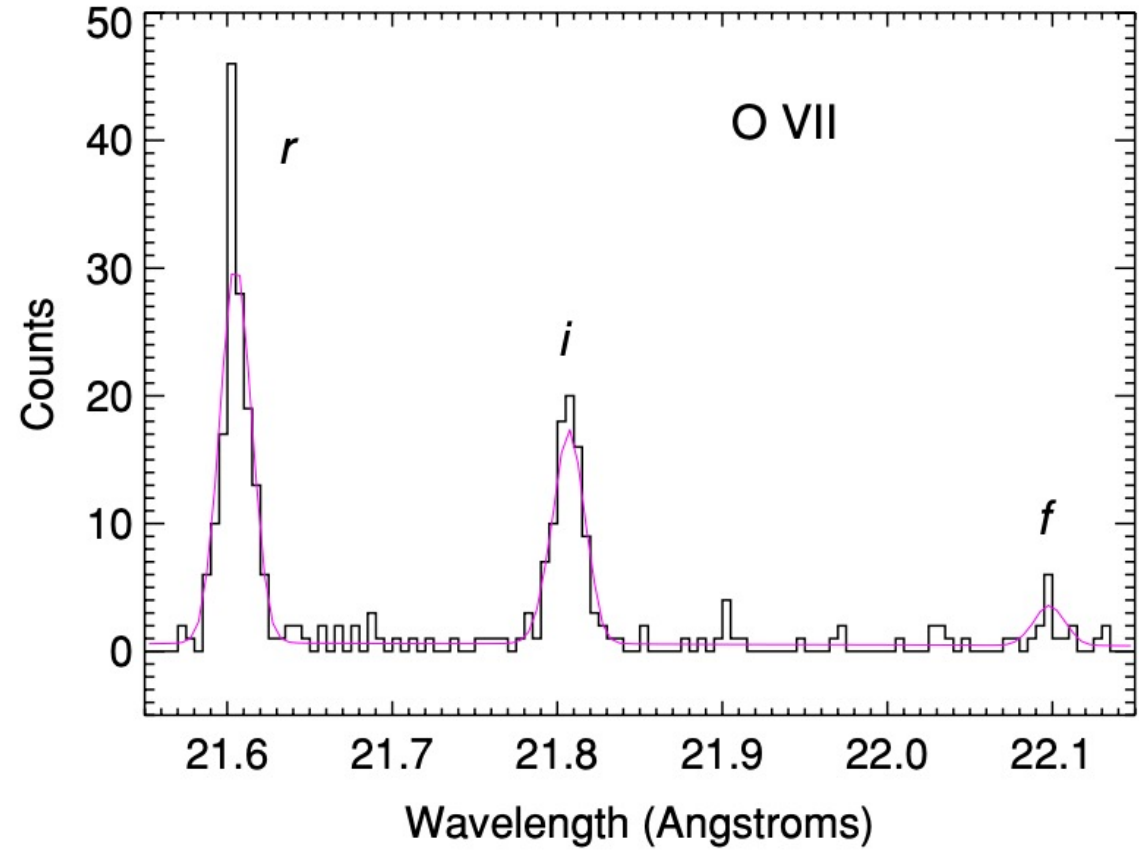
Left: for **high** temperature collisional-dominated plasmas (e.g., stellar coronae)
Right: for **low** temperature photoionized plasmas (e.g., NLR in AGN)

Ratio (theory vs. observation)

Porquet et al. 2010

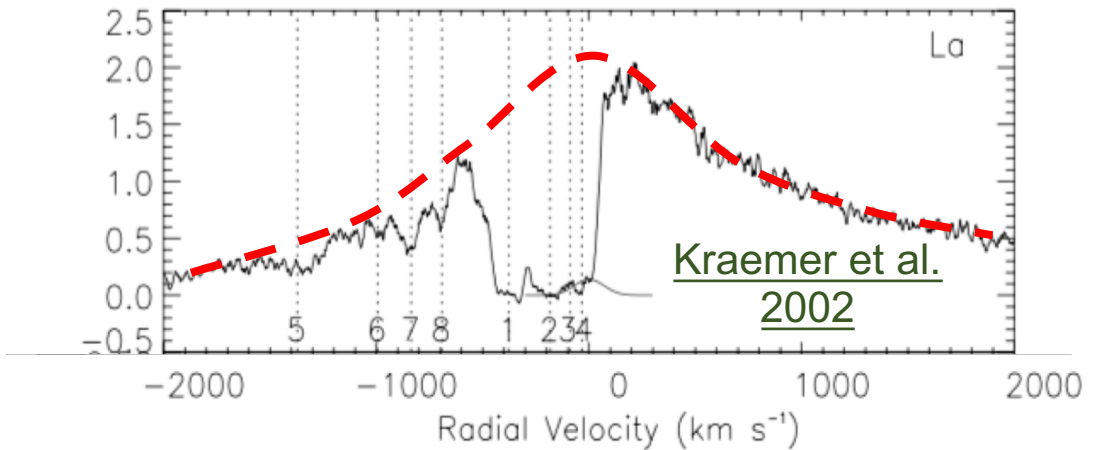
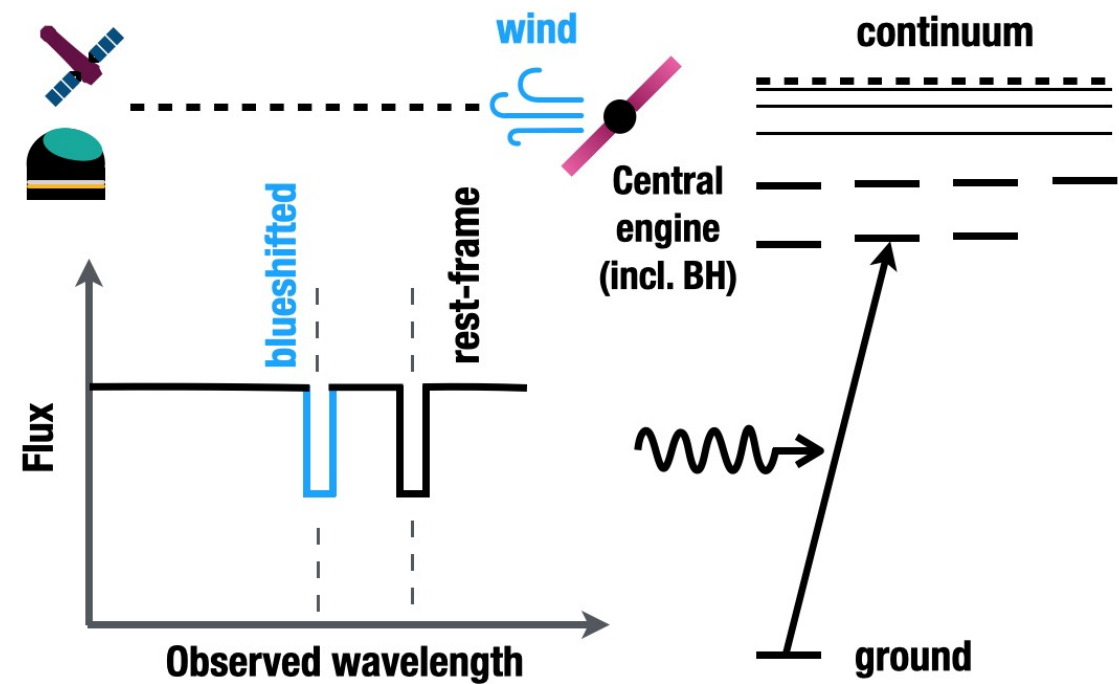


Brickhouse et al. 2010
TW Hydrae (observation)
 $n_e(\text{O VII}) \sim 5.7 \times 10^{11} \text{ cm}^{-3}$

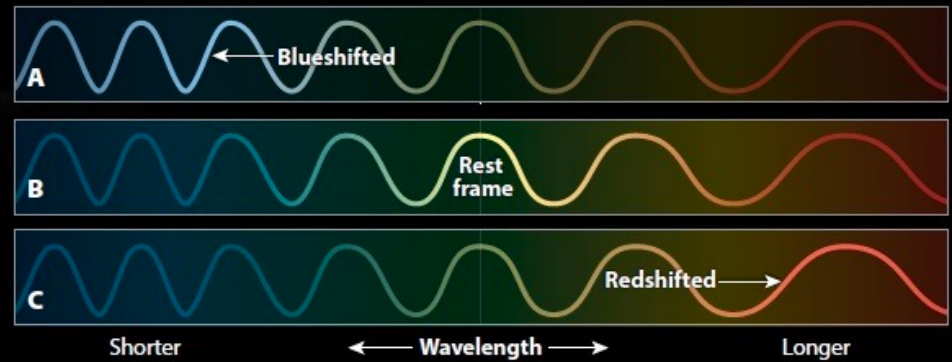
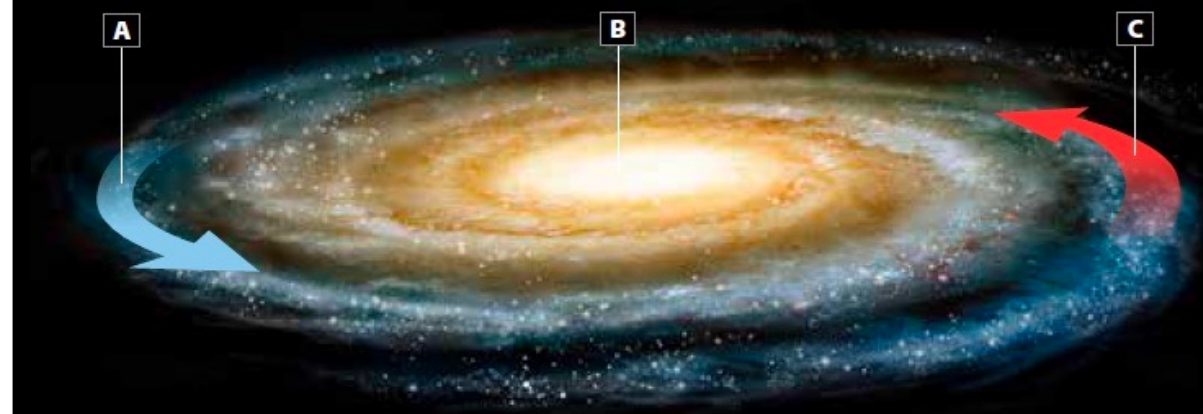


$$\mathcal{G}(T_e) \equiv \frac{z + (x + y)}{w} \quad \left(\text{or } \equiv \frac{F + I}{R} \right) \quad \mathcal{R}(n_e) \equiv \frac{z}{x + y} \quad \left(\text{or } \equiv \frac{F}{I} \right)$$

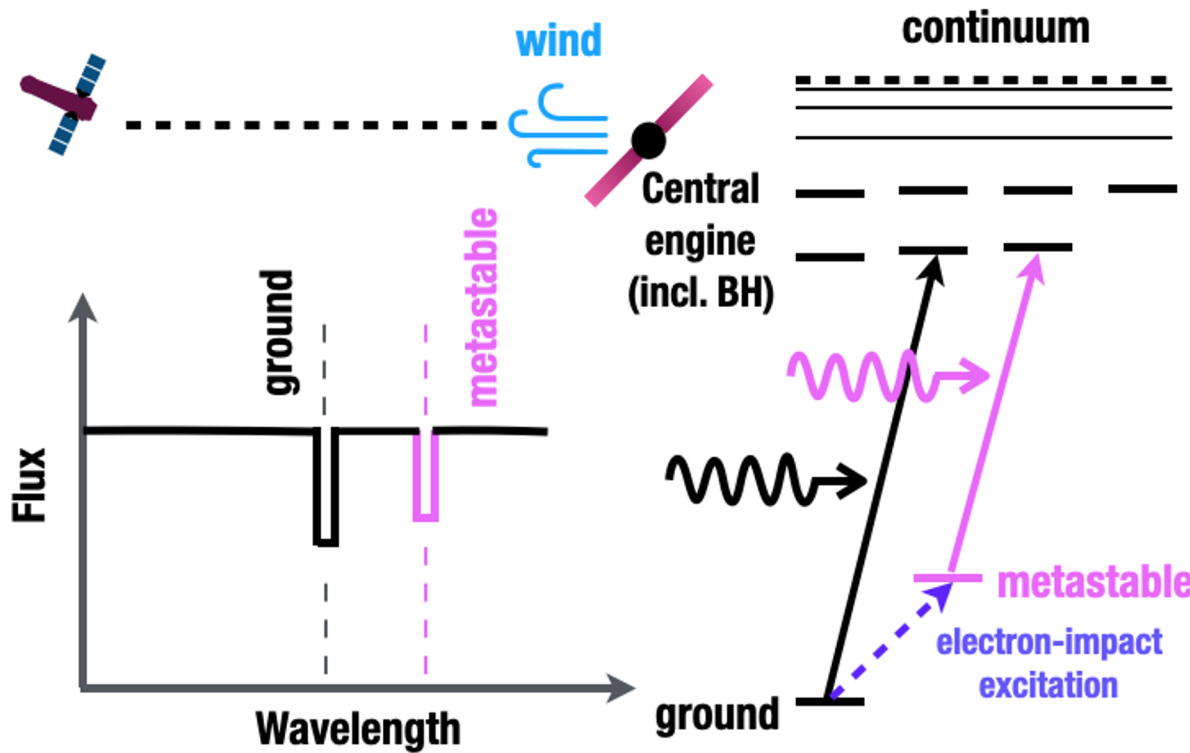
Black hole ionized winds



Ionized winds driven away from black holes are mainly probed via absorption spectroscopy



Metastable absorption lines



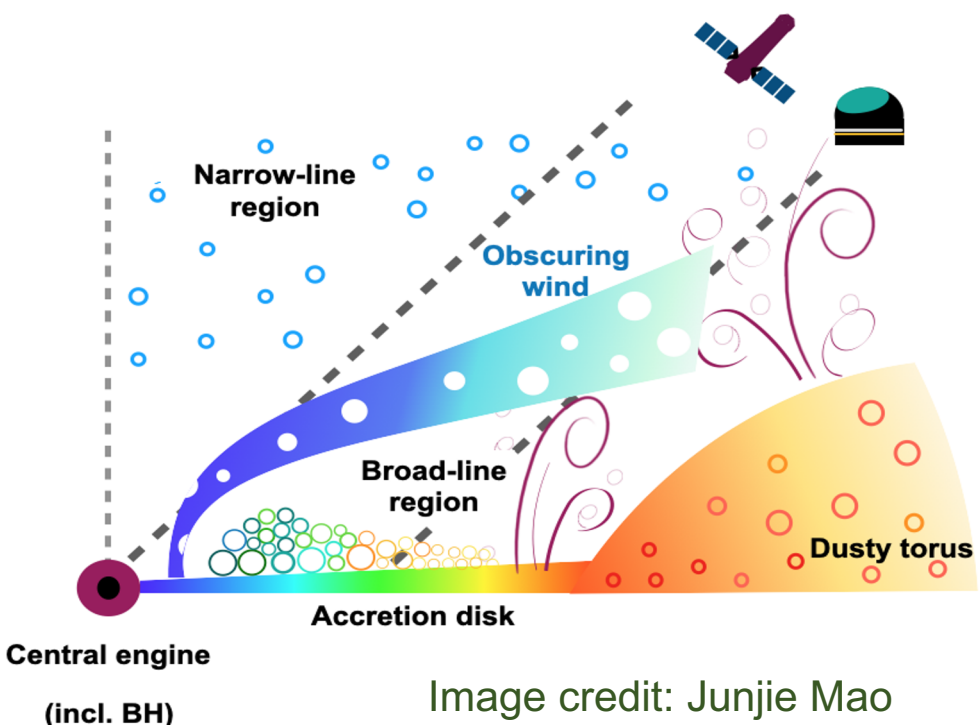
High-density winds are mainly probed via absorption spectroscopy

Index	1		2	
n_j	Lower	Upper (\dagger)	Lower	Upper
2–2	$2s^2 2p\ (^2P_{1/2})$	$2s 2p^2\ (^2P_{1/2})$	$2s^2 2p\ (^2P_{3/2})$	$2s 2p^2\ (^2P_{3/2})$
Ion	λ (Å)	f	λ (Å)	f
C II	903.962	0.33	904.142	0.42
N III	685.515	0.28	685.818	0.36
O IV	554.076	0.23	554.514	0.29
Ne VI	401.146	0.17	401.941	0.22
Mg VIII	313.754	0.13	315.039	0.18
Si X	256.384	0.09	258.372	0.15
S XII	227.490	0.07 ($^2S_{1/2}$)	218.200	0.13
Ar XIV	194.401	0.08 ($^2S_{1/2}$)	187.962	0.12
Ca XVI	168.868	0.08 ($^2S_{1/2}$)	164.165	0.11
Fe XXII	117.144	0.08	114.409	0.09
n_j	Lower	Upper	Lower	Upper
2–3	$2s^2 2p\ (^2P_{1/2})$	$2s^2 3d\ (^2D_{3/2})$	$2s^2 2p\ (^2P_{3/2})$	$2s^2 3d\ (^2D_{5/2})$
Ion	λ (Å)	f	λ (Å)	f
C II	687.053	0.33	687.346	0.30
N III	374.198	0.44	374.434	0.39
O IV	238.360	0.50	238.570	0.45
Ne VI	122.516	0.56	122.701	0.50
Mg VIII	74.858	0.60	75.034	0.54
Si X	50.524	0.62	50.691	0.56
S XII	36.399	0.63	36.564	0.57
Ar XIV	27.469	0.64	27.631	0.58
Ca XVI	21.451	0.65	21.609	0.58
Fe XXII	11.767	0.67	11.921	0.59

Ionization parameter

density (n_{H}) & distance to the BH (r)

- Origin of the winds
- Structure of the (multi-phase) winds
- Power of the winds to the environment



Tarter et al. 1969

$$\xi = \frac{L_{1-1000 \text{ Ry}}}{n_{\text{H}} r^2}$$

(cgs units): $\text{erg s}^{-1} \text{ cm}^{-2}$

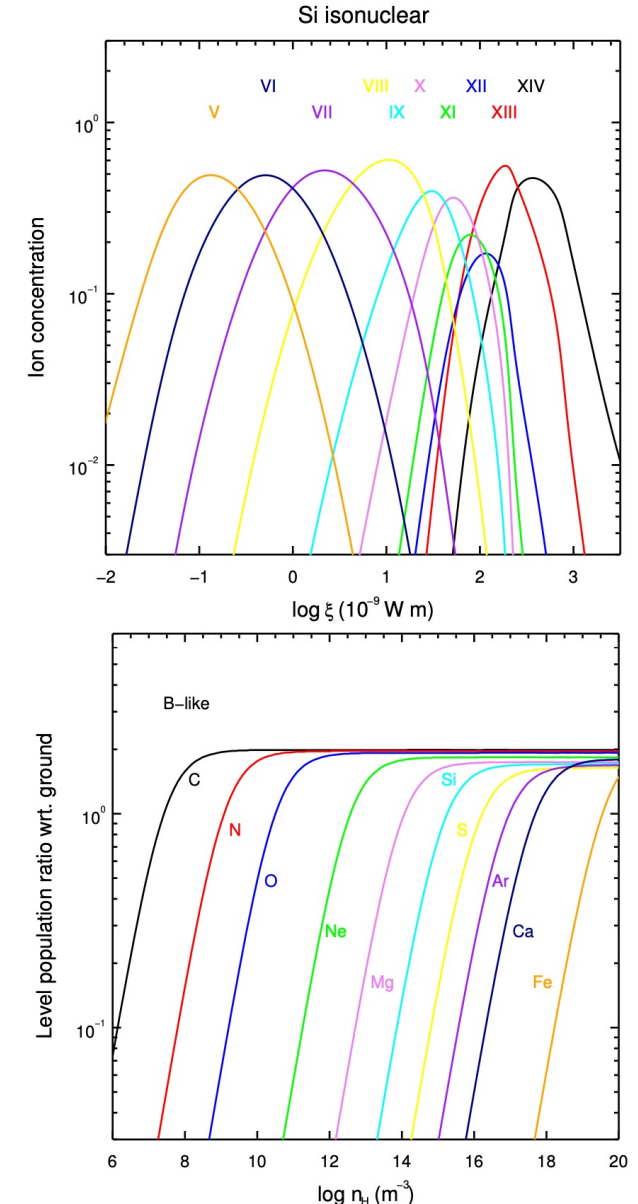
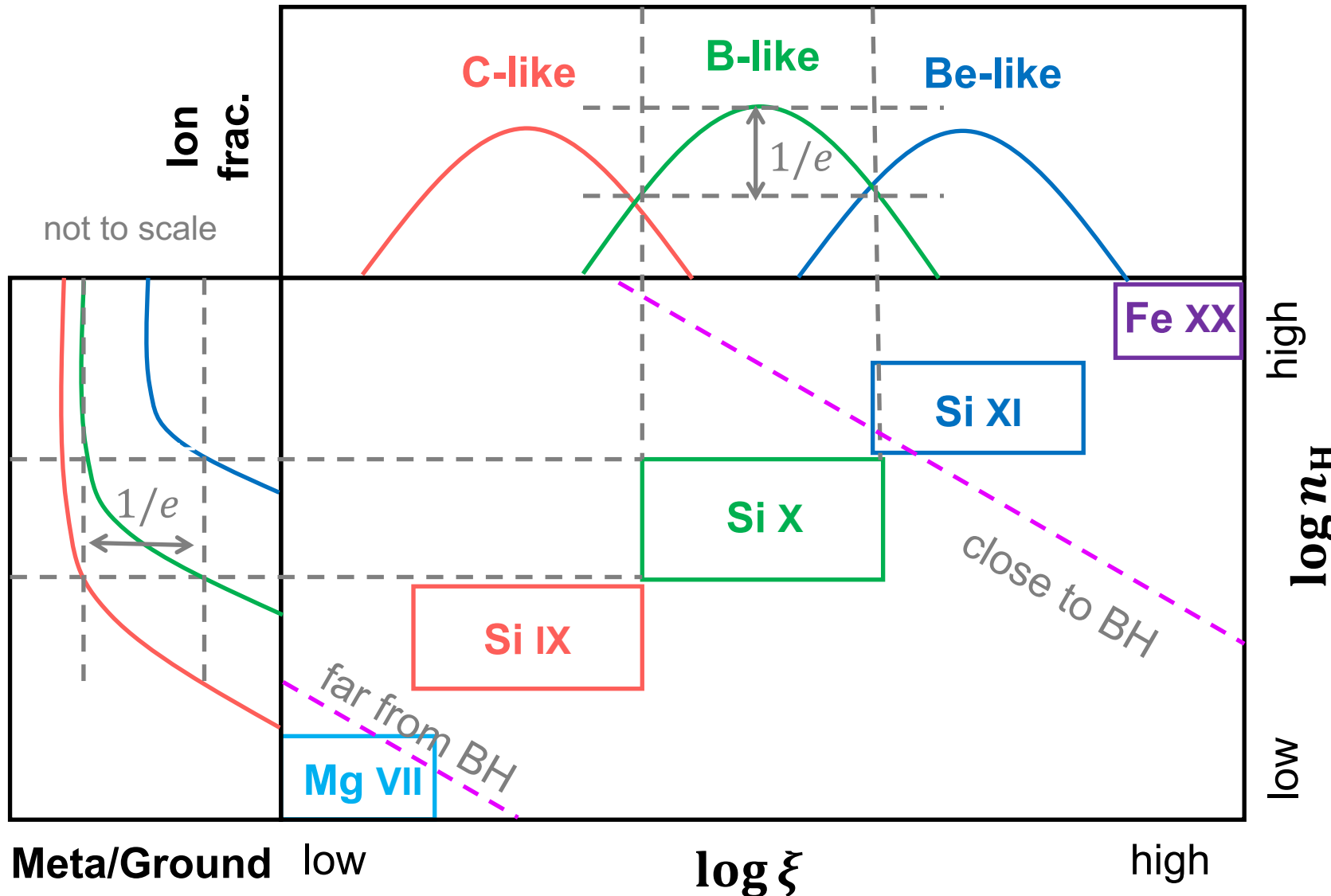
The alternative definition of ionization parameter

Osterbrock 2006

$$U = \frac{1}{4\pi r^2 c n_{\text{H}}} \int_{\nu_0}^{\infty} \frac{L_{\nu}}{h\nu} d\nu$$

dimensionless

Density and temperature diagnostics



Mao et al. 2017b